CAPITAL UNIVERSITY OF SCIENCE AND
TECHNOLOGY, ISLAMABAD

A Numerical Study of Boundary Layer Flow and Heat Transfer in Magneto-Micropolar Fluids with Influence of Micromagnetorotation

by

Sumaira Khatoon

A thesis submitted in partial fulfillment for the
degree of Master of Philosophy

in the

Faculty of Computing
Department of Mathematics

2024

*I dedicate my dissertation work to my **family** and dignified **teachers**. A special feeling of gratitude to my loving parents who have supported me in my studies*

CERTIFICATE OF APPROVAL

A Numerical Study of Boundary Layer Flow and Heat Transfer in Magneto-Micropolar Fluids with Influence of Micromagnetorotation.

by

Sumaira Khatoon

(Registration No: MMT213003)

THESIS EXAMINING COMMITTEE

S. No.	Examiner	Name	Organization
(a)	External Examiner	Dr. Yasir Mehmood	UOL, Sargodha
(b)	Internal Examiner	Dr. Muhammad Sabeel Khan	CUST, Islamabad
(c)	Supervisor	Dr. Muhammad Sagheer	CUST, Islamabad

Dr. Muhammad Sagheer
Thesis Supervisor
September, 2024

Dr. Muhammad Sagheer
Head
Dept. of Mathematics
September, 2024

Dr. M. Abdul Qadir
Dean
Faculty of Computing
September, 2024

Author's Declaration

I, **Sumaira Khatoon** hereby state that my MPhil thesis titled "**A Numerical Study of Boundary Layer Flow and Heat Transfer in Magneto-Micropolar Fluids with Influence of Micromagnetorotation**" is my own work and has not been submitted previously by me for taking any degree from Capital University of Science and Technology, Islamabad or anywhere else in the country/abroad.

At any time if my statement is found to be incorrect even after my graduation, the University has the right to withdraw my MPhil Degree.

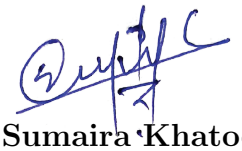

(Sumaira Khatoon)

Registration No: MMT213003

Plagiarism Undertaking

I solemnly declare that research work presented in this thesis titled "**A Numerical Study of Boundary Layer Flow and Heat Transfer in Magneto-Micropolar Fluids with Influence of Micromagnetorotation**" is solely my research work with no significant contribution from any other person. Small contribution/help wherever taken has been duly acknowledged and that complete thesis has been written by me.

I understand the zero tolerance policy of the HEC and Capital University of Science and Technology towards plagiarism. Therefore, I as an author of the above titled thesis declare that no portion of my thesis has been plagiarized and any material used as reference is properly referred/cited.

I undertake that if I am found guilty of any formal plagiarism in the above titled thesis even after award of MPhil Degree, the University reserves the right to withdraw/revoke my MPhil degree and that HEC and the University have the right to publish my name on the HEC/University website on which names of students are placed who submitted plagiarized work.

(Sumaira Khatoon)

Registration No: MMT213003

Acknowledgement

I got no words to articulate my cordial sense of gratitude to **Almighty Allah** who is the most merciful and most beneficent to his creation.

I also express my gratitude to the last prophet of **Almighty Allah, Prophet Muhammad (PBUH)** the supreme reformer of the world and knowledge for human being.

I would like to be thankful to all those who provided and encourged me during this work.

I would like to be grateful to my thesis supervisor **Dr. Muhammad Sagheer,** the Head of the Department of Mathematics, for guiding and encouraging towards writing this thesis. It would have remained incomplete without his endeavours. Due to his efforts I was able to write and complete this assertation.

I would like to pay great tribute to my parents, for their prayers, moral support encouragment and apperciation.

I would like to be thankful to my elder brother **Syed Akbar Shah**, for being an incredible source of inspiration, guidance, and support throughout this journey. Your belief in me has been a guiding light, and I am honored to have you by my side every step of the way.

Last but not the least, I want to express my gratitude to my collegue and friends who helped me throughout in my Mphil degree.

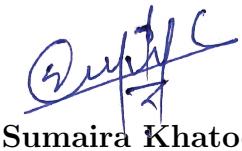

(Sumaira Khatoon)

Registration No: MMT213003

Abstract

This paper investigates the intricate interplay of heat transfer phenomenon within micropolar magnetohydrodynamic (MHD) flows, with a specific emphasis on the influential role of micromagnetrotation (MMR). A comprehensive analysis of an incompressible, laminar, two-dimensional MHD micro-polar fluid flow subject to an externally applied magnetic field has been conducted. Numerical technique; the shooting method, effectively solved the converted coupled system of ordinary differential equations. The inclusion of micro-polar and magnetization effects is shown to distinctly influence the magnetic induction, temperature, and macro-rotational velocity profiles, along with notable variations in their rates of change. Furthermore, the examination underscores the significant impact of magnetic reynolds number and Eckert numbers in enhancing heat transfer efficiency, thereby fostering improved thermal diffusion within the system. The effects of MMR are thoroughly analyzed on hydrodynamics, temperature, macro-rotational, and magnetic induction profiles, revealing intriguing features of the flow. To enhance the comprehensiveness of the study, the results of skin friction and local Nusselt number are presented in tabular and graphical formats, with a detailed discussion. These outcomes contribute to a deeper understanding of the intricate dynamics involved in the micro-polar flows, emphasizing the practical implications of MMR on key flow parameters. The findings of this research offer valuable insights into the pivotal role of MMR in MHD flows and its consequential influence on heat transfer characteristics, with potential applications in magnetic cooling systems, advanced thermal management, energy conversion, material processing, environmental fluid dynamics, and innovations in magneto-hydrodynamics.

Contents

List of Figures

List of Tables

Abbreviations

BCs	Boundary conditions
IVPs	Initial value problems
MHD	Magnetohydrodynamics
MMR	Micromagnetorotation
ODEs	Ordinary differential equations
PDEs	Partial differential equations
RK-4	Range Kutta order 4

Symbols

u	x-component of fluid velocity
v	y-component of fluid velocity
μ	Viscosity
ν	Kinematic viscosity
ρ	Density
B_o	Magnetic induction strength
τ	Stress tensor
k	Thermal conductivity
α	Thermal diffisuitivity
σ	Electrical conductivity
ρc_p	Heat capacity
$\mathbf{J}$	Current density
t	Time
l	Moment of interia
I	Identical tensor
K^*	absorption coefficient
$\mathbf{H}$	External magnetic field
M_0	Magnetization strength
H_0	Magnetic field strength
$\mathbf{B}$	Magnetic induction vector
μ	Coefficient of friction
ζ_1	Vortex viscosity coefficient
$\mathbf{T}$	Fluid temperature
γ	Angular viscosity coefficient

$\mathbf{M}$	Magnetization vector
p	Pressure
β	Magnetization parameter
β^*	Micro-inertial coupling parameter
K	Micropolar constant
μ_0	Magnetic premeability
B_0	Magnetic induction strength
ϵ	Levi-Civical symbol
$\mathbf{W}$	Microrotation vector
$\mathbf{w}$	vorticity
T_w	Temperature of the wall
T_∞	Ambient temperature of the fluid
q	Heat generation constant
q_w	Heat flux
ζ	Similarity variable
$f(\zeta)$	Dimensionless velocity
$\theta(\zeta)$	Dimensionless temperature
Ec	Eckert number
Q	Heat source
Re	Reynolds number
Re_x	Local Reynolds number
Nu	Nusselt number
Nu_x	Local Nusselt number
Cf	Skin fraction coefficient

Chapter 1

Introduction

1.1 Background

Micropolar fluids, characterized by the presence of micro-constituents capable of undergoing rotation, exhibit non-Newtonian hydrodynamics and have wide-ranged practical applications. Applications of such fluids include the analysis of exotic lubricants, colloidal suspensions, solidification of liquid crystals, extrusion of polymer fluids, cooling of metallic plates in a bath, and the study of biological fluids such as animal blood. Eringen [1] is acknowledged as the pioneer in formulating the theory of micropolar fluids. His groundbreaking theory introduces new material parameters, an additional independent vector field;the microrotation,and new constitutive equations, requiring simultaneous solution with the standard equations for Newtonian fluid flow. The field of micropolar fluids boasts a rich literature, with various aspects extensively investigated. Notable studies include Nazar et al. [2] which is focused on the numerical exploration of stagnation point flow in a micropolar fluid over a stretching sheet, by the Keller–box method. Bhattacharyya et al. [3] delved into the effects of thermal radiation on micropolar fluid flow past a porous shrinking sheet, employing the shooting method for numerical solution. Nadeem et al. [4] analytically investigated the micropolar fluid flow over an exponentially stretching surface under multislip conditions, employing the Optimal Homotopy Analysis Method. Ghasemi and Gouran [5] studied the physical behavior of incompressible micropolar fluid flow between two porous disks, employing the differential transformation

scheme and the differential quadrature method to find sdution of the nonlinear problem. Magnetohydrodynamics is considered to be an interdisciplinary field that integrates the foundational principles of classical electromagnetism with the complexities of fluid dynamics. Its scope involves the study of electrically conductive fluids under the influence of magnetic field. Eringen [6] extensively explored the magnetohydrodynamics and electrodynamics of micropolar fluids, a branch of physics addressing phenomena related to moving charged bodies within varying electric and magnetic fields, recognizing that moving charges generate a magnetic field. Building upon Eringen's work [7], numerous researchers have delved into MHD micropolar flows. Chaudhary and Jha [8] investigated the an unsteady MHD micropolar fluid flow through a porous medium bounded by a semi-infinite vertical plate, considering a first-order homogeneous chemical reaction. Sharma et al. [9] utilized the Matlab solver bvp4c to analyze MHD micropolar fluids induced by a permeable and continuously stretching sheet, accounting for slip effects in a porous medium. Appidi et al. [10] applied the Galerkin finite element technique to explore an unstable two-dimensional laminar flow around a viscous fluid over a semi-infinite, vertically absorbent surface.

Analyzing fluid flow with heat transfer characteristics induced by a stretching sheet holds significant implications for engineering and industrial applications, including wire drawing, polymer sheet extrusion, glass blowing, and textile and paper production. Turkyilmazoglu [11] conducted an analytical investigation of a micropolar fluid flow over a permeable stretching sheet, examining heat transfer under conditions of constant wall temperature, constant heat flux, and Newtonian heating. In a numerical study, Mandal et al. [12] explored the effects of velocity slip and radiation on the MHD flow and melting heat transfer of a micropolar fluid due to an exponentially stretched sheet. Bakarand Soid [13] numerically investigated MHD stagnation point flow and heat transfer in a micropo-lar fluid over an exponentially vertical stretching/shrinking sheet, conside ring buoyancy effects and employing the bvp4c solver.Usafzai and Aly [14] found an exact solution for a heat transfer problem on a flexible surface subjected to linear stretc hing/shrinking. Agrawal et al. [15] numerically explored the impact of Joul heating and thermal radiation on melting heat transfer for an MHD micropolar fluid flow.

The MMR effect plays a significant role in shaping the flow characteristics of micropolar fluids. This effect introduces additional stresses and angular momentum into the flow,

resulting in alterations to both velocity and microrotation profiles. Moreover, the MMR effect extends its influence to heat transfer and mass transfer phenomena within micropolar fluids. Aslani and Sarris [16] employed analytical methods to explore the impact of MMR on velocity and microrotation fields.

The intricate interplay between heat transfer, magneto-micropolar flow, and MMR has attracted significant attention in recent years. Despite some notable advancements in the field, there are still noticeable gaps in this area. Particularly, the influence of magnetization on microrotation in magneto-micropolar flows has received limited investigation. To address these shortcomings, this study is designed to explore the heat transfer in magneto-micropolar flow under the influence of the MMR effect. Employing an effecient numerical approach, the shooting method with fourth-order Runge-Kutta method as as major component, the intricate interplay between the MMR effect and the flow behavior has been unravelled. The present work provides a comprehensive analysis to dissec tthe behaviors of the micropolar flow, enabling us to elucidate the effects of various dimensionless parameters on velocity, temperature, and microrotation.

The present investigation sheds light on the differences arising due to the MMR term, providing a deeper understanding of the behavior of micropolar fluids under the influe nce of magnetic fields. Moreover, the present findings highlight the significance of con sidering the lateral magnetization effect, which has often been neglected in previous st udies on micropolar boundary layer flows.

1.1.1 Thesis contributions

The numerical analysis of micromagnetorotation-related heat transfer and boundary layer flow in a magnetomicropolar fluid are the main topics of this work. The formulaic PDEs are transformed into a system of ODEs with the use of similarity transforms. Moreover, the shooting method is applied to acquire the numerical results of the given ODEs. MATLAB is used to compute the results that are obtained numerically. Graphs and tables are used to assess and display the effects of important parameters on the skin friction, Nusselt number, magnetic induction profile, hydrodynamic velocity profile, and macrorotational velocity profile.

1.1.2 Layout of Thesis

Chapter 2 contains some basic definitions and terminology that are helpful in understanding the ideas that will be covered later.

In **Chapter 3** offers a study on boundary layer flow in a fluid that is magneto-micropolar. The numerical results of the governing flow equations are derived by the shooting method.

Chapter 4 adds the consequences of heat transfer to the model flow that was covered in Chapter 3. This chapter also includes the computation and discussion of the skin friction coefficient and Nusselt number numerical values. Graphs and tables are used to illustrate how various physical factors behave.

Chapter 5gives the thesis's concluding remarks.

Every reference consulted during the study project is included in **Bibliography**.

Chapter 2

Preliminaries

This chapter includes some basic definitions, notions, and concepts related to fluid dynamics. Particular attention has been paid to the terminology pertinent to the remainder of the thesis. The majority of these are from.

2.1 Foundational Concepts

2.1.1 Fluid

"A substance in the liquid or gas phase is referred to as a fluid. Distinction between a solid and a fluid is made on the basis of the substances ability to resist an applied shear (or tangential) stress that to change its shape. A solid can resist an applied shear stress by deforming, whereas a fluid deforms continuously under the influence of shear stress no matter how small." [17]

2.1.2 Fluid Mechanics

"Fluid mechanics is that branch of science which deals with the behavior of the fluid (liquids or gases) at rest as well as in motion. Thus this branch of science deals with the static kinematics and dynamics aspects of fluids." [18]

2.1.3 Fluid Dynamics

"Fluid dynamics is the branch of science that studies the behavior of fluids (liquids and gases) in motion, including the effects of pressure forces" [19]

2.1.4 Fluid statics

" The study of fluid at rest is called fluid statics." [19]

2.1.5 Viscosity

" Viscosity is defined as the property of a fluid which offers resistance to the movement of one layers of fluid over another adjacent layer of the fluid. When two layers of a fluid. Mathematically,

$$\Rightarrow \quad \mu = \frac{\tau}{\frac{\partial u}{\partial y}}, \tag{2.1}$$

where μ is viscosity coefficient, τ is shear stress, $\frac{\partial u}{\partial y}$ represents the velocity gradient." [19]

2.1.5 Kinematic Viscosity

"It is defined as the ratio between the dynamic viscosity and density of fluid. It is denoted by the symbol ν called **'nu'** . Mathematically,

$$\nu = \frac{\text{Viscosity}}{\text{Density}} = \frac{\mu}{\rho},$$

where the unit of kinematic viscosity is m^2/sec." [19]

2.1.6 Pressure

"The ratio of applied force to the unit area is said to be pressure. It is represented by P and mathematically, written as

$$P = \frac{F}{A},$$

where A and F denote the unit area and the applied force, respectively."[19]

2.1.7 Density

"The mass per unit volume of a material is known as its density. symbolically, it is denoted by ρ and mathematically, it is expressed as

$$\rho = \frac{m}{\nu},$$

where v and m are the volume and mass of the material, respectively."[19]

2.1.8 Magnetohydrodynamics

"Magnetohydrodynamics (MHD) is concerned with the flow of electrically conduct- ing fluids in the presence of magnetic fields, either externally applied or generated within the fluid by inductive action." [20]

2.1.9 Hydrodynamics

"The study of the motion of fluids that are practically incompressible such as liquids, especially water and gases at low speeds is usually referred to as hydrodynamics." [21]

2.2 Classification of Fluid

2.2.1 Ideal Fluid

"A fluid which is incompressible and has no viscosity, is known as an ideal fluid. Ideal fluid is only an imaginary fluid as all the fluids, which exist, have some viscosity." [19]

2.2.2 Real Fluid

"A fluid, which possesses viscosity, is known as a real fluid. In actual practice, all the fluids are real fluids." [19]

2.2.3 Newtonian Fluid

"A real fluid, in which shear stress is directly, proportional to the rate of shear strain (or velocity gradient), is known as a Newtonian fluid." [19]

2.2.4 Non-Newtonian Fluid

"A real fluid, in which the shear stress is not directly proportional to the rate of shear strain (or velocity gradient), is known as a Non-Newtonian fluid." [19]

2.2.5 Ideal plastic Fluid

"A fluid, in which shear stress is more than the yield value and shear stress is proportional to the rate of shear strain (or velocity gradient), is known as ideal plastic fluid." [19]

2.2.6 Micropolar Fluid

"Micro polar fluids are special non-Newtonian fluids with microscopic effects like micro rotational and rotational inertia. Eringen has put out the theory of micro polar fluids. Physical examples of micro polar fluids can be seen in ferrofluids, blood flows, bubbly liquids, liquid crystals, and so on, all of them containing intrinsic polarities."[1]

2.3 Modes of Heat Transfer

2.3.1 Conduction

"The conduction mode of heat transfer occurs either because of an exchange of energy

from one molecule to another, without the actual motion of the molecules, or because of the motion of the free electrons of they present. Therefore, this form of heat transport depends heavily on the properties of the medium and takes palce in solids, liquids and gases if a difference in temperature exists." [22]

Example: When you cook food using a metal pot on a stove, heat conduction plays a crucial role. The heat from the stove is transferred to the metal pot through conduction. The molecules in the metal gain energy and vibrate more rapidly as they absorb heat. This increased molecular motion is then passed on to the adjacent molecules in the pot. As a result, the entire pot becomes hot, and this heat is conducted to the food inside the pot. The process continues until the food reaches the desired temperature. In this way, conduction is responsible for distributing heat evenly and cooking the food throughout the pot.

2.3.2 Convection

"Molecules present in liquids and gases have freedom of motion, and by moving from hot to cold region, they carry energy with them. The transfer of heat from one region to another, due to such macroscopic motion in a liquid and gas, added to the energy by conduction within the fluid, is called heat transfer by convection." [22]

Example: When you boil water on the stove, you observe convection in action. As the water is heated at the bottom of the pot, the molecules near the heat source gain energy, become less dense, and rise. This creates a convection current where the hotter, lighter water rises to the top, and the cooler, denser water descends to replace it. This continuous cycle forms a convection current within the water.

2.3.3 Forced Convection

"When fluid motion is caused by external force, such as pumping or blowing, the state is defined as being one of forced convection." [22]

2.3.4 Mixed Convection

"A mixed convection state is one in which both natural and forced convection are present. convection haet transfer also occurs in boling and condenstion processes." [22]

2.3.5 Radiation

"Radiation is the energy transfer due to the release of photons or electromagnetic waves from a surface volume. Radiation does not require any medium to transfer heat. The energy produced by radiation is transformed by electromagnetic waves." [23]

Example: Sunlight is a common and vital example of radiation. The Sun emits electromagnetic waves, including visible light, infrared radiation, and ultraviolet radiation. These waves travel through the vacuum of space and reach the Earth. When sunlight reaches the Earth's surface, it warms the land, oceans, and atmosphere.

2.3.6 Boundary Layer

"Viscous effects a particularly important near the solid surfaces, where the strong inter-action of the molecules of the fluid with molecules of the solid causes the relative velocity between the fluid and the solid to become almost exactly zero for a stationary surface. Therefore, the fluid velocity in the region near the wall must reduce to zero.

This is called no slip condition. In that condition there is no relative motion between the fluid and the solid surface at their point of contact. It follows that the flow velocity varies with distance from the wall; f rom zero at the wall to its full value some distance away, so that significant velocity gradients are established close to the wall. In most cases this region is thin (compared to the typical body dimension), and it is called a bou ndary layer." [24]

2.4 Types of Flow

2.4.1 Rotational Flow

" Rotational flow is that type of flow in which the fluid particles while flowing along stream-lines, also rotate about their own axis." [19]

2.4.2 Irrotational Flow

" Irrotational flow is that type of flow in which the fluid particles while flowing along stream-lines, do not rotate about their own axis then this type of flow is called irrotational flow." [19]

2.4.3 Compressible Flow

" Compressible flow is that type of flow in which the density of the fluid changes from point to point in other words the density ρ is not constant for the the fluid. Thus, mathematically, for compressible flow

$$\rho \neq k,$$

where k is constant." [19]

2.4.4 Incompressible Flows

"Incompressible flow is that type of flow in which the density is constant for the fluid flow. Liquids are generally incompressible while gases are compressible. Mathematically, for incompressible flow

$$\rho = k,$$

where k is constant." [19]

2.4.5 Steady Flow

"If the flow characteristics such as depth of flow, velocity of flow, rate of flow at any point in open channel flow do not change with respect to time, the flow is said to be staedy flow. Mathematically,

$$\frac{\partial Q}{\partial t} = 0,$$

where Q is any fluid property." [19]

2.4.6 Unsteady Flow

"If any point in open channel flow, the velocity of flow, depth of flow or rate of flow chnages with respect to time, the flow is said to be unsteady. Mathematically,

$$\frac{\partial Q}{\partial t} \neq 0,$$

where Q is any fluid property." [19]

2.4.7 Internal Flow

" Flows completely bounded by a solid surfaces are called internal or duct flows." [23]

2.4.8 External Flow

" Flows over bodies immersed in an unbounded fluid are said to be an external flow." [23]

2.4.9 Laminar Flow

"A laminar flow is one in which path taken by the individual particles do not cross one another and move along well defined path. This type of flow is also called stream line flow or viscous flow, for example, blood in veins." [25]

2.4.10 Turbulent Flow

"A turbulent flow is that flow in which fluid particles move in a zig zag way, for example, high velocity flow in conduit of large size."[25]

2.5 Porous Material

2.5.1 Porous Material

"A solid containing holes or voids, either connected or non-connected, dispersed within it in either a regular or random manner known as porous material provided that holes occur relatively frequently within the solid. Pores are either interconnected or non-interconnected. A fluid can flow through a porous material only if at least some of the pores are interconnected. Some natural porous materials are beach sand, limestone, sandstone, wood, loaf of bread and human lung etc."[26]

2.5.2 Porosity

"The porosity of a porous material is the fraction of the bulk volume of the material occupied by voids. The symbol usually employed for this parameter is ϕ. Thus

$$\phi = \frac{V_P}{V_B} = \frac{\text{Volume of pores}}{\text{Bulk volume}}$$

Bulk volume , which is a dimensionless quantity. Since that portion of the bulk volume not occupied by pores is occupied by the solid grains or matrix of the material, it follows that

$$1 - \phi = \frac{V_S}{V_B} = \frac{\text{Volume of solids}}{\text{Bulk volume}}."[26]$$

2.5.3 Permeability

"Permeability is the property of a porous material which characterizes the ease with which a fluid may be made to ow through the material by an applied pressure gradient. Permeability is the fluid conductivity of the porous material. If horizontal linear ow of an incompressible fluid is established through a sample of porous material of length L in the direction of flow, and cross sectional area A,then the permeability K of the material is defined as

$$K = \frac{q\mu}{A\left(\frac{\delta P}{L}\right)}$$

Here q is the fluid flow rate in volume per unit time, μ is the viscosity of the fluid and δP is the applied pressure difference across the length of the specimen."[26]

2.6 Conservation Laws

2.6.1 Law of Conservation of Mass

"The principle of conservation of mass can be stated as the time rate of change of mass in a fixed volume is equal to the net rate of flow of mass across the surface".

$$\frac{\partial \rho}{\partial t} + \nabla . \left(\rho U\right) .[27] \tag{2.2}$$

2.6.2 Law of Conservation of Momentum

"The momentum equation states that the time rate of change of linear momentum of a given set of particles is equal to the vector sum of all the external forces acting on the particles of the set, provided Newton's Third Law of action and reaction governs the internal forces. Mathematically it can be written as".

$$\frac{\partial}{\partial t}\left(\rho U\right) + \nabla . \left[\left(\rho U\right) U\right] = \nabla . T + \rho g .[27] \tag{2.3}$$

2.6.3 Law of Conservation of Energy

"The law of conservation of energy (or the First Law of Thermodynamics) states that the time rate of change of the total energy is equal to the sum of the rate of work done by applied forces and the change of heat content per unit time. In the general case, the First Law of Thermodynamics can be expressed in conservation form as

$$\frac{\partial \rho}{\partial t} + \nabla . \rho u = -\nabla . q + Q + \phi, \tag{2.4}$$

Where ϕ is the dissipation function". [27]

2.4.4 Newton's Law of Viscosity

"It states that the shear stress (τ) on a fluid element layer is proportional to the rate of shear strain. The constant of proportionally is called coefficient of viscosity. Mathematically, it is expressed as

$$\tau = \mu \frac{\partial u}{\partial y} ."[19]$$

2.7 Dimensionless Parameters

2.7.1 Reynolds Number (R_e)

"It is the most significant dimensionless number which is used to identify the different flow behaviors like laminar or turbulent flow. Mathematically, it is expressed as

$$Re = \frac{LU}{\nu},$$

where U denotes the free stream velocity, L is the characteristic length and ν stands for kinematic viscosity." [28]

2.7.2 Skin Friction Coefficient (Cf_x)

"The skin friction coefficient is typically defined as

$$Cf = \frac{\tau_w}{\rho u_w^2},$$

where τ_w is the local wall shear stress, ρ is the fluid density and u_w is the free stream velocity (usually taken outside the boundary layer or at the inlet)." [28] **2.7.3 Nusselt number (Nu)**

"It is the relationship between the convective to the conductive heat transfer through the boundary of the surface. Mathematically, it is defined as

$$Nu = \frac{qL}{k},$$

where q stands for the convection heat transfer, L stands for characteristic length and k stands for thermal conductivity." [28]

2.8 Shooting Method

To elaborate the shooting method, take into account the subsequent nonlinear boundary value problem.

$$\left.\begin{aligned} &2f'''(x) + f(x)f''(x) = 0 \\ &f(0) = 0, f'(0) = 0 \quad f'(G) = 1. \end{aligned}\right\} \tag{2.5}$$

To reduce the order of the above boundary value problem, introduce the following notations.

$$f = S_1, \quad f' = S_1' = S_2, \quad f'' = S_2' = S_3, \quad f''' = S_3', \tag{2.6}$$

As a result, (2.5) converted into the system of first order ODEs is as follows:

$$S_1' = S_2, \qquad S_1(0) = 0. \tag{2.7}$$

$$S_2' = S_3, \qquad S_2(0) = 0. \tag{2.8}$$

$$S_3' = -\frac{1}{2} S_1 S_3, \qquad S_3(0) = w. \tag{2.9}$$

where w is the missing initial condition which will be guessed. The above IVP will be numerically solved by the RK-4 method. The missing condition w is to be chosen such that.

$$S_2\left(G, w\right) = 1. \tag{2.10}$$

For convenience, now onward, $S_2(G, w)$ will be denoted by $S_2(w)$.
Let us further denote $S_2(w) - 1$ by $H(w)$, so that

$$H(w) = 0. \tag{2.11}$$

The above equation can be solved by using Newton's method, which has the following iterative formula.

$$w^{(n+1)} = w^{(n)} - \frac{H(w^n)}{\frac{\partial H(w^n)}{\partial w}},$$

OR

$$w^{(n+1)} = w^{(n)} - \frac{S_2(w^n) - 1}{\frac{\partial S_2(w^n)}{\partial w}}. \tag{2.12}$$

To find $\left(\frac{\partial S_2(w^n)}{\partial w}\right)$, introduced the following notations:

$$\frac{\partial S_1}{\partial w} = S_4, \quad \frac{\partial S_2}{\partial w} = S_5, \quad \frac{\partial S_3}{\partial w} = S_6. \tag{2.13}$$

As a result of these new notations the Newton's iterative scheme, will then get the following form.

$$w^{(n+1)} = w^{(n)} - \frac{S_2\left(w^n\right) - 1}{S_5\left(w^n\right)}. \tag{2.14}$$

Now differentiating the system of two first order ODEs (2.7), (2.8) and (2.9) with respect to w, we get another system of ODEs, as follows.

$$S_4' = S_5, \qquad S_4(0) = 0. \tag{2.15}$$

$$S_5' = S_6, \qquad S_5(0) = 0. \tag{2.16}$$

$$S_6' = -\frac{1}{2}\Big[S_1 S_6 + S_3 Q_4\Big], \qquad S_6(0) = 1. \tag{2.17}$$

Writing all the four ODEs (2.7), (2.8), (2.9),(2.15), (2.16) and (2.17) together, following IVP is obtained.

$$\begin{aligned}
S_1' &= S_2, && S_1(0) = 0.\\
S_2' &= S_3, && S_2(0) = 0.\\
S_3' &= -\frac{1}{2} S_1 S_3, && S_3(0) = w.\\
S_4' &= S_5, && S_4(0) = 0.\\
S_5' &= S_6, && S_5(0) = 0.\\
S_6' &= -\frac{1}{2}\Big[S_1 S_6 + S_3 S_4\Big], && S_6(0) = 1.
\end{aligned}$$

The above system together will be solved numerically by Runge-Kutta method of order four. The missing condition will be updated by the Newton's formula in (2.14). The stopping criteria for the Newton's technique is set as,

$$|S_2(w) - 1| < \epsilon,$$

where $\epsilon > 0$ is an arbitrary small positive number.

Chapter 3

Numerical Analysis of Boundary Layer Flow of a Magneto-Micropolar Fluid

3.1 Introduction

This chapter presents a detailed investigation on the numerical analysis of boundary layer flow of a magneto-micropolar fluid. Through numerical simulations, we endeavor to unravel the intricate dynamics governing the boundary layer flow in such fluids, with a particular emphasis on elucidating the effects of magnetic field and micropolar properties. The relevant nonlinear PDEs are converted to a system of non-dimensional ODEs with the help of some appropriate transformations. For solving the ODEs, the shooting technique is applied with the help of MATLAB code. The numerical results of various parameters are elaborated at the end of this chapter for the dimensionless hydrodynamics velocity profile $f'(\zeta)$, macrorotational velocity profile $g'(\zeta)$ and magnetic induction profile $h'(\zeta)$.

3.2 Physical Model

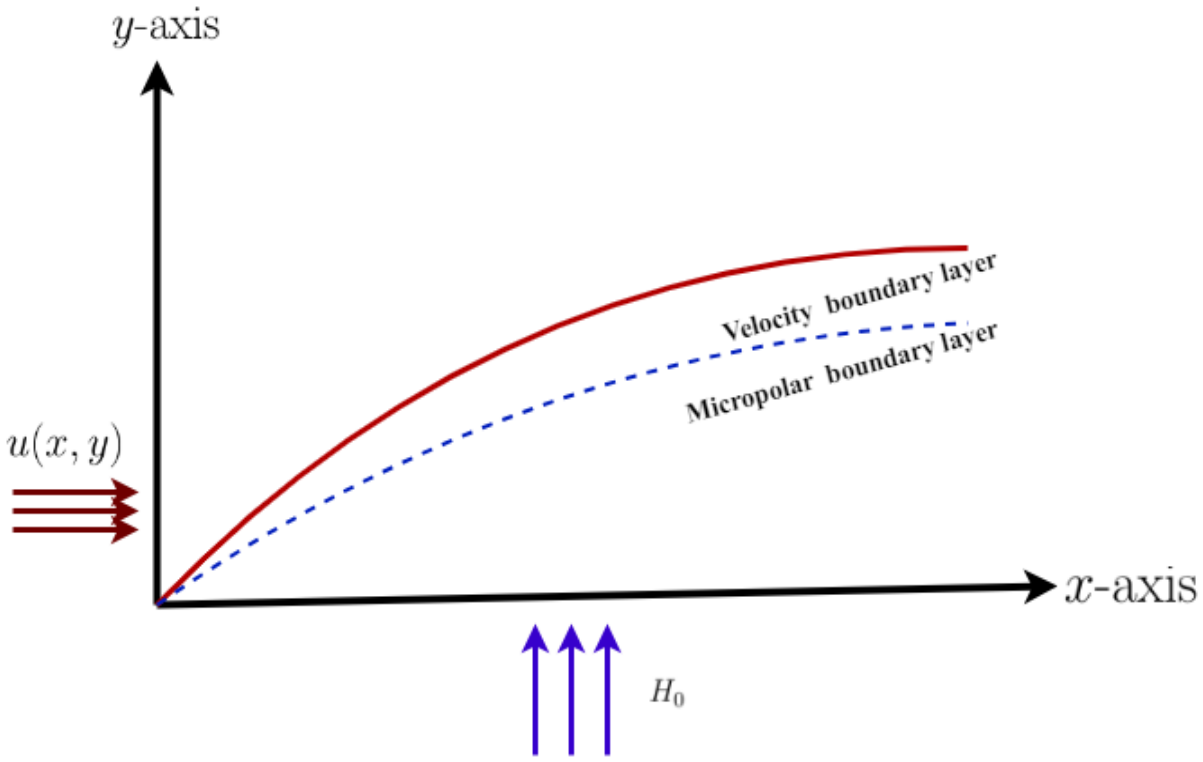

FIGURE 3.1: Flow configuration.

The vector form of the governing equation is as follows:

$$\boldsymbol{\nabla}.\mathbf{U} = 0, \tag{3.1}$$

$$\boldsymbol{\nabla}.\mathbf{H} = 0, \tag{3.2}$$

$$\rho\left(\frac{d\mathbf{U}}{dt} + \mathbf{U}.\boldsymbol{\nabla}\mathbf{U}\right) = -\boldsymbol{\nabla}(p) + \mu\boldsymbol{\nabla}^{\mathbf{2}}\mathbf{U} + 2\zeta_1\boldsymbol{\nabla}\times(\mathbf{W}-\mathbf{w}) + \mathbf{J}\times\mathbf{B}, \tag{3.3}$$

$$\rho\left(\frac{d\mathbf{H}}{dt} + \mathbf{U}.\boldsymbol{\nabla}\mathbf{H} - \mathbf{H}.\boldsymbol{\nabla}\mathbf{U}\right) = \mu_0\boldsymbol{\nabla}^{\mathbf{2}}\mathbf{H}, \tag{3.4}$$

$$l\left(\frac{d\mathbf{W}}{dt} + \mathbf{U}.\boldsymbol{\nabla}\mathbf{W}\right) = \gamma\boldsymbol{\nabla}^{\mathbf{2}}\mathbf{W} + 4\zeta_1(\mathbf{w}-\mathbf{W}), \tag{3.5}$$

$$\mathbf{B} = \mu_0\mathbf{H} + \mathbf{M}, \tag{3.6}$$

$$\mathbf{w} = \boldsymbol{\nabla}\times\frac{\mathbf{U}}{2}, \tag{3.7}$$

$$\mathbf{M} = \frac{M_0(\mathbf{I}-\tau\mathbf{W}.\epsilon).\mathbf{H}}{\bar{H}}, \tag{3.8}$$

$$\mathbf{J} = \sigma\Big(\mathbf{E} + \mathbf{U}\times\mathbf{B}\Big). \tag{3.9}$$

3.3 Governing Equations in the Operator-Form

In this section, we present the process of transforming the governing equations in the vector form to the operator form. Vector equations encapsulate the foundational principles governing a system in abstract mathematical terms, whereas the operator form offers a more concrete representation in terms of the physical variables and parameters.
In this model, we have discussed steady-state flow, where the fluid characteristics at a point do not change with time. Equations (3.3) and (3.5) are the conservation laws of linear and angular momentum, respectively. Equation (3.7) defines the vorticity **(w)**, which is a pseudovector field that describes the local spinning motion of a continuum near some point, as would be seen by an observer located at that point and traveling along with the flow. Scale analysis simplifies equations by determining the approximate magnitudes of their terms and ignoring negligibly small ones. Use of scale analysis, it has been assumed that the pressure p does not depend on the spatial coordinates. The relaxation time of magnetization τ being very small, has been ignored. Assume that no electric field $\mathbf{E}$ is applied on the flow [16]. No-slip boundary conditions are imposed for the linear velocity, in accordance with the assumptions used in [16] and the boundary layer approximations.

3.3.1 Continuity Equations

$$\boldsymbol{\nabla}.\mathbf{U} = 0$$

$$\Rightarrow \left(\frac{\partial}{\partial x}, \frac{\partial}{\partial y}, 0\right).(u, v, 0) = 0$$

$$\Rightarrow \frac{\partial u}{\partial x} + \frac{\partial v}{\partial y} = 0.$$

$$\boldsymbol{\nabla}.\mathbf{H} = 0$$

$$\Rightarrow \left(\frac{\partial}{\partial H_1}, \frac{\partial}{\partial H_2}, 0\right).(H_1, H_2, 0) = 0$$

$$\Rightarrow \frac{\partial H_1}{\partial x} + \frac{\partial H_2}{\partial y} = 0$$

3.3.2 Momentum Equation

For the momentum equation (3.3) the following operators are required:

$$\begin{aligned}
\mathbf{U}.\boldsymbol{\nabla}\mathbf{U} &= (u,v,0).\left(\frac{\partial}{\partial x},\frac{\partial}{\partial y},0\right)(u,v,0)\\
&= \left(u\frac{\partial}{\partial x}+v\frac{\partial}{\partial y}+0\right)(u,v,0)\\
&= u\frac{\partial}{\partial x}(u,v,0)+v\frac{\partial}{\partial y}(u,v,0)+0(u,v,0)\\
&= \left(u\frac{\partial u}{\partial x},u\frac{\partial v}{\partial x},0\right)+\left(v\frac{\partial u}{\partial y},v\frac{\partial v}{\partial y},0\right)+(0)\\
&= \left(u\frac{\partial u}{\partial x}+v\frac{\partial u}{\partial y},u\frac{\partial v}{\partial x}+v\frac{\partial v}{\partial y},0\right). \qquad (3.10)\\
\boldsymbol{\nabla}^{\mathbf{2}}\mathbf{U} &= \left(\frac{\partial}{\partial x},\frac{\partial}{\partial y},0\right).\left(\frac{\partial}{\partial x},\frac{\partial}{\partial y},0\right)(u,v,0)\\
&= \left(\frac{\partial^2}{\partial x^2}+\frac{\partial^2}{\partial y^2}+0\right)(u,v,0)\\
&= \left(\frac{\partial^2 u}{\partial x^2},\frac{\partial^2 v}{\partial x^2},0\right)+\left(\frac{\partial^2 u}{\partial y^2},\frac{\partial^2 v}{\partial y^2},0\right)+(0)\\
&= \left(\frac{\partial^2 u}{\partial x^2}+\frac{\partial^2 u}{\partial y^2},\frac{\partial^2 v}{\partial x^2}+\frac{\partial^2 v}{\partial y^2},0\right). \qquad (3.11)\\
2\zeta_1\boldsymbol{\nabla}\times(\mathbf{W}-\mathbf{w}) &= 2\zeta_1(\boldsymbol{\nabla}\times\mathbf{W})-2\zeta_1(\boldsymbol{\nabla}\times\mathbf{w})\\
&= 2\zeta_1(\boldsymbol{\nabla}\times\mathbf{W})-2\zeta_1\left(\boldsymbol{\nabla}\times\boldsymbol{\nabla}\times\frac{\mathbf{U}}{2}\right)\\
&= 2\zeta_1(\boldsymbol{\nabla}\times\mathbf{W})-\zeta_1\left(\boldsymbol{\nabla}\times(\boldsymbol{\nabla}\times\mathbf{U})\right) \qquad (3.12)
\end{aligned}$$

$$\begin{aligned}
\boldsymbol{\nabla}\times\mathbf{W} &= \begin{vmatrix}\hat{i} & \hat{j} & \hat{k}\\ \frac{\partial}{\partial x} & \frac{\partial}{\partial y} & 0\\ 0 & 0 & N\end{vmatrix}\\
&= \frac{\partial N}{\partial y}\hat{i}-\frac{\partial N}{\partial x}\hat{j}+(0)\hat{k}.\boldsymbol{\nabla}\times\mathbf{U} \qquad (3.13)\\
&= \begin{vmatrix}\hat{i} & \hat{j} & \hat{k}\\ \frac{\partial}{\partial x} & \frac{\partial}{\partial y} & 0\\ u & v & 0\end{vmatrix}\\
&= (0)\hat{i}-(0)\hat{j}+\left(\frac{\partial v}{\partial x}-\frac{\partial u}{\partial y}\right)\hat{k}.
\end{aligned}$$

$$\boldsymbol{\nabla}\times(\boldsymbol{\nabla}\times\mathbf{U}) = \begin{vmatrix} \hat{i} & \hat{j} & \hat{k} \\ \frac{\partial}{\partial x} & \frac{\partial}{\partial y} & 0 \\ 0 & 0 & \frac{\partial v}{\partial x} - \frac{\partial u}{\partial y} \end{vmatrix}$$
$$= \left(\frac{\partial^2 v}{\partial y \partial x} - \frac{\partial^2 u}{\partial y^2}\right)\hat{i} - \left(\frac{\partial^2 v}{\partial x^2} - \frac{\partial^2 u}{\partial x \partial y}\right)\hat{j}$$
$$+ (0)\hat{k} \tag{3.14}$$

Now using (3.13) and (3.14) in (3.12), we get

$$2\zeta_1\boldsymbol{\nabla}\times(\mathbf{W}-\mathbf{w}) = 2\zeta_1\left(\frac{\partial N}{\partial y}, -\frac{\partial N}{\partial x}, 0\right)$$

$$- \zeta_1\left(\frac{\partial^2 v}{\partial y \partial x} - \frac{\partial^2 u}{\partial y^2}, -\frac{\partial^2 v}{\partial x^2} - \frac{\partial^2 u}{\partial x \partial y}, 0\right). \tag{3.15}$$

$$\mathbf{J}\times\mathbf{B} = \sigma(\mathbf{E}+\mathbf{U}\times\mathbf{B})\times\mathbf{B}$$

$$= \sigma(\mathbf{U}\times\mathbf{B})\times\mathbf{B} \quad (\text{using} \quad (3.6)) \tag{3.16}$$

$$\mathbf{U}\times\mathbf{B} = \mu_0 \begin{vmatrix} \hat{i} & \hat{j} & \hat{k} \\ u & v & 0 \\ H_1 + M_0 & H_2 - \tau M_0 N & 0 \end{vmatrix}$$
$$= \mu_0((0)\hat{i} - (0)\hat{j} + (uH_2 - u\tau M_0 N - vH_1 - vM_0)\hat{k}).$$

$$(\mathbf{U}\times\mathbf{B})\times\mathbf{B} = \mu_0 \begin{vmatrix} \hat{i} & \hat{j} & \hat{k} \\ 0 & 0 & uH_2 - u\tau M_0 N - vH_1 - vM_0 \\ H_1 + M_0 & H_2 - \tau M_0 N & 0 \end{vmatrix}$$

$$= \mu_0((0 - uH_2^2 - uH_2\tau M_0 N - vH_1 H_2 - vM_0 H_2 + uH_2\tau M_0 N$$
$$+ u\tau^2 M_0^2 N^2 + vH_1\tau M_0 N + v\tau M_0^2 N)\hat{i} - (0 - uH_2 H_1 - uH_2\tau M_0 N$$
$$- vH_1^2 - vM_0 H_1 - uH_2 M_0 - u\tau M_0^2 N$$
$$- vH_1 M_0 - vM_0^2)\hat{j} + (0)\hat{k}) \tag{3.17}$$

Now using (3.17) in (3.16) we get

$$
\begin{aligned}
&=\sigma\mu_0(-uH_2^2 - vH_1H_2 - vM_0H_2 + u\tau^2M_0^2N^2 + vH_1\tau M_0N + v\tau M_0^2N),\\
&uH_2H_1 + uH_2\tau M_0N + vH_1^2 + vM_0H_1 + uH_2M_0 + u\tau M_0^2N\\
&+ vH_1M_0 + vM_0^2, 0)
\end{aligned}
\tag{3.18}
$$

All the expressions (3.10)-(3.18), have now been substituted into equation (3.3) to get the following:

$$
\begin{aligned}
&\rho\left(\frac{du}{dt}, \frac{dv}{dt}, 0\right) + \left(u\frac{\partial u}{\partial x} + v\frac{\partial u}{\partial y}, u\frac{\partial v}{\partial x} + v\frac{\partial v}{\partial y}, 0\right)\\
&= -\left(\frac{\partial p}{\partial x}, \frac{\partial p}{\partial y}, 0\right) + \mu\left(\frac{\partial^2 u}{\partial x^2} + \frac{\partial^2 u}{\partial y^2}, \frac{\partial v^2}{\partial x} + \frac{\partial^2 v}{\partial y}, 0\right) + 2\zeta_1\left(\frac{\partial N}{\partial y}, -\frac{\partial N}{\partial x}, 0\right)\\
&\quad - \zeta_1\left(\frac{\partial^2 v}{\partial y\partial x} - \frac{\partial^2 u}{\partial y^2}, -\frac{\partial^2 v}{\partial x^2} - \frac{\partial^2 u}{\partial x\partial y}, 0\right) + \sigma\mu_0(-uH_2^2 - vH_1H_2 - vM_0H_2\\
&\quad + u\tau^2M_0^2N^2 + vH_1\tau M_0N + v\tau M_0^2N, uH_2H_1 + uH_2\tau M_0N + vH_1^2 + vM_0H_1\\
&\quad + uH_2M_0 + u\tau M_0^2N + vH_1M_0 + vM_0^2, 0).
\end{aligned}
$$

$$
\begin{aligned}
\Rightarrow \quad \frac{du}{dt} + \left(u\frac{\partial u}{\partial x} + v\frac{\partial u}{\partial y} + 0\right) &= -\frac{1}{\rho}.\frac{\partial p}{\partial x} + \frac{\mu}{\rho}\left(\frac{\partial^2 u}{\partial x^2} + \frac{\partial^2 u}{\partial y^2}\right) + \frac{2\zeta_1}{\rho}\left(\frac{\partial N}{\partial y}\right)\\
&\quad - \frac{\zeta_1}{\rho}\left(\frac{\partial^2 v}{\partial y\partial x} - \frac{\partial^2 u}{\partial y^2}\right) + \frac{\sigma}{\rho}\mu_0(-uH_2^2).
\end{aligned}
$$

$$
\Rightarrow \quad u\frac{\partial u}{\partial x} + v\frac{\partial u}{\partial y} = \left(\frac{\mu + \zeta_1}{\rho}\right)\frac{\partial^2 u}{\partial y^2} - \frac{\sigma}{\rho}\mu_0 H_2^2 u + \frac{2\zeta_1}{\rho}\frac{\partial N}{\partial y}. \tag{3.19}
$$

3.3.3 Magnetic Induction Equation

For the magnetic induction equation (3.4) the following operators are required:

$$
\mathbf{U}.\boldsymbol{\nabla}\mathbf{H} = (u, v, 0).\left(\frac{\partial}{\partial x}, \frac{\partial}{\partial y}, 0\right)(H_1, H_2, 0)
$$

$$
= \left(u\frac{\partial}{\partial x} + v\frac{\partial}{\partial y} + 0\right)(H_1, H_2, 0)
$$

$$
\begin{aligned}
&= u\frac{\partial}{\partial x}(H_1, H_2, 0) + v\frac{\partial}{\partial y}(H_1, H_2, 0) + (0) \\
&= \left(u\frac{\partial H_1}{\partial x}, u\frac{\partial H_2}{\partial x}, 0\right) + \left(v\frac{\partial H_1}{\partial y}, v\frac{\partial H_2}{\partial y}, 0\right) + (0) \\
&= \left(u\frac{\partial H_1}{\partial x} + v\frac{\partial H_1}{\partial y}, u\frac{\partial H_2}{\partial x} + v\frac{\partial H_2}{\partial y}, 0\right). \qquad (3.20)
\end{aligned}
$$

$$
\begin{aligned}
\mathbf{H}.\boldsymbol{\nabla}\mathbf{U} &= (H_1, H_2, 0).\left(\frac{\partial}{\partial x}, \frac{\partial}{\partial y}, 0\right)(u, v, 0) \\
&= \left(H_1\frac{\partial}{\partial x} + H_2\frac{\partial}{\partial y} + 0\right)(u, v, 0) \\
&= H_1\frac{\partial}{\partial x}(u, v, 0) + H_2\frac{\partial}{\partial y}(u, v, 0) \\
&= \left(H_1\frac{\partial u}{\partial x}, H_1\frac{\partial v}{\partial x}\right) + \left(H_2\frac{\partial u}{\partial y}, H_2\frac{\partial v}{\partial y}\right) \\
&= \left(H_1\frac{\partial u}{\partial x} + H_2\frac{\partial u}{\partial y}, H_1\frac{\partial v}{\partial x} + H_2\frac{\partial v}{\partial y}, 0\right). \qquad (3.21)
\end{aligned}
$$

$$
\begin{aligned}
\boldsymbol{\nabla}^{\mathbf{2}}\mathbf{H} &= \left(\frac{\partial}{\partial x}, \frac{\partial}{\partial y}, 0\right).\left(\frac{\partial}{\partial x}, \frac{\partial}{\partial y}, 0\right)(H_1, H_2, 0) \\
&= \left(\frac{\partial^2}{\partial x^2} + \frac{\partial^2}{\partial y^2} + 0\right)(H_1, H_2, 0) \\
&= \left(\frac{\partial^2 H_1}{\partial x^2}, \frac{\partial^2 H_2}{\partial x^2}, 0\right) + \left(\frac{\partial^2 H_1}{\partial y^2}, \frac{\partial^2 H_2}{\partial y^2}, 0\right) + (0) \\
&= \left(\frac{\partial^2 H_1}{\partial x^2} + \frac{\partial^2 H_1}{\partial y^2}, \frac{\partial^2 H_2}{\partial x^2} + \frac{\partial^2 H_2}{\partial y^2}, 0\right). \qquad (3.22)
\end{aligned}
$$

Now, we put all expressions (3.20)-(3.22) in equation (3.4) to get the following:

$$
\rho\left(\frac{dH_1}{dt}, \frac{dH_2}{dt}, 0\right) + \left(u\frac{\partial H_1}{\partial x} + v\frac{\partial H_1}{\partial y}, u\frac{\partial H_2}{\partial x} + v\frac{\partial H_2}{\partial y}, 0\right)
$$

$$
-\left(H_1\frac{\partial u}{\partial x} + H_2\frac{\partial u}{\partial y}, H_1\frac{\partial v}{\partial x} + H_2\frac{\partial v}{\partial y}, 0\right) = \mu_0\left(\frac{\partial^2 H_1}{\partial x^2} + \frac{\partial^2 H_1}{\partial y^2}, \frac{\partial^2 H_2}{\partial x^2} + \frac{\partial^2 H_2}{\partial y^2}, 0\right).
$$

$$
\Rightarrow \qquad \frac{dH_1}{dt} + \left(u\frac{\partial H_1}{\partial x} + v\frac{\partial H_1}{\partial y}\right) - \left(H_1\frac{\partial u}{\partial x} + H_2\frac{\partial u}{\partial y}\right) = \frac{\mu_0}{\rho}\left(\frac{\partial^2 H_1}{\partial x^2} + \frac{\partial^2 H_1}{\partial y^2} + 0\right).
$$

$$
\Rightarrow \quad u\frac{\partial H_1}{\partial x} + v\frac{\partial H_1}{\partial y} = H_1\frac{\partial u}{\partial x} + H_2\frac{\partial u}{\partial y} + \nu_0\frac{\partial^2 H_1}{\partial y^2}. \qquad (3.23)
$$

3.3.4 Microrotation Equation

For the microrotation equation (3.5) the following operators are required:

$$\begin{aligned}
\mathbf{U}.\boldsymbol{\nabla}\mathbf{W} &= (u,v,0).\left(\frac{\partial}{\partial x},\frac{\partial}{\partial y},0\right)(0,0,N)\\
&= \left(u\frac{\partial}{\partial x}+v\frac{\partial}{\partial y}+0\right)(0,0,N)\\
&= u\frac{\partial}{\partial x}(0,0,N)+v\frac{\partial}{\partial y}(0,0,N)+0(0,0,N)\\
&= \left(u\frac{\partial(0)}{\partial x},u\frac{\partial(0)}{\partial x},u\frac{\partial N}{\partial x}\right)+\left(v\frac{\partial(0)}{\partial y},v\frac{\partial(0)}{\partial y},v\frac{\partial N}{\partial y}\right)+(0)\\
&= \left(0,0,u\frac{\partial N}{\partial x}\right)+\left(0,0,v\frac{\partial N}{\partial y}\right)+(0)\\
&= \left(0,0,u\frac{\partial N}{\partial x}+v\frac{\partial N}{\partial y}\right) \qquad (3.24)\\
\gamma\boldsymbol{\nabla}^{\mathbf{2}}\mathbf{W} &= \gamma\left(\frac{\partial}{\partial x},\frac{\partial}{\partial y},0\right).\left(\frac{\partial}{\partial x},\frac{\partial}{\partial y},0\right)(0,0,N)\\
&= \gamma\left(\frac{\partial^2}{\partial x^2}+\frac{\partial^2}{\partial y^2}+0\right)(0,0,N)\\
&= \gamma\left(\frac{\partial^2(0)}{\partial x^2},\frac{\partial^2(0)}{\partial x^2},\frac{\partial^2 N}{\partial x^2}+\frac{\partial^2(0)}{\partial y^2},\frac{\partial^2(0)}{\partial y^2},\frac{\partial^2 N}{\partial y^2}+(0)\right)\\
&= \gamma\left(0,0,\frac{\partial^2 N}{\partial x^2}+0,0,\frac{\partial^2 N}{\partial y^2}+(0)\right)\\
&= \gamma\left(0,0,\frac{\partial^2 N}{\partial x^2}+\frac{\partial^2 N}{\partial y^2}\right). \qquad (3.25)
\end{aligned}$$

$$\begin{aligned}
4\zeta_1(\mathbf{w}-\mathbf{W}) &= 4\zeta_1\mathbf{w}-4\zeta_1\mathbf{W}\\
&= 4\zeta_1\left(\boldsymbol{\nabla}\times\frac{\mathbf{U}}{2}\right)-4\zeta_1\mathbf{W} \quad \text{(using (3.7))}\\
&= 2\zeta_1(\boldsymbol{\nabla}\times\mathbf{U}-2\mathbf{W}) \qquad (3.26)
\end{aligned}$$

$$\begin{aligned}
\boldsymbol{\nabla}\times\mathbf{U} &= \begin{vmatrix} \hat{i} & \hat{j} & \hat{k}\\ \frac{\partial}{\partial x} & \frac{\partial}{\partial y} & 0\\ u & v & 0 \end{vmatrix}\\
&= (0)\hat{i}-(0)\hat{j}+\left(\frac{\partial v}{\partial x}-\frac{\partial u}{\partial y}\right)\hat{k}. \qquad (3.27)
\end{aligned}$$

Now using (3.27) in (3.26), we get

$$\begin{aligned}
&= 2\zeta_1\left(0,0,\frac{\partial v}{\partial x}-\frac{\partial u}{\partial y}\right)-4\zeta_1(0,0,N)\\
&= 2\zeta_1\left(0,0,\frac{\partial v}{\partial x}-\frac{\partial u}{\partial y}-2(0,0,N)\right)\\
&= 2\zeta_1\left(0,0,\frac{\partial v}{\partial x}-\frac{\partial u}{\partial y}-(0,0,2N)\right).
\end{aligned} \tag{3.28}$$

Now, we substitute the all expressions (3.24)-(3.28) into (3.5), to get:

$$\begin{aligned}
l\left(0,0,\frac{dN}{dt}+0,0,u\frac{\partial N}{\partial x}+v\frac{\partial N}{\partial y}\right) &= \gamma\left(0,0,\frac{\partial^2 N}{\partial x^2}+\frac{\partial^2 N}{\partial y^2}\right)\\
&\quad +2\zeta_1\left(0,0,\frac{\partial v}{\partial x}-\frac{\partial u}{\partial y}-0,0,2N\right).\\
\Rightarrow\quad \left(u\frac{\partial N}{\partial x}+v\frac{\partial N}{\partial y}\right) &= \frac{\gamma}{l}\left(\frac{\partial^2 N}{\partial x^2}+\frac{\partial^2 N}{\partial y^2}\right)+\frac{2\zeta_1}{l}\left(\frac{\partial v}{\partial x}-\frac{\partial u}{\partial y}-2N\right).\\
\Rightarrow\quad u\frac{\partial N}{\partial x}+v\frac{\partial N}{\partial y} &= \frac{\gamma}{l}\frac{\partial^2 N}{\partial y^2}-\frac{2\zeta_1}{l}\left(2N+\frac{\partial u}{\partial y}\right).
\end{aligned} \tag{3.29}$$

The final form of the governing equations:

$$\frac{\partial u}{\partial x}+\frac{\partial v}{\partial y}=0, \tag{3.30}$$

$$\frac{\partial H_1}{\partial x}+\frac{\partial H_2}{\partial y}=0, \tag{3.31}$$

$$u\frac{\partial u}{\partial x}+v\frac{\partial u}{\partial y}=\left(\frac{\mu+\zeta_1}{\rho}\right)\frac{\partial^2 u}{\partial y^2}-\frac{\sigma}{\rho}\mu_0 H_2^2 u+\frac{2\zeta_1}{\rho}\frac{\partial N}{\partial y}, \tag{3.32}$$

$$u\frac{\partial H_1}{\partial x}+v\frac{\partial H_1}{\partial y}=H_1\frac{\partial u}{\partial x}+H_2\frac{\partial u}{\partial y}+\nu_0\frac{\partial^2 H_1}{\partial y^2}, \tag{3.33}$$

$$u\frac{\partial N}{\partial x}+v\frac{\partial N}{\partial y}=\frac{\gamma*}{\rho j}\frac{\partial^2 N}{\partial y^2}-\frac{2\zeta_1}{\rho j}\left(2N+\frac{\partial u}{\partial y}\right). \tag{3.34}$$

Boundary conditions:

$$\left.\begin{aligned}
&u=cx,\quad v=0,\quad \frac{\partial H_1}{\partial y}=H_2=0,\quad N=-N_0\frac{\partial u}{\partial y}\quad at\quad y=0,\\
&u=ax,\quad H_1=H_e(x)=H_0x,\quad N\longrightarrow 0,\ as\ \ y\longrightarrow\infty.
\end{aligned}\right\} \tag{3.35}$$

3.4 Non-dimensionalization

In this section, we present the process of non-dimensionalization of the mathematical model governing the behavior of the proposed micropolar boundary layer flow. The procedure requires introducing the dimensionless variables and parameters to transform the original equations into a normalized form. By using the dimensionless quantities, we gain a deeper insight into the physical phenomena and make the analysis more tractable. The mathematical model will be transformed into a system of ODEs using the following similarity transformation:

$$\left.\begin{aligned} u &= cxf'(\zeta),\ v = \sqrt{\nu}cf(\zeta), \quad \zeta = \sqrt{\frac{c}{\nu}}y, \\ N &= cx\sqrt{\frac{c}{\nu}}g(\zeta), \quad H_1 = H_0xh'(\zeta), \quad H_2 = -H_0\sqrt{\frac{\nu}{c}}h(\zeta). \end{aligned}\right\} \tag{3.36}$$

Different parameters arising in (3.30)-(3.34) are dimensionless with the following formulation:

$$K = \frac{\zeta_1}{\mu}, \quad \frac{R_m}{R_e} = \frac{\sigma H_0^2\nu}{\rho c^2}, \quad R_m = \sigma\mu_0 v_0 L, \quad R_e = \frac{v_0 L}{\nu}, \quad d = \frac{H_0^2}{c^2 l},$$
$$\lambda = \frac{\nu_0}{\nu}, \quad \gamma^* = \left(\mu + \frac{\zeta_1}{2}\right)j, \quad \frac{\beta}{\alpha} = \frac{\tau M_0\bar{H}}{c}, \quad \beta = \frac{\tau M_0 H_0^2}{\rho\bar{H}c}, \quad \beta^* = \frac{2\zeta_1}{\rho j c}.$$

The following derivatives are required to satisfy the continuity equation (3.28):

$$\begin{aligned} \frac{\partial u}{\partial x} &= \frac{\partial}{\partial x}\left(cxf'(\zeta)\right) \\ &= cf'(\zeta)\frac{\partial}{\partial x}(x) \\ &= cf'(\zeta). \end{aligned} \tag{3.37}$$

$$\begin{aligned} \frac{\partial v}{\partial y} &= \frac{\partial}{\partial y}(-\sqrt{\nu c}f(\zeta)) \\ &= -\sqrt{\nu c}f'(\zeta)\frac{\partial}{\partial y}(\zeta) \\ &= -\sqrt{\nu c}f'(\zeta)\sqrt{\frac{c}{\nu}} \\ &= -cf'(\zeta) \end{aligned} \tag{3.38}$$

Using Equations (3.37) and (3.38) in (3.30), we obtain

$$cf'(\zeta) - cf'(\zeta) = 0.$$

Hence, Equation (3.30) is identically satisfied.

Now for Equation (3.31), the following derivaties are needed:

$$\begin{aligned}\frac{\partial H_1}{\partial x} &= \frac{\partial}{\partial x} H_0 x h'(\zeta) \\ &= H_0 h'(\zeta) \frac{\partial}{\partial x}(x) \\ &= H_0 h'(\zeta). \end{aligned} \tag{3.39}$$

$$\begin{aligned}\frac{\partial H_2}{\partial y} &= \frac{\partial}{\partial y}\left(- H_0 \sqrt{\frac{\nu}{c}} h(\zeta)\right) \\ &= -H_0 \sqrt{\frac{\nu}{c}} h'(\zeta) \frac{\partial}{\partial y}(\zeta) \\ &= -H_0 \sqrt{\frac{\nu}{c}} h'(\zeta) \sqrt{\frac{c}{\nu}} \\ &= -H_0 h'(\zeta). \end{aligned} \tag{3.40}$$

Using Equations (3.39) and (3.40) in (3.31), we obtain:

$$H_0 h'(\zeta) - H_0 h'(\zeta) = 0.$$

Hence, Equation (3.31) is identically satisfied.

3.4.1 Non-Dimensionalization of Momentum Equation

For the momentum equation (3.32), the following derivatives are needed:

$$\begin{aligned}\frac{\partial u}{\partial x} &= \frac{\partial}{\partial x}\left(c x f'(\zeta)\right) \\ &= c f'(\zeta) \frac{\partial}{\partial x}(x) \\ &= c f'(\zeta). \end{aligned} \tag{3.41}$$

$$\begin{aligned}
\frac{\partial u}{\partial y} &= \frac{\partial}{\partial y}\left(cxf'(\zeta)\right) \\
&= cxf''(\zeta)\frac{\partial}{\partial y}(\zeta) \qquad \text{(using (3.36))} \\
&= cxf''(\zeta)\sqrt{\frac{c}{\nu}}. \qquad (3.42)
\end{aligned}$$

$$\begin{aligned}
\Rightarrow \quad \frac{\partial^2 u}{\partial y^2} &= \frac{\partial}{\partial y}\left(cxf''(\zeta)\sqrt{\frac{c}{\nu}}\right) \\
&= cxf'''(\zeta)\sqrt{\frac{c}{\nu}}\frac{\partial}{\partial y}(\zeta) \\
&= c^2xf'''(\zeta).\frac{1}{\nu}. \qquad (3.43)
\end{aligned}$$

$$\begin{aligned}
\frac{\partial N}{\partial y} &= \frac{\partial}{\partial y}\left(cx\sqrt{\frac{c}{\nu}}g(\zeta)\right) \\
&= cx\sqrt{\frac{c}{\nu}}g'(\zeta)\frac{\partial}{\partial y}(\zeta) \\
&= cx\sqrt{\frac{c}{\nu}}g'(\zeta)\sqrt{\frac{c}{\nu}} \\
&= c^2xg'(\zeta)\frac{1}{\nu}. \qquad (3.44)
\end{aligned}$$

Now, we substitute all the partial derivatives (3.41)- (3.44) and the velocity components u and v from (3.36) into Equation (3.32) to get the following:

$$\begin{aligned}
&(cxf'(\zeta))(cf'(\zeta)) + (-\sqrt{\nu c}f(\zeta))\left(cxf''(\zeta)\sqrt{\frac{c}{\nu}}\right) \\
&= \left(\frac{\mu+\zeta_1}{\rho}\right)c^2xf'''(\zeta).\frac{1}{\nu} - \frac{\sigma}{\rho}\mu_0\left(H_0^2\left(\sqrt{\frac{\nu}{c}}\right)^2 h^2(\zeta)\right)(cxf'(\zeta)) \\
&\quad + \frac{2\zeta_1}{\rho}c^2xg'(\zeta).\frac{1}{\nu}.
\end{aligned}$$

$$\begin{aligned}
\Rightarrow \quad c^2x\big(f'(\zeta)\big)^2 - c^2xf(\zeta)f''(\zeta) &= \left(\frac{\mu}{\rho}+\frac{\zeta_1}{\rho}\right)c^2xf'''(\zeta).\frac{1}{\nu} \\
&\quad - \frac{\sigma}{\rho}\mu_0H_0^2.\frac{\nu}{c}h^2(\zeta)cxf'(\zeta) + \frac{2\zeta_1}{\rho}c^2xg'(\zeta).\frac{1}{\nu}.
\end{aligned}$$

$$\begin{aligned}
\Rightarrow \quad c^2x(f'(\zeta)^2 - f(\zeta)f''(\zeta)) &= \left(\frac{\mu}{\rho}+\frac{\zeta_1}{\rho}\right)c^2xf'''(\zeta).\frac{\rho}{\mu} - \frac{\sigma}{\rho}\mu_0H_0^2.\frac{\nu}{c}h^2(\zeta)cxf'(\zeta) \\
&\quad + \frac{2\zeta_1}{\rho}c^2xg'(\zeta).\frac{\rho}{\mu}.
\end{aligned}$$

$$\Rightarrow \quad f'(\zeta)^2 - f(\zeta)f''(\zeta) = \frac{\mu}{\rho}f'''(\zeta).\frac{\rho}{\mu} + \frac{\zeta_1}{\rho}f'''(\zeta).\frac{\rho}{\mu} - \frac{\sigma\mu_0H_0^2\nu}{\rho c^2}h^2f'(\zeta) + \frac{2\zeta_1}{\mu}g'(\zeta).$$

$$\Rightarrow \quad f'(\zeta)^2 - f(\zeta)f''(\zeta) = f'''(\zeta)\left(1+\frac{\zeta_1}{\mu}\right) - \frac{R_m}{R_e}h^2 f'(\zeta) + 2Kg'(\zeta).$$

$$\Rightarrow \quad f'(\zeta)^2 - f(\zeta)f''(\zeta) = (1+K)f'''(\zeta) - \frac{R_m}{R_e}h^2 f'(\zeta) + 2Kg'(\zeta).$$

$$\Rightarrow \qquad (1+K)\,f''' - \left(\frac{R_m}{R_e}\right)h^2 f' + 2Kg' - f'^2 + ff'' = 0. \tag{3.45}$$

3.4.2 Non-Dimensionalization of the Magnetic Induction Equation

For the non-dimensionalization of Equation (3.33), the following derivatives are required:

$$\begin{aligned}
\frac{\partial H1}{\partial x} &= \frac{\partial}{\partial x}(H_0 x h'(\zeta)) \\
&= H_0 h'(\zeta)\frac{\partial}{\partial x}(x) \\
&= H_0 h'(\zeta). \qquad (3.46) \\
\frac{\partial H1}{\partial y} &= \frac{\partial}{\partial y}(H_0 x h'(\zeta)) \\
&= H_0 x h''(\zeta)\frac{\partial}{\partial y}(\zeta) \\
&= H_0 x h''(\zeta)\sqrt{\frac{c}{\nu}}. \qquad (3.47) \\
\Rightarrow \quad \frac{\partial^2 H1}{\partial y^2} &= \frac{\partial}{\partial y}\left(H_0 x h''(\zeta)\sqrt{\frac{c}{\nu}}\right) \\
&= H_0 x h'''(\zeta)\sqrt{\frac{c}{\nu}}\frac{\partial}{\partial y}(\zeta) \\
&= H_0 x h'''(\zeta)\sqrt{\frac{c}{\nu}}.\sqrt{\frac{c}{\nu}} \\
&= cH_0 x h'''(\zeta)\frac{1}{\nu}. \qquad (3.48)
\end{aligned}$$

Now, we substitute the partial derivatives (3.41), (3.42), (3.46), (3.47) and (3.48) and the velocity components u and v from (3.36) into the equation (3.33), to get:

$$cxf'(\zeta))(H_0 h'(\zeta)) + -\sqrt{\nu c}f(\zeta)\left(H_0 x h''(\zeta)\sqrt{\frac{c}{\nu}}\right)$$

$$= H_0 x h'(\zeta)(cf'(\zeta)) + (-H_0\sqrt{\frac{\nu}{c}}h(\zeta))\left(cxf''(\zeta)\sqrt{\frac{c}{\nu}}\right) + \nu_0 c H_0 x h'''(\zeta).\frac{1}{\nu}.$$

$$\Rightarrow \quad cH_0xf'h' - cH_0xfh'' = cH_0xh'f' - cH_0xf''h + \nu_0 cH_0xh'''.\frac{1}{\nu}.$$

$$\Rightarrow \quad f'h' - fh'' = h'f' - f''h + \frac{\nu_0}{\nu}h'''.$$

$$\Rightarrow \quad h'f' - f''h - f'h' + fh'' + \frac{\nu_0}{\nu}h''' = 0.$$

$$\Rightarrow \quad \frac{\nu_0}{\nu}h''' - f''h(\zeta) + fh'' = 0.$$

$$\Rightarrow \quad \lambda h''' - f''h + fh'' = 0. \tag{3.49}$$

3.4.3 Non-Dimensionalization of Microrotation Equation

In this subsection, we discuss the non-dimensionalization process of the microrotation equation (3.33). For this purpose, the following derivaties are required:

$$\begin{aligned}\frac{\partial N}{\partial x} &= \frac{\partial}{\partial x}\left(cx\sqrt{\frac{c}{\nu}}g(\zeta)\right)\\ &= c\sqrt{\frac{c}{\nu}}g(\zeta).\frac{\partial}{\partial x}x\\ &= c\sqrt{\frac{c}{\nu}}g(\zeta).\end{aligned} \tag{3.50}$$

$$\begin{aligned}\frac{\partial N}{\partial y} &= \frac{\partial}{\partial y}\left(cx\sqrt{\frac{c}{\nu}}g(\zeta)\right)\\ &= cx\sqrt{\frac{c}{\nu}}g'(\zeta)\frac{\partial}{\partial y}(\zeta)\\ &= cx\sqrt{\frac{c}{\nu}}g'(\zeta)\sqrt{\frac{c}{\nu}}.\end{aligned} \tag{3.51}$$

$$\begin{aligned}\Rightarrow \quad \frac{\partial^2 N}{\partial y^2} &= \frac{\partial}{\partial y}(c^2xg'(\zeta)).\frac{1}{\nu}\\ &= c^2xg''(\zeta).\frac{1}{\nu}\frac{\partial}{\partial y}(\zeta)\\ &= c^2xg''(\zeta)\frac{1}{\nu}\sqrt{\frac{c}{\nu}}.\end{aligned} \tag{3.52}$$

Now, we substitute the partial derivatives (3.50)- (3.51) into (3.34), to get:

$$\begin{aligned}&(cxf'(\zeta))\left(c\sqrt{\frac{c}{\nu}}g(\zeta)\right) + (-\sqrt{\nu c}f(\zeta)\left(cx\left(\sqrt{\frac{c}{\nu}}\right)g'(\zeta)\sqrt{\frac{c}{\nu}}\right)\\ &= \frac{\gamma*}{\rho j}\left(c^2xg''(\zeta)\sqrt{\frac{c}{\nu}}\right).\frac{1}{\nu} - \frac{2\zeta_1}{\rho j}\left(2cx\sqrt{\frac{c}{\nu}}g(\zeta) + cxf''(\zeta)\sqrt{\frac{c}{\nu}}\right).\end{aligned}$$

$$\Rightarrow \quad \left(c^2xf'(\zeta)\left(\sqrt{\frac{c}{\nu}}\right)g(\zeta)\right)-\left(c^2xf(\zeta)\sqrt{\frac{c}{\nu}}g'(\zeta)\right)$$
$$=\frac{(\mu+\frac{\zeta_1}{2}).j}{\rho j}c^2xg''(\zeta)\sqrt{\frac{c}{\nu}}.\frac{1}{\nu}-\frac{2\zeta_1}{\rho j}\left(2cx\sqrt{\frac{c}{\nu}}g(\zeta)+cxf''(\zeta)\sqrt{\frac{c}{\nu}}\right).$$

$$\Rightarrow \quad c^2x\sqrt{\frac{c}{\nu}}\left(f'g-fg'\right)=\frac{(\mu+\frac{\zeta_1}{2})}{\rho}c^2xg''\left(\sqrt{\frac{c}{\nu}}\right).\frac{1}{\nu}$$
$$-\frac{2\zeta_1}{\rho j}cx\sqrt{\frac{c}{\nu}}\left(2g+f''\right).$$

$$\Rightarrow \quad f'(\zeta)g(\zeta)-(f(\zeta)g'(\zeta)=\frac{\mu(1+\frac{\zeta_1}{2\mu})}{\rho}g''(\zeta).\frac{1}{\nu}-\frac{2\zeta_1}{\rho jc}(2g(\zeta)+f''(\zeta)).$$

$$\Rightarrow \quad f'(\zeta)g(\zeta)-(f(\zeta)g'(\zeta)=\frac{\mu(1+\frac{\zeta_1}{2\mu})}{\rho}g''(\zeta).\frac{\rho}{\mu}-\frac{2\zeta_1}{\rho jc}(2g(\zeta)+f''(\zeta)).$$

$$\Rightarrow \quad f'g-fg'=\left(1+\frac{\zeta_1}{2\mu}\right)g''-\beta^*(2g+f'').$$

$$\Rightarrow \quad \left(1+\frac{K}{2}\right)g''-\beta^*(2g+f'')-f'g(\zeta)+fg'=0.$$

$$\Rightarrow \quad \left(1+\frac{K}{2}\right)g''-\beta^*(2g+f'')-f'g+fg'=0. \tag{3.53}$$

3.4.4 Non-Dimensionalization of Boundary Conditions

The BCs (3.35) are transformed into the non-dimensional form through the following procedure:

- $u=cx, \qquad at \quad y=0.$

$$\Rightarrow \quad cxf'(\zeta)=cx, \qquad at \quad \zeta=0.$$

$$\Rightarrow \quad f'(\zeta)=1, \qquad at \quad \zeta=0.$$

- $v=0, \qquad at \quad y=0.$

$$\Rightarrow \quad -\sqrt{\nu}cf(\zeta)=0, \qquad at \quad \zeta=0.$$

$$\Rightarrow \quad f(\zeta)=0, \qquad at \quad \zeta=0.$$

- $\frac{\partial H_1}{\partial y}=H_2=0, \qquad at \quad y=0.$

$$\Rightarrow \qquad H_0 x h''(\zeta)\left(\sqrt{\frac{c}{\nu}}\right) = -H_0\sqrt{\frac{\nu}{c}}h(\zeta), \qquad at \quad \zeta = 0.$$

$$\Rightarrow \qquad H_0 x\left(\sqrt{\frac{c}{\nu}}\right)h''(\zeta) = h(\zeta), \qquad at \quad \zeta = 0.$$

$$\Rightarrow \quad h''(\zeta) = h(\zeta), \qquad at \quad \zeta = 0.$$

$$\Rightarrow \quad N = -N_0\frac{\partial u}{\partial y}, \qquad at \quad y = 0.$$

$$\Rightarrow \qquad cx\left(\sqrt{\frac{c}{\nu}}\right)g(\zeta) = -N_0\left(cxf''(\eta)\right)\sqrt{\frac{c}{\nu}}, \qquad at \quad \zeta = 0.$$

$$\Rightarrow \quad cx\left(\sqrt{\frac{c}{\nu}}\right)g(\zeta) = -\left(cx\sqrt{\frac{c}{\nu}}\right)N_0 f''(\eta), \qquad at \quad \zeta = 0.$$

$$\Rightarrow \qquad g(\zeta) = -N_0 f''(\zeta) \qquad , \qquad at \quad \zeta = 0.$$

- $u = ax \qquad as \quad y \longrightarrow \infty.$

$$\Rightarrow \qquad cxf'(\zeta) = ax, \qquad as \quad \zeta \longrightarrow \infty.$$

$$\Rightarrow \quad f'(\zeta) = \frac{a}{c}, \qquad as \quad \zeta \longrightarrow \infty.$$

- $H_1 = H_0 x, \qquad as \quad y \longrightarrow \infty.$

$$\Rightarrow \quad H_0 x h'(\zeta) = H_0 x, \qquad as \quad \zeta \longrightarrow \infty.$$

$$\Rightarrow \quad h'(\zeta) = 1, \qquad as \quad \zeta \longrightarrow \infty.$$

- $N \longrightarrow 0, \qquad as \quad \tilde{y} \longrightarrow \infty.$

$$\Rightarrow \qquad cx\sqrt{\frac{c}{\nu}}g(\zeta) \longrightarrow 0, \qquad as \quad \zeta \longrightarrow \infty.$$

$$\Rightarrow \quad g(\zeta) \longrightarrow 0, \qquad as \quad \zeta \longrightarrow \infty.$$

3.4.5 Non-dimensionalization of the skin-friction

This sub-section focuses on the non-dimesionalization of important parameter skin friction coefficient.

$$C_f = \frac{\tau_w}{\rho u_w^2}, \qquad \left(\tau_w = (\mu + \zeta_1)\frac{\partial u}{\partial y} + \zeta_1 N\right)$$

$$C_f = \frac{(\mu+\zeta_1)cxf''(\zeta)\sqrt{\frac{c}{\nu}} + \zeta_1\left(cx\sqrt{\frac{c}{\nu}}g(\zeta)\right)}{\rho u_w^2}$$

$$= cx\sqrt{\frac{c}{\nu}}\frac{(\mu+\zeta_1)f'(\zeta)+\zeta_1 g(\zeta)}{\rho u_w^2}$$

$$= u_w\sqrt{\frac{c}{\nu}}\frac{(\mu+\zeta_1)f''(\zeta)+\zeta_1 g(\zeta)}{\rho u_w^2}$$

$$= \sqrt{\frac{c}{\nu}}\frac{(\mu+\zeta_1)f''(\zeta)+\zeta_1 g(\zeta)}{\rho u_w}$$

$$\begin{aligned}
&= \mu\sqrt{\frac{c}{\nu}}\frac{(1+\frac{\zeta_1}{\mu})f''(\zeta)+\frac{\zeta_1}{\mu}g(\zeta)}{\rho u_w}\\
&= \nu\sqrt{\frac{c}{\nu}}\frac{(1+K)f''(\zeta)+Kg(\zeta)}{u_w}\\
&= \sqrt{\nu}\sqrt{c}\frac{(1+K)f''(\zeta)+Kg(\zeta)}{u_w}\\
&= \sqrt{\nu}\frac{\sqrt{cx}}{\sqrt{x}}\frac{(1+K)f''(\zeta)+Kg(\zeta)}{u_w}\\
&= \sqrt{\nu}\frac{\sqrt{u_w}}{\sqrt{x}}\cdot\frac{\sqrt{x}}{\sqrt{x}}\frac{(1+K)f''(\zeta)+Kg(\zeta)}{u_w}\\
&= \sqrt{\nu}\frac{\sqrt{u_w x}}{\sqrt{\nu}}\cdot\sqrt{\nu}.\frac{1}{x}\frac{(1+K)f''(\zeta)+Kg(\zeta)}{u_w}\\
&= \frac{\sqrt{u_w x}}{\sqrt{\nu}}\cdot\frac{\nu}{x}\frac{(1+K)f''(\zeta)+Kg(\zeta)}{u_w}\\
&= \sqrt{\frac{u_w x}{\nu}}\frac{(1+K)f''(\zeta)+Kg(\zeta)}{\frac{u_w x}{\nu}}
\end{aligned}$$

$$\begin{aligned}
&= \frac{(1+K)f''(\zeta)+Kg(\zeta)}{\sqrt{\frac{u_w x}{\nu}}}\\
&= (1+K)f''(\zeta)+Kg(\zeta)
\end{aligned}$$

$$\Rightarrow \quad \frac{}{\sqrt{Re_x}}\sqrt{Re_x}C_f = Kg(0)+(1+K)f''(0),$$

where $Re_x = \frac{u_w x}{\nu}$ is the local Reynolds number.

3.5 Solution Framework

In order to solve the ODEs (3.45), (3.49) and (3.53) by the shooting method, the following notations have been considered:

$\mathrm{f}(\zeta) = Y_1,\ f'(\zeta) = Y_1' = Y_2,\ f''(\zeta) = Y_2' = Y_3,\ \mathrm{h}(\zeta) = Y_4,\ h'(\zeta) = Y_4' = Y_5,$

$h''(\zeta) = Y_5' = Y_6, \qquad \mathrm{g}(\zeta) = Y_7, \qquad g'(\zeta) = Y_7' = Y_8.$

The system of equations (3.45), (3.49) and (3.53) can be represented in the form of the following first-order coupled ODEs:

$$
\begin{aligned}
Y_1' &= Y_2, && Y_1(0) = 0,\\
Y_2' &= Y_3, && Y_2(0) = 1,\\
Y_3' &= \frac{1}{1+K}\left(\frac{Rm}{Re}(Y_4)^2 Y_2 - 2KY_8 + Y_2^2 - Y_1Y_3\right), && Y_3(0) = p,\\
Y_4' &= Y_5, && Y_4(0) = 0,\\
Y_5' &= Y_6, && Y_5(0) = q,\\
Y_6' &= \frac{1}{\lambda}(Y_4Y_3 - Y_6Y_1), && Y_6(0) = 0,\\
Y_7' &= Y_8, && Y_7(0) = -N_0(t),\\
Y_8' &= \frac{2}{K+2}\left(\beta^*(2Y_7 + Y_3) + Y_2Y_7 - Y_1Y_8\right), && Y_8(0) = w,
\end{aligned}
$$

where p, q and w are the missing initial conditions. Now, the Runge-Kutta method of order four will be used to solve the above mentioned first order initial value problem. It is necessary to choose the missing conditions, such that:

$$
\left.
\begin{aligned}
Y_2(p,q,w) - A^* &= 0,\\
Y_5(p,q,w) - 1 &= 0,\\
Y_7(p,q,w) &= 0,
\end{aligned}
\right\} \tag{3.54}
$$

Newton's method has been used to solve the algebraic equations (3.54) numerically. This formula has the following itreative form:

$$
\begin{bmatrix} p \\ q \\ w \end{bmatrix}_{(n+1)} = \begin{bmatrix} p \\ q \\ w \end{bmatrix}_{(n)} \begin{bmatrix} \frac{\partial Y_2}{\partial p} & \frac{\partial Y_2}{\partial q} & \frac{\partial Y_2}{\partial w} \\ \frac{\partial Y_5}{\partial p} & \frac{\partial Y_5}{\partial q} & \frac{\partial Y_5}{\partial w} \\ \frac{\partial Y_7}{\partial p} & \frac{\partial Y_7}{\partial q} & \frac{\partial Y_7}{\partial w} \end{bmatrix}_{(n)} \begin{bmatrix} Y_2 - A^* \\ Y_5 - 1 \\ Y_7 \end{bmatrix}_{(n)}
$$

To successfully iterate the above formula, we need the following new notations:

$$\frac{\partial Y_1}{\partial p} = Y_9, \quad \frac{\partial Y_2}{\partial p} = Y_{10}, \quad \frac{\partial Y_3}{\partial p} = Y_{11}, \quad \frac{\partial Y_4}{\partial p} = Y_{12}, \frac{\partial Y_5}{\partial p} = Y_{13}, \quad \frac{\partial Y_6}{\partial p} = Y_{14},$$

$$\frac{\partial Y_7}{\partial p} = Y_{15}, \quad \frac{\partial Y_8}{\partial p} = Y_{16}, \quad \frac{\partial Y_1}{\partial q} = Y_{17}, \quad \frac{\partial Y_2}{\partial q} = Y_{18}, \quad \frac{\partial Y_3}{\partial q} = Y_{19}, \frac{\partial Y_4}{\partial q} = Y_{20},$$

$$\frac{\partial Y_5}{\partial q} = Y_{21}, \quad \frac{\partial Y_6}{\partial q} = Y_{22}, \quad \frac{\partial Y_7}{\partial q} = Y_{23}, \quad \frac{\partial Y_8}{\partial q} = Y_{24}, \quad \frac{\partial Y_1}{\partial w} = Y_{25}, \frac{\partial Y_2}{\partial w} = Y_{26},$$

$$\frac{\partial Y_3}{\partial w} = Y_{27}, \quad \frac{\partial Y_4}{\partial w} = Y_{28}, \quad \frac{\partial y_5}{\partial w} = Y_{29}, \quad \frac{\partial Y_6}{\partial w} = Y_{30}, \quad \frac{\partial Y_7}{\partial w} = Y_{31}, \quad \frac{\partial Y_8}{\partial w} = Y_{32},$$

The Netwon's iterative technique takes on the following form, as a result of the above notations:

$$\begin{bmatrix} p \\ q \\ w \end{bmatrix}_{(n+1)} = \begin{bmatrix} p \\ q \\ w \end{bmatrix}_{(n)} \begin{bmatrix} Y_9 & Y_{17} & Y_{25} \\ Y_{12} & Y_{20} & Y_{28} \\ Y_{15} & Y_{23} & Y_{31} \end{bmatrix}_{(n)} \begin{bmatrix} Y_2 - A^* \\ Y_5 - 1 \\ Y_7 \end{bmatrix}_{(n)} .$$

To find the missing derivatives present in the Newton formula, the following initial value problem, will have to be tackled:

$$Y_9' = Y_{10}, \qquad Y_9(0) = 0,$$

$$Y'_{10} = Y_{11}, \qquad Y_{10}(0) = 0,$$

$$\text{Y'}_{11} = \tfrac{1}{1+K}\left(\tfrac{Rm}{Re}Y_4^2Y_{10} + Y_2 2y_4 Y_{12} - 2KY_{16} + 2Y_2Y_{10} - Y_1Y_{11} + Y_3Y_9\right), \quad Y_{11}(0) = 1.$$

$$\text{Y'}_{12} = Y_{13}, \qquad Y_{12}(0) = 0,$$

$$Y_{13}' = Y_{14}, \qquad Y_{13}(0) = 0,$$

$$Y_{14}' = \lambda\left(Y_4Y_{11} + Y_3Y_{12} - Y_6Y_9 - Y_1Y_{14}\right), \qquad Y_{14}(0) = 0.$$

$$Y_{15}' = Y_{16}, \qquad Y_{15}(0) = -N_0,$$

$$Y_{16}' = \tfrac{2}{K+2}\left(\beta^*(2Y_{15} + Y_{11}) + Y_2Y_{15} + Y_7Y_{10} - Y_1Y_{16} - Y_8Y_9\right), \qquad Y_{16}(0) = 0.$$

$$Y_{17}' = Y_{18}, \qquad Y_{17}(0) = 0,$$

$$Y_{18}' = Y_{19}, \qquad Y_{18}(0) = 0,$$

$$Y_{19}' = \tfrac{1}{1+K}\left(\tfrac{Rm}{Re}Y_4^2Y_{18} + Y_2 2Y_4Y_{20} - 2KY_{24} + 2Y_2Y_{18}\right.$$

$$\left. - Y_1Y_{19} + Y_3Y_{17}\right), \qquad Y_{19}(0) = 0.$$

$$Y_{20}' = Y_{21}, \qquad Y_{20}(0) = 0,$$

$$Y_{21}' = Y_{22}, \qquad Y_{21}(0) = 1,$$

$$Y_{22}' = \lambda\Big(Y_4Y_{19} + Y_3Y_{20} - Y_6Y_{17} - Y_1Y_{22}\Big), \qquad Y_{22}(0) = 0.$$
$$Y_{23}' = Y_{24}, \qquad Y_{23}(0) = 0,$$
$$Y_{24}' = \tfrac{2}{K+2}\Big(\beta^*(2Y_{23} + Y_{19}) + Y_2Y_{23} + Y_7Y_{18} - Y_1Y_{24} - Y_8Y_{17}\Big), \qquad Y_{24}(0) = 0.$$
$$Y_{25}' = Y_{26}, \qquad Y_{25}(0) = 0,$$
$$Y_{26}' = Y_{27}, \qquad Y_{26}(0) = 0,$$
$$Y_{27}' = \tfrac{1}{1+K}\Big(\tfrac{Rm}{Re}Y_4^2Y_{26} + Y_2 2Y_4Y_{28} - 2KY_{32} + 2Y_2Y_{26}$$
$$- Y_1Y_{27} + Y_3Y_{25}\Big), \qquad Y_{27}(0) = 0.$$
$$Y_{28}' = Y_{29}, \qquad Y_{28}(0) = 0,$$

$$Y_{29}' = Y_{30}, \qquad Y_{29}(0) = 0,$$
$$Y_{30}' = \lambda\Big(Y_4Y_{27} + Y_3Y_{28} - Y_6Y_{25} - Y_1Y_{30}\Big), \qquad Y_{30}(0) = 0.$$

$$Y_{31}' = Y_{32}, \qquad Y_{31}(0) = 0,$$

$$Y_{32}' = \frac{2}{K+2}\Big(\beta^*(2Y_{31} + Y_{27}) + Y_2Y_{31} + Y_7Y_{26} - Y_1Y_{32} - Y_8Y_{25}\Big), \qquad Y_{32}(0) = 1.$$

Following stopping criteria is used for Newtons's method:

$$\max\left\{\left|Y_2\left(\zeta_\infty, p, q, w\right) - A^*\right|, \left|Y_5\left(\zeta_\infty, p, q, w\right) - 1\right|, \left|Y_7\left(\zeta_\infty, p, q, w\right)\right|\right\} < \epsilon,$$

where $\epsilon > 0$ is an arbitrarily small positive number. From now onward, ϵ has been taken as 10^{-6}.

3.5.1 Results Interpretation

This section aims to evaluate the physical characteristics of microrotational velocity profile, hydrodynamics velocity profile and magnetic induction profiles considering the variations in several significant physical parameters, such as Reylonds number (Rm), magnetic Reylonds number (Re), micropolar constant (K) and micro-inertial coupling parameter (β^*). The evaluation is conducted by utilizing graphical representations of microrotational velocity profiles and magnetic induction profiles. Furthermore, by modifying the values of different dimensionless parameters, the effects of these parameters on skin friction has been examined and presented in tabular form. The graphical representations

of microrotational velocity profile, hydrodynamic velocity profile and magnetic induction profiles provide visual insights into the behavior of the system as the physical parameters vary.

3.5.2 Analysis of Computational Results

Table 3.1 provides computational results of skin friction coefficient for various parameter values in the analysis of the mentioned boundary layer flow. Skin friction coefficients varies with different parameter combinations, indicating sensitivity to changes in fluid properties and flow conditions. As the values of α (the magnetic field parameter) and K (the micropolar fluid parameter) increase, the magnitude of skin friction coefficient is observed to decrease.

The same is the impact of Reynolds number (Re) on the skin friction indicating reduced viscous effects at higher flow rates. In Table 3.2, interval I_f, I_h and I_g are shown where from the missing initial conditions $f''(0)$, $h'(0)$ and $g'(0)$ respectively, have been chosen.

TABLE 3.1: The numerical result of $(Re_x)^{1/2}Cf_x$.

α	K	λ	β^*	R_e	R_m	N_0	A_s	$Re^{1/2}Cf_x$
1.0	0.2	0.5	0.1	10	0.1	2.0	1.0	-0.316773
0.6								-0.799288
0.7								-0.715898
0.8								-0.611989
	0.05							-0.255146
	0.1							-0.271721
	0.15							-0.291762
		0.1						-0.314011
		0.2						-0.316834
		0.3						-0.317745
			0.0					-0.313656
			0.15					-0.318196
			0.2					-0.319542
				6				-0.424292
				12				-0.281515
				18				-0.211418
					0.2			-0.464382
					0.3			-0.553064
					0.4			-0.613212
						2.1		-0.322315
						2.12		-0.323484
						2.13		-0.324076
							1.0	-0.521344
							1.2	-0.643113
							1.3	-0.721537

TABLE 3.2: Numerical Results for the Missing Initial Value Problem (IVP).

α	K	λ	β^*	R_e	R_m	N_0	A_s	$f''(0)$	$h'(0)$	$g'(0)$
1.0	0.2	0.5	0.1	10	0.1	2.0	1.0	-0.395966	0.864433	-0.940300
0.6								-0.999111	0.659849	-2.153325
0.7								-0.894873	0.699982	-1.969709
0.8								-0.764987	0.746660	-1.723286
	0.05							-0.268575	0.888654	-0.666810
	0.1							-0.301912	0.882694	-0.739201
	0.15							-0.343250	0.874889	-0.828157
		0.1						-0.392514	0.906685	-0.929124
		0.2						-0.396043	0.886855	-0.938425
		0.3						-0.397182	0.875953	-0.941887
			0.0					-0.392070	0.864489	-0.884365
			0.15					-0.397745	0.864420	-0.967127
			0.2					-0.399428	0.864416	-0.993219
				6				-0.530365	0.814315	-1.233867
				12				-0.351894	0.880360	-0.840923
				18				-0.264273	0.911345	-0.639149
					0.2			-0.580471	0.794983	-1.339370
					0.3			-0.691330	0.750867	-1.564145
					0.4			-0.766515	0.719848	-1.709018
						2.1		-0.413225	0.860977	-1.029607
						2.12		-0.416860	0.860247	-1.048374
						2.13		-0.418703	0.859877	-1.057877
							1.1	-0.651681	0.721602	-1.498046
							1.2	-0.803892	0.623892	-1.805781
							1.3	-0.901921	0.552715	-1.992738

3.6 Hydrodynamic Velocity Profile

In Figure 3.2, the hydrodynamics velocity profile with an increaseing micropolar constant (K) can be elucidated by considering different characteristics of the micropolar fluids. A higher K signifies a stronger coupling between macroscopic fluid motion and microstructural effects within the fluid. As K increases, microstructural interactions such as micro-rotations and micro-deformations become more influential in shaping the velocity profile. In essence, the higher values of K enhance the rotational aspects of the flow, causing the velocity to change more dramatically near the boundary.

In Figure 3.3, the influence of increasing Reynolds number on the hydrodynamic velocity

profile, particularly in the presence of a varying magnetization parameter, entails the acceleration of fluid particles. With increasing Reynolds number, the ratio of inertial forces to viscous forces becomes greater. This amplification of inertia causes fluid particles near the boundary to accelerate more rapidly, resulting in a steeper velocity gradient and a more pronounced velocity profile. Essentially, higher Reynolds numbers indicate that the fluid is less influenced by viscosity and more by inertia, resulting in a more dynamic flow with a sharper velocity change near the boundary.

Figure 3.4 exhibits the diminishing hydrodynamics velocity profile as the magnetic Reynolds number (Rm) increases. The effect of the magnetic reynolds number (Rm) velocity profile in magnetohydrodynamic (MHD) flows is deeply intertwined with the interaction between magnetic forces, fluid motion, and boundary conditions. Magnetic forces exert influence on the fluid motion by inducing Lorentz forces, which interact with the velocity field. As Rm increases, magnetic forces become more signifi-cant relative to viscous forces, affecting the fluid flow patterns. In MHD flows, magnetic fields interact with the fluid, exerting forces that can significantly affect fluid motion. As Rm increases, the influence of magnetic forces becomes more pronounced relative to the viscous forces.

3.7 Macrorotational Velocity Profile

In the study of the magneto-micropolar boundary layer models, the macrorotational velocity profile $g(\zeta)$ takes centeral stage due to its crucial role in understanding the fluid's overall rotational behavior, especially in the presence of micromagnetorotation (MMR) effects. Figures 3.5 to 3.7 investigate how various parameters influence this profile. In Figure 3.5 the micropolar constant K increases, its influence which becomes apparent as the macro rotational velocity profile rises. This escalation is linked to the amplified involvement of microrotation, which enhances the fluid rotation and consequently augments the overall macro rotational velocity profile.

Figure 3.6 reveals an unexpected behavior; as the (Re) increases, initially the macrorotational velocity profile near the stretching plate decreases. This decline is attributed to the dominance of fluid inertia at higher Re. However, as we move away from the plate,

the boundary layer characteristics evolve, and rotational effects start to prevail, leading to a reversal in the profile's behavior. This intriguing reversal signifies the transition from an inertia-dominated region close to the plate to a rotationally influenced area further away.

Figure 3.7 illuminates the impact of the magnetic Reynolds number (Rm) on the macrorotational velocity profile. As Rm increases, magnetic influences strengthen, enhancing the fluid rotation and raising the macrorotational profile. However, in the vicinity of the stretching plate, this pattern shifts due to the intricate interplay of magnetic forces, leading to a nuanced dynamic with a reversal near the plate:

3.8 Magnetic Induction Profile

Figure 3.8 directs attention to the micro-inertial coupling parameter (β^*) and its impact on the magnetic induction profile. Here, an interesting pattern is observed which reflects a rise in the magnetic induction profile as the values of (β^*)increases. This pattern indicates an increased interaction between micro-inertial effects and magnetization. Higher β^* values indicate a more significant involvement of micro-polar fluid characteristics in the fluid's response to the magnetic field, thereby enhancing the magnetic induction profile.

Figure 3.9 examines the influence of the micro-polar constant K on shaping the magnetic induction profile. As K increases, a significant rise in the magnetic induction profile becomes apparent. This increase is linked to the heightened impact of micro-polar characteristics on the fluid's reaction to the magnetic field, leading to an intensified magnetic induction profile.

Figure 3.10 presents the effect of Reylonds number (Re) on the magnetic induction profile. Significantly, as Reynolds number increases, a noticeable augmentation in the magnetic induction profile becomes evident. This phenomenon arises from the intensified fluid dynamics propelled by the heightened inertia. As Reynolds number increases, the fluid's momentum intensifies, allowing it to more efficiently propagate the magnetic effects across the boundary layer.

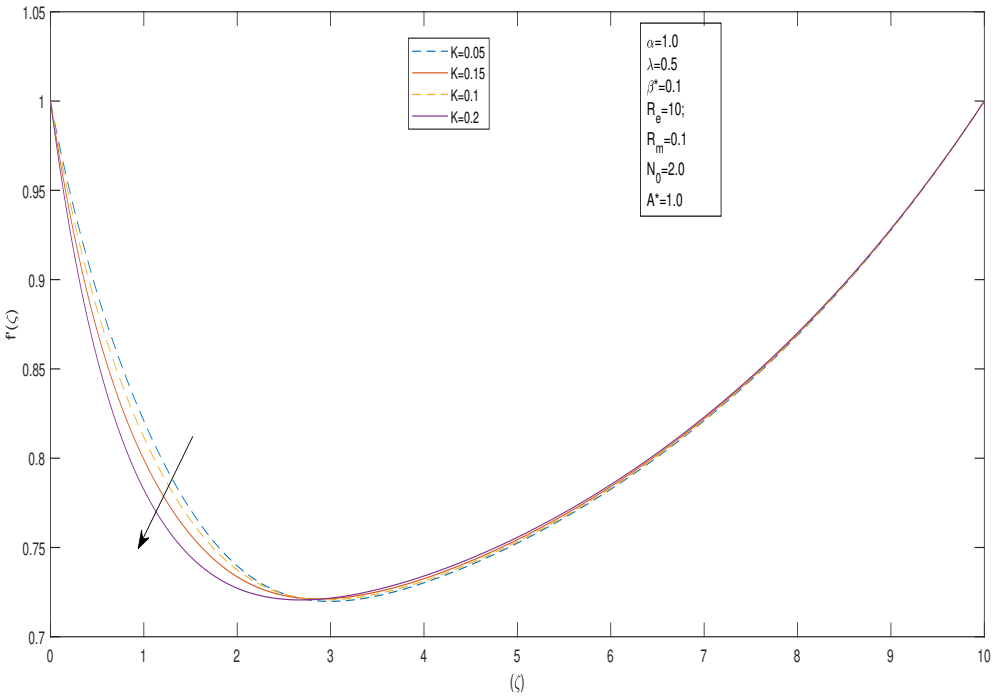

FIGURE 3.2: Effect of K on $f'(\zeta)$

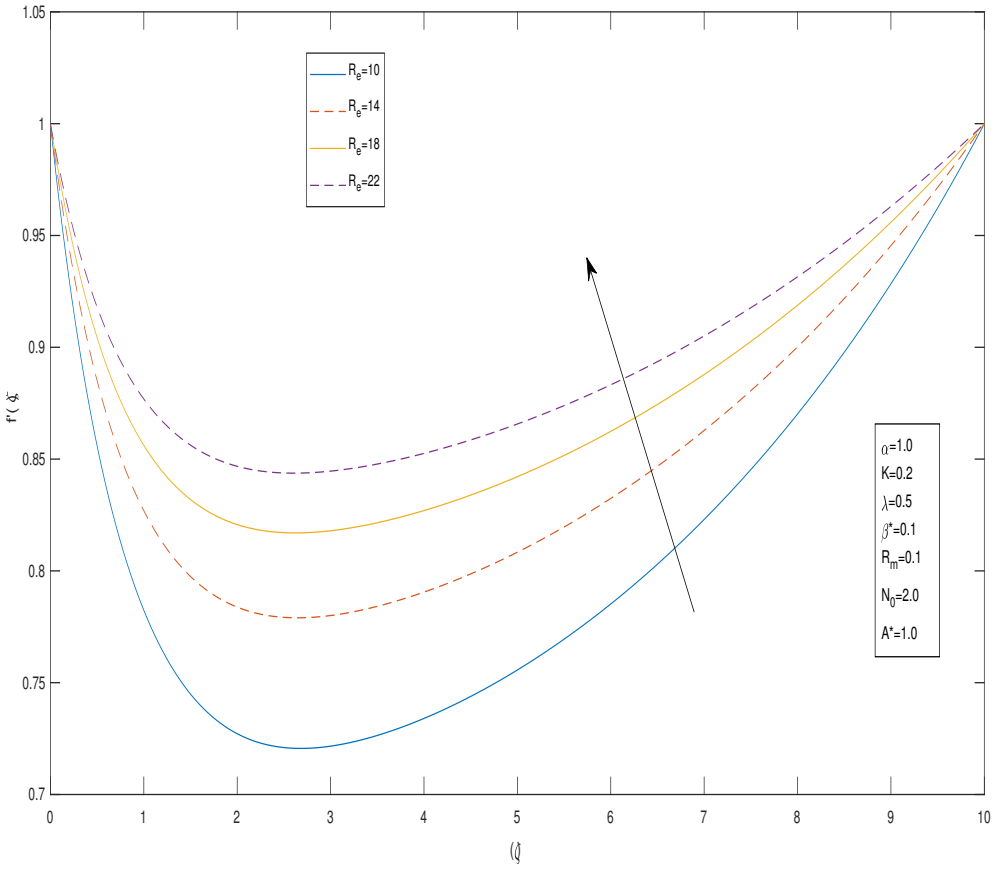

FIGURE 3.3: Effect of R_e on $f'(\zeta)$

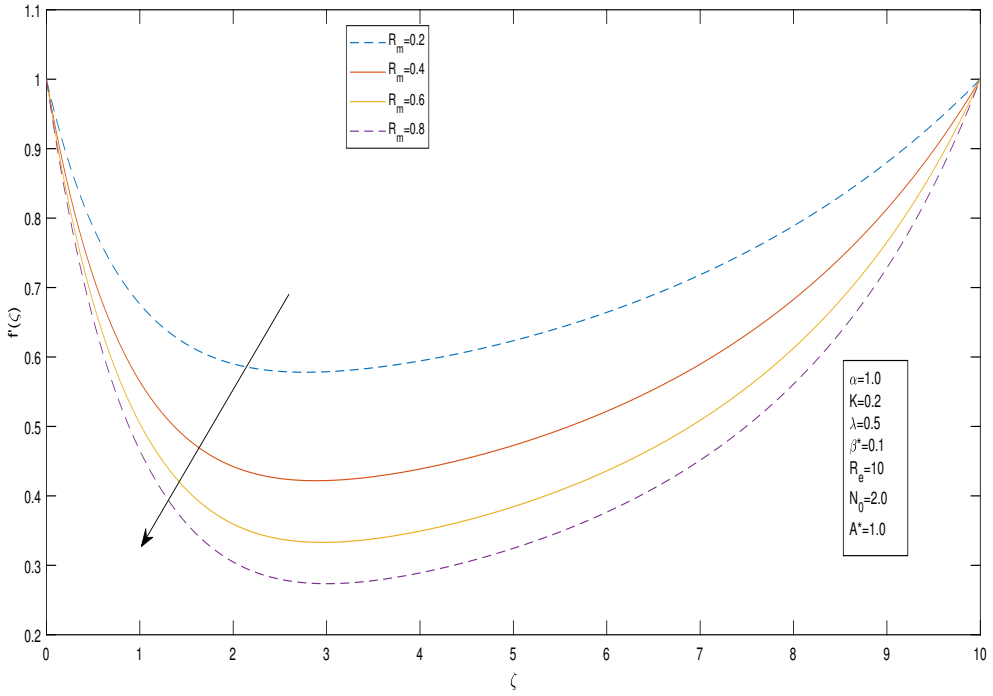

FIGURE 3.4: Effect of R_m on $f'(\zeta)$

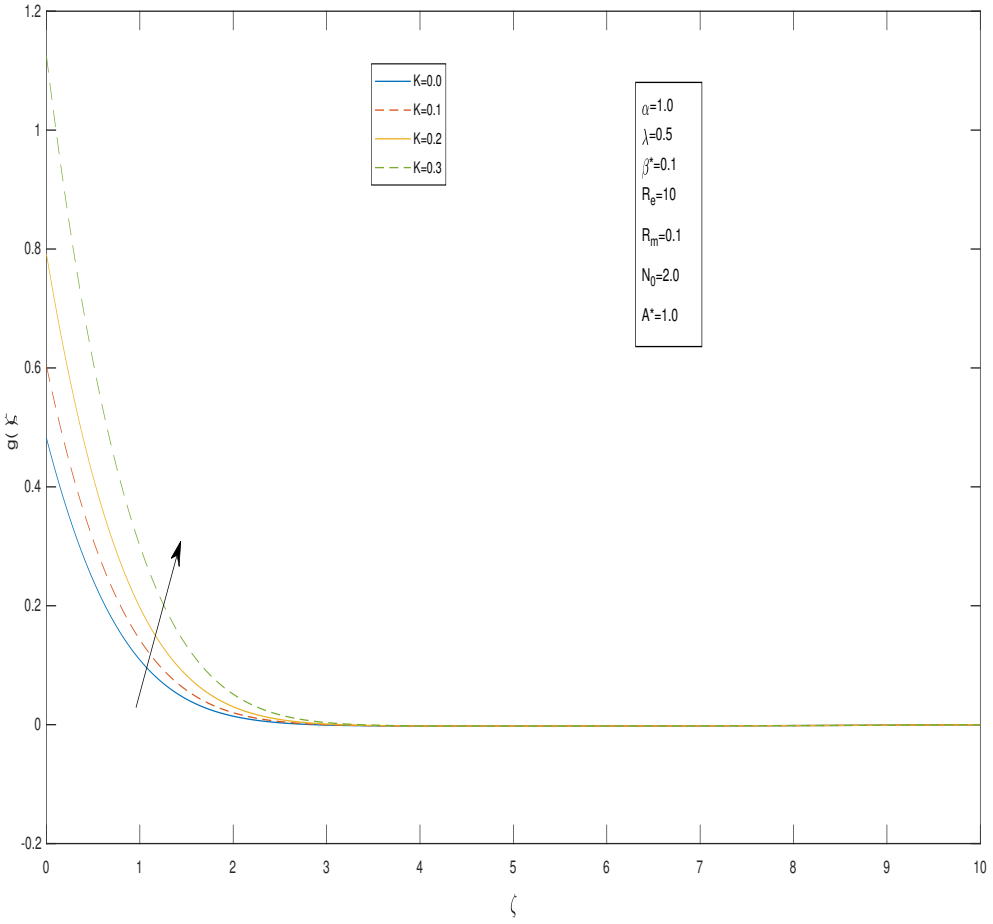

FIGURE 3.5: Effect of K on $g(\zeta)$

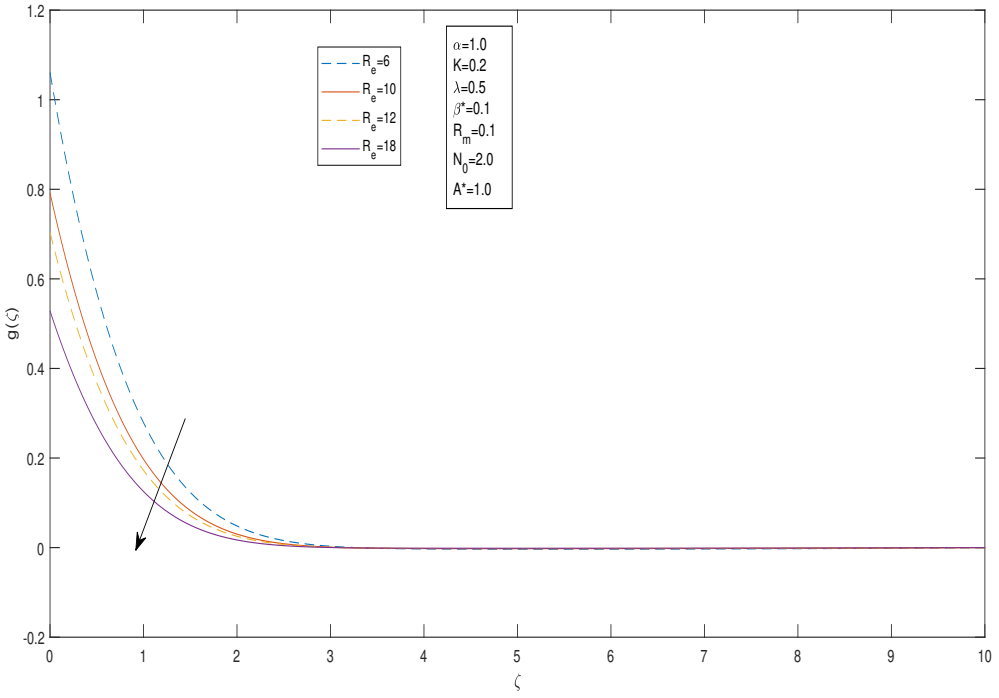

FIGURE 3.6: Effect of R_e on $g(\zeta)$

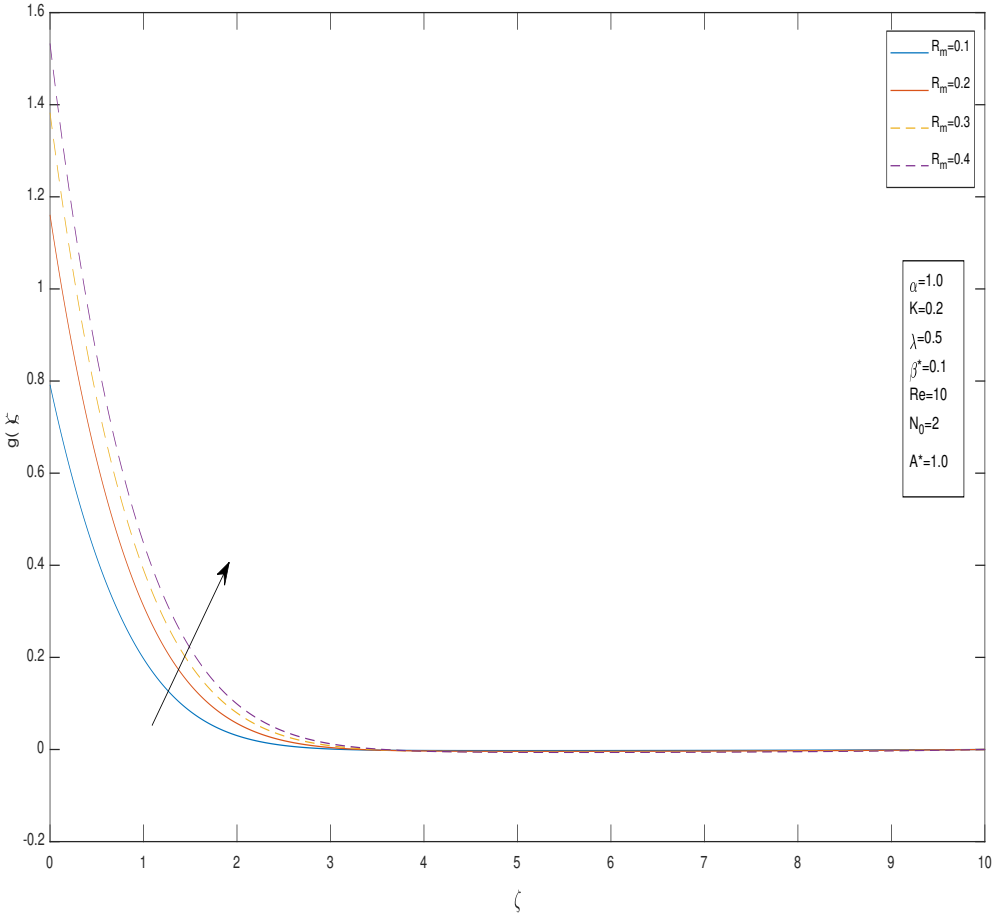

FIGURE 3.7: Effect of R_m on $g(\zeta)$

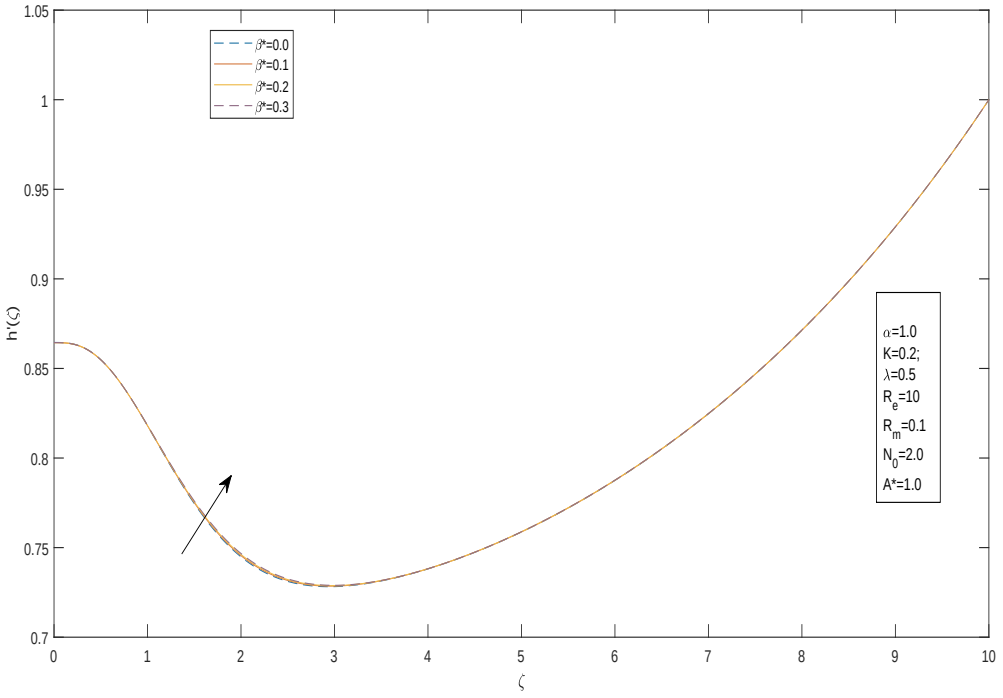

FIGURE 3.8: Effect of β^* on $h'(\zeta)$

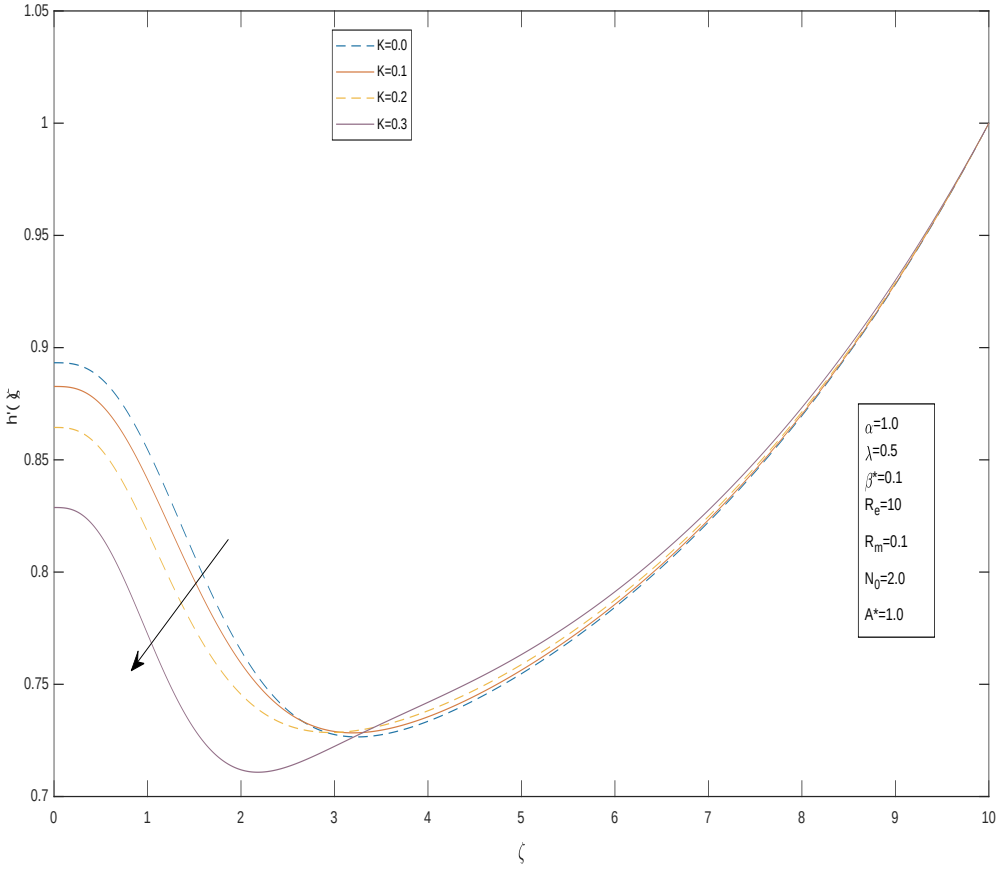

FIGURE 3.9: Effect of K on $h'(\zeta)$

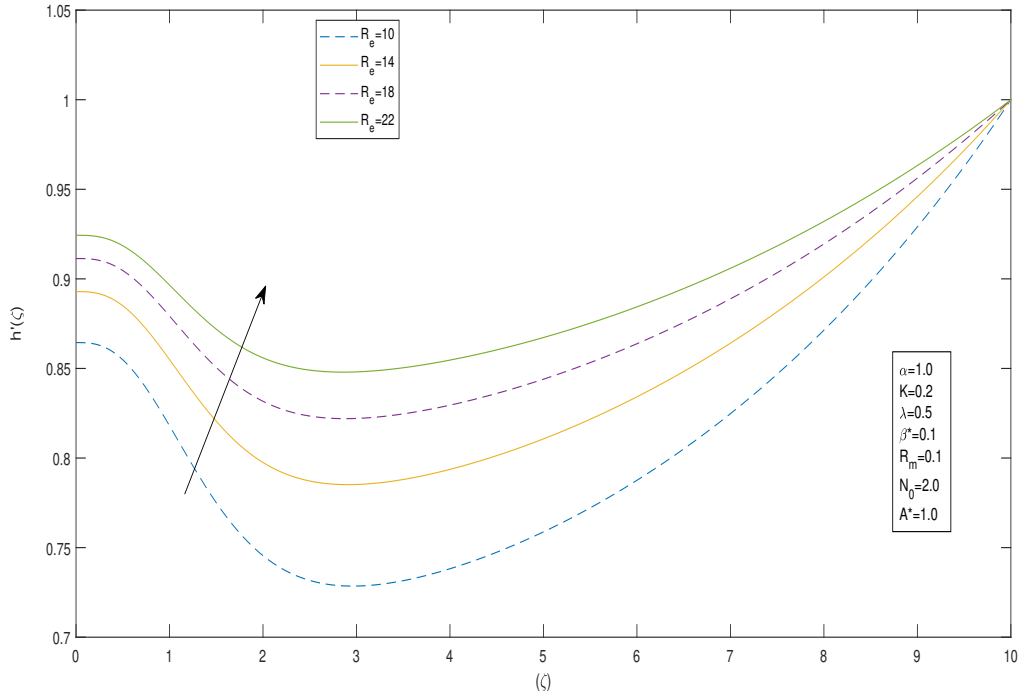

FIGURE 3.10: Effect of Re on $h'(\zeta)$

Chapter 4

Numerical Investigation of Micromagnetorotation Effects on Boundary Layer Flow and Heat Transfer in Magneto-Micropolar Fluids

4.1 Introduction

The current chapter extends the model discussed in the previous chapter by incorporating additional discussion on heat transfer in the energy equation. The effects of the magnetic field, as well as heat and mass transfer, have been incorporated into the energy equation in this chapter. The governing nonlinear PDEs are converted into a system of dimensionless ODEs by utilizing the similarity transformations. The numerical solution of ODEs is obtained by applying numerical method known as the shooting method. At the end of this chapter, the final results are discussed for significant parameters affecting hydrodynamic velocity profile, microrotation velocity profile, magnetic induction profile and temperature profile, which are displaced through tables and graphs.

4.2 Mathematical Modeling

Figure 3.1 shows the setup of the physical model. In this system, x and y denote the Cartesian coordinates along the surface and perpendicular to it, respectively. The velocity components are u in the x-direction and v in the y-direction. The study focuses on an incompressible, laminar, two-dimensional flow of a micropolar fluid subject to magnetohydrodynamic (MHD) convection, under the influence of an externally applied magnetic field. Below are the governing equations for the fluid flow, along with the constitutive relations for magnetization, in the vector form:

$$\boldsymbol{\nabla}.\mathbf{U} = 0, \tag{4.1}$$

$$\boldsymbol{\nabla}.\mathbf{H} = 0, \tag{4.2}$$

$$\rho\left(\frac{d\mathbf{U}}{dt} + \mathbf{U}.\boldsymbol{\nabla}\mathbf{U}\right) = -\boldsymbol{\nabla}(p) + \mu\boldsymbol{\nabla}^{\mathbf{2}}\mathbf{U} + 2\zeta_1\boldsymbol{\nabla}\times(\mathbf{W}-\mathbf{w}) + \mathbf{J}\times\mathbf{B} + (\mathbf{M}.\boldsymbol{\nabla})\mathbf{H} + \mathbf{M}\times(\boldsymbol{\nabla}\times\mathbf{H}), \tag{4.3}$$

$$\rho\left(\frac{d\mathbf{H}}{dt} + \mathbf{U}.\boldsymbol{\nabla}\mathbf{H} - \mathbf{H}.\boldsymbol{\nabla}\mathbf{U}\right) = \mu_0\boldsymbol{\nabla}^{\mathbf{2}}\mathbf{H}, \tag{4.4}$$

$$l\left(\frac{d\mathbf{W}}{dt} + \mathbf{U}.\boldsymbol{\nabla}\mathbf{W}\right) = \gamma\boldsymbol{\nabla}^{\mathbf{2}}\mathbf{W} + 4\zeta_1(\mathbf{w}-\mathbf{W}) + \mathbf{M}\times\mathbf{H}, \tag{4.5}$$

$$\rho c_p\left(\frac{\partial\mathbf{T}}{\partial t} + \mathbf{U}.\boldsymbol{\nabla}\mathbf{T}\right) = k\boldsymbol{\nabla}^{\mathbf{2}}\mathbf{T} + \frac{\mathbf{J}^2}{\sigma}, \tag{4.6}$$

$$\mathbf{B} = \mu_0\mathbf{H} + \mathbf{M}, \tag{4.7}$$

$$\mathbf{M} = \frac{M_0(\mathbf{I}-\tau\mathbf{W}.\epsilon).\mathbf{H}}{\bar{H}}, \tag{4.8}$$

$$\mathbf{J} = \sigma\Big(\mathbf{E} + \mathbf{U}\times\mathbf{B}\Big), \tag{4.9}$$

$$\mathbf{w} = \boldsymbol{\nabla}\times\frac{\mathbf{U}}{2}. \tag{4.10}$$

The expression $\mathbf{M}\times\mathbf{H}$ represents the MMR term, delineating the impact of magnetization on microrotation [16]. The applied magnetic field is defined as $H(H_1, H_2, 0)$. The second term $\mathbf{J}$ in the right hand side of equation (4.6), is the current density vector due to the magnetic field and electric field [29]. Equations (4.7) and (4.8) represent the constitutive equations for magnetization.

4.3 Governing Equations in the Operator-Form

In this section, we present the process of transforming the governing equations in the vector form to the operator form. Vector equations encapsulate the foundational principles governing a system in the abstract mathematical terms, whereas the operator form offers a more concrete representation in terms of the physical variables and parameters.
In this model, we have discussed steady-state flow, where the fluid characteristics at a point do not change with time. Equations (3.3) and (3.5) are the conservation laws of linear and angular momentum, respectively. Equation (3.7) defines the vorticity **(w)**, which is a pseudovector field that describes the local spinning motion of a continuum near some point, as would be seen by an observer located at that point and traveling along with the flow. Scale analysis simplifies equations by determining the approximate magnitudes of their terms and ignoring negligibly small ones. Using scale analysis, it has been assumed that the pressure p does not depend on the spatial coordinates. The relaxation time of magnetization τ being very small, has been ignored. Assume that no electric field **E** is applied on the flow [16]. No-slip boundary conditions are imposed for the linear velocity, in accordance with the assumptions used in [16] and the boundary layer approximations.

4.3.1 Continuity Equations

The continuity equations in the operator form have already been discussed in Chapter 3.

4.3.2 Momentum Equation

For the momentum equations (4.3) the following operators are required:

$$
\begin{aligned}
(\mathbf{M}.\boldsymbol{\nabla})\mathbf{H} &= \left(M_0\frac{(H_1+\tau H_2 N)}{H_1}, M_0\frac{(H_2-\tau H_1 N)}{H_2}, 0\right).\left(\frac{\partial}{\partial x}, \frac{\partial}{\partial y}, 0\right)(H_1, H_2, 0) \\
&= \left(M_0\frac{(H_1+\tau H_2 N)}{H_1}\frac{\partial}{\partial x} + M_0\frac{(H_2-\tau H_1 N)}{H_2}\frac{\partial}{\partial y} + 0\right)(H_1, H_2, 0) \\
&= M_0\frac{(H_1+\tau H_2 N)}{H_1}\frac{\partial}{\partial x}(H_1, H_2, 0) + M_0\frac{(H_2-\tau H_1 N)}{H_2}\frac{\partial}{\partial y}(H_1, H_2, 0) \\
&\quad + 0(H_1, H_2, 0)
\end{aligned}
$$

$$
\begin{aligned}
&= \left(M_0 \frac{(H_1 + \tau H_2 N)}{H_1} \frac{\partial H_1}{\partial x}, M_0 \frac{(H_1 + \tau H_2 N)}{H_1} \frac{\partial H_2}{\partial x}, 0 \right) \\
&\quad + \left(M_0 \frac{(H_2 - \tau H_1 N)}{H_2} \frac{\partial H_1}{\partial y}, M_0 \frac{(H_2 - \tau H_1 N)}{H_2} \frac{\partial H_2}{\partial y}, 0 + 0 \right) \\
&= \left(M_0 \frac{(H_1 + \tau H_2 N)}{H_1} \frac{\partial H_1}{\partial x} + M_0 \frac{(H_2 - \tau H_1 N)}{H_2} \frac{\partial H_1}{\partial y}, \right. \\
&\quad \left. M_0 \frac{(H_1 + \tau H_2 N)}{H_1} \frac{\partial H_2}{\partial x} + M_0 \frac{(H_2 - \tau H_1 N)}{H_2} \frac{\partial H_2}{\partial y}, 0 \right). \qquad (4.11)
\end{aligned}
$$

Now, the cross product $\mathbf{M} \times (\boldsymbol{\nabla} \times \mathbf{H})$ is computed as follows:

$$
\begin{aligned}
\boldsymbol{\nabla} \times \mathbf{H} &= \begin{vmatrix} \hat{i} & \hat{j} & \hat{k} \\ \frac{\partial}{\partial x} & \frac{\partial}{\partial y} & 0 \\ H_1 & H_2 & 0 \end{vmatrix} \\
&= (0)\hat{i} - (0)\hat{j} + \left(\frac{\partial H_2}{\partial x} - \frac{\partial H_1}{\partial y} \right) \hat{k}. \\
\mathbf{M} \times (\boldsymbol{\nabla} \times \mathbf{H}) &= \begin{vmatrix} \hat{i} & \hat{j} & \hat{k} \\ M_0 \frac{(H_1 + \tau H_2 N)}{H_1} & M_0 \frac{(H_2 - \tau H_1 N)}{H_2} & 0 \\ 0 & 0 & \frac{\partial H_2}{\partial x} - \frac{\partial H_1}{\partial y} \end{vmatrix} \\
&= \left(M_0 \frac{(H_2 - \tau H_1 N)}{H_2} \frac{\partial H_2}{\partial x} - M_0 \frac{(H_2 - \tau H_1 N)}{H_2} \frac{\partial H_1}{\partial y} \hat{i} \right. \\
&\quad - M_0 \frac{(H_1 + \tau H_2 N)}{H_1} \frac{\partial H_2}{\partial x} + M_0 \frac{(H_1 + \tau H_2 N)}{H_1} \frac{\partial H_1}{\partial y} \hat{j} \\
&\quad \left. + 0\hat{k} \right). \qquad (4.12)
\end{aligned}
$$

Now, we substitute all the expressions (3.10)-(3.18) and (4.11), (4.12) into equation (4.3) to get the following:

$$
\begin{aligned}
&\rho \left(\frac{du}{dt}, \frac{dv}{dt}, 0 \right) + \left(u \frac{\partial u}{\partial x} + v \frac{\partial u}{\partial y}, u \frac{\partial v}{\partial x} + v \frac{\partial v}{\partial y}, 0 \right) \\
&= -\left(\frac{\partial p}{\partial x}, \frac{\partial p}{\partial y}, 0 \right) + \mu \left(\frac{\partial^2 u}{\partial x^2} + \frac{\partial^2 u}{\partial y^2}, \frac{\partial^2 v}{\partial x^2} + \frac{\partial^2 v}{\partial y^2}, 0 \right) \\
&\quad + 2\zeta_1 \left(\frac{\partial N}{\partial y} - \frac{\partial N}{\partial x}, 0 \right) - \zeta_1 \left(\frac{\partial^2 v}{\partial y \partial x} - \frac{\partial^2 u}{\partial y^2}, -\frac{\partial^2 v}{\partial x^2} - \frac{\partial^2 u}{\partial x \partial y}, 0 \right) \\
&\quad + \sigma \mu_0 (-u H_2^2 - v H_1 H_2 - v M_0 H_2 + u \tau^2 M_0^2 N^2 + v H_1 \tau M_0 N \\
&\quad + v \tau M_0^2 N, u H_2 H_1 + u H_2 \tau M_0 N + v H_1^2 + v M_0 H_1 \\
&\quad + u H_2 M_0 + u \tau M_0^2 N + v H_1 M_0 + v M_0^2, 0)
\end{aligned}
$$

$$\left(M_0\frac{(H_1+\tau H_2N)}{H_1}\frac{\partial H_1}{\partial x}+M_0\frac{(H_2-\tau H_1N)}{H_2}\frac{\partial H_1}{\partial y},\right.$$
$$\left.M_0\frac{(H_1+\tau H_2N)}{H_1}\frac{\partial H_2}{\partial x}+M_0\frac{(H_2-\tau H_1N)}{H_2}\frac{\partial H_2}{\partial y},0\right)$$
$$+\left(M_0\frac{(H_2-\tau H_1N)}{H_2}\frac{\partial H_2}{\partial x}-M_0\frac{(H_2-\tau H_1N)}{H_2}\frac{\partial H_1}{\partial y},\right.$$
$$\left.-M_0\frac{(H_1+\tau H_2N)}{H_1}\frac{\partial H_2}{\partial x}+M_0\frac{(H_1+\tau H_2N)}{H_1}\frac{\partial H_1}{\partial y},0\right).$$

$$\Rightarrow \quad \frac{du}{dt}+\left(u\frac{\partial u}{\partial x}+v\frac{\partial u}{\partial y}\right)=-\frac{1}{\rho}.\frac{\partial p}{\partial x}+\frac{\mu}{\rho}\left(\frac{\partial^2u}{\partial x^2}+\frac{\partial^2u}{\partial y^2}\right)+\frac{2\zeta_1}{\rho}\left(\frac{\partial N}{\partial y}\right)$$
$$-\frac{\zeta_1}{\rho}\left(\frac{\partial^2v}{\partial y\partial x}-\frac{\partial^2u}{\partial y^2}\right)+\frac{\sigma}{\rho}\mu_0(-uH_2^2)$$
$$+\frac{1}{\rho}M_0\frac{(H_1+\tau H_2N)}{H_1}\frac{\partial H_1}{\partial x}+M_0\frac{(H_2-\tau H_1N)}{H_2}\frac{\partial H_1}{\partial y}$$
$$+M_0\frac{(H_2-\tau H_1N)}{H_2}\frac{\partial H_2}{\partial x}-M_0\frac{(H_2-\tau H_1N)}{H_2}\frac{\partial H_1}{\partial y}.$$

$$\Rightarrow \quad u\frac{\partial u}{\partial x}+v\frac{\partial u}{\partial y}=\left(\frac{\mu+\zeta_1}{\rho}\right)\frac{\partial^2u}{\partial y^2}-\frac{\sigma}{\rho}\mu_0H_2^2u+\frac{2\zeta_1}{\rho}\frac{\partial N}{\partial y}$$
$$+\frac{1}{\rho}\frac{M_0}{\bar{H}}(H_1+\tau H_2N)\frac{\partial H_1}{\partial x}+(H_2-\tau H_1N)\frac{\partial H_2}{\partial x}. \tag{4.13}$$

4.3.3 Magnetic Induction Equation

The detailed procedure for the conversion of (4.4) into the dimensional form has already been discussed in chapter 3. Therefore, the dimensional form of the magnetic induction equation is

$$u\frac{\partial H_1}{\partial x}+v\frac{\partial H_1}{\partial y}=H_1\frac{\partial u}{\partial x}+H_2\frac{\partial u}{\partial y}+\nu_0\frac{\partial^2H_1}{\partial y^2}. \tag{4.14}$$

4.3.4 Microrotation Equation

The cross product $\mathbf{M}\times\mathbf{H}$ is computed as follows:

$$\mathbf{M}\times\mathbf{H}=\begin{vmatrix}\hat{i} & \hat{j} & \hat{k}\\ M_0 & -\tau M_0N & 0\\ H_1 & H_2 & 0\end{vmatrix}$$

$$=(0)\hat{i}-(0)\hat{j}+(M_0H_2-(-M_0\tau H_1N))\hat{k}$$

$$= (0)\hat{i} - (0)\hat{j} + (M_0H_2 + M_0\tau H_1 N)\hat{k}. \tag{4.15}$$

We substitute all the expressions (3.20)-(3.22) and (4.15) into (4.5), to get:

$$\begin{aligned} l\left(0,0,\frac{dN}{dt}+0,0,u\frac{\partial N}{\partial y}+v\frac{\partial N}{\partial y}\right) &= \gamma\left(0,0,\frac{\partial^2 N}{\partial x^2}+\frac{\partial^2 N}{\partial y^2}\right) \\ &\quad + 2\zeta_1\left(0,0,\frac{\partial v}{\partial x}-\frac{\partial u}{\partial y}-0,0,2N\right) \\ &\quad + (0,0,M_0H_2+M_0\tau H_1 N) \end{aligned}$$

$$\begin{aligned} \Rightarrow \quad \left(0,0,\frac{dN}{dt}+0,0,u\frac{\partial N}{\partial x}+v\frac{\partial N}{\partial y}\right) &= \frac{\gamma}{l}\left(0,0,\frac{\partial^2 N}{\partial x^2}+\frac{\partial^2 N}{\partial y^2}\right) \\ &\quad + \frac{2\zeta_1}{l}\left(0,0,\frac{\partial v}{\partial x}-\frac{\partial u}{\partial y}-0,0,2N\right) \\ &\quad + \frac{1}{l}(0,0,M_0H_2+M_0\tau H_1 N) \end{aligned}$$

$$\Rightarrow \quad u\frac{\partial N}{\partial x}+v\frac{\partial N}{\partial y} = \frac{\gamma}{l}\frac{\partial^2 N}{\partial y^2} - \frac{2\zeta_1}{l}\left(2N+\frac{\partial u}{\partial y}\right) + \frac{1}{l}M_0\tau\bar{H}N. \tag{4.16}$$

4.3.5 Energy equation

For the energy equation (4.6) the following operators are required:

$$\begin{aligned} \mathbf{U}.\boldsymbol{\nabla}\mathbf{T} &= (u,v,0).\left(\frac{\partial}{\partial x},\frac{\partial}{\partial y},0\right)(T_1,T_2,0) \\ &= \left(u\frac{\partial}{\partial x}+v\frac{\partial}{\partial y}+0\right)(T_1,T_2,0) \\ &= u\frac{\partial}{\partial x}(T_1,T_2,0)+v\frac{\partial}{\partial y}(T_1,T_2,0)+0(T_1,T_2,0) \\ &= \left(u\frac{\partial T_1}{\partial x},u\frac{\partial T_2}{\partial x},0\right)+\left(v\frac{\partial T_1}{\partial y},v\frac{\partial T_2}{\partial y},0\right)+(0) \\ &= \left(u\frac{\partial T_1}{\partial x}+v\frac{\partial T_1}{\partial y},u\frac{\partial T_2}{\partial x}+v\frac{\partial T_2}{\partial y},0\right). \end{aligned} \tag{4.17}$$

$$\begin{aligned} \boldsymbol{\nabla}^2\mathbf{T} &= \left(\frac{\partial}{\partial x},\frac{\partial}{\partial y},0\right).\left(\frac{\partial}{\partial x},\frac{\partial}{\partial y},0\right)(T_1,T_2,0) \\ &= \left(\frac{\partial^2}{\partial x^2}+\frac{\partial^2}{\partial y^2}+0\right)(T_1,T_2,0) \\ &= \left(\frac{\partial^2 T_1}{\partial x^2},\frac{\partial^2 T_2}{\partial x^2},0\right)+\left(\frac{\partial^2 T_1}{\partial y^2},\frac{\partial^2 T_2}{\partial y^2},0\right)+0(T_1,T_2,0) \end{aligned}$$

$$= \left(\frac{\partial^2 T_1}{\partial x^2} + \frac{\partial^2 T_1}{\partial y^2}, \frac{\partial^2 T_2}{\partial x^2} + \frac{\partial^2 T_2}{\partial y^2}, 0\right). \tag{4.18}$$

$$\mathbf{U} \times \mathbf{B} = \begin{vmatrix} \hat{i} & \hat{j} & \hat{k} \\ u & v & 0 \\ H_1 + M_0 & H_2 - \tau M_0 N & 0 \end{vmatrix}$$

$$= (0)\hat{i} - (0)\hat{j} + (uH_2 - u\tau M_0 N - vH_1 - vM_0)\hat{k}. \tag{4.19}$$

$$\begin{aligned} \frac{\mathbf{J}^2}{\boldsymbol{\sigma}} &= \frac{1}{\sigma}\sigma^2(\mathbf{E} + \mathbf{U} \times \mathbf{B})^2 \\ &= \frac{1}{\sigma}\sigma^2(\mathbf{U} \times \mathbf{B})^2 \\ &= \frac{1}{\sigma}\sigma^2(0, 0, uH_2 - u\tau M_0 N - vH_1 - vM_0)^2 \\ &= \sigma(0, 0, u^2 H_2^2 - u^2\tau^2 M_0^2 N^2 - v^2 H_1^2 - v^2 M_0^2) \\ &= \sigma(0, 0, u^2 H_2^2). \end{aligned} \tag{4.20}$$

Now, we substitute all the expressions (4.17)-(4.18) into (4.6) to get the following:

$$\begin{aligned} &\rho c_p\left(\frac{\partial T_1}{\partial t}, \frac{\partial T_2}{\partial t}, 0\right) + \left(u\frac{\partial T_1}{\partial x} + v\frac{\partial T_1}{\partial y}, u\frac{\partial T_2}{\partial x} + v\frac{\partial T_2}{\partial y}, 0\right) \\ &= k\left(\frac{\partial^2 T_1}{\partial x^2} + \frac{\partial^2 T_1}{\partial y^2}, \frac{\partial^2 T_2}{\partial x^2} + \frac{\partial^2 T_2}{\partial y^2}, 0\right) + \sigma(0, 0, u^2 H_2^2). \end{aligned}$$

$$\Rightarrow \quad \frac{dT_1}{dt} + \left(u\frac{\partial T_1}{\partial x} + v\frac{\partial T_1}{\partial y}\right) = \frac{k}{\rho c_p}\left(\frac{\partial^2 T_1}{\partial x^2} + \frac{\partial^2 T_1}{\partial y^2}\right) + \frac{\sigma}{\rho c_p}u^2 H_2^2.$$

$$\Rightarrow \quad u\frac{\partial T_1}{\partial x} + v\frac{\partial T_1}{\partial y} = k_\alpha\left(\frac{\partial^2 T_1}{\partial y^2}\right) + \frac{\sigma}{\rho c_p}u^2 H_2^2. \tag{4.21}$$

The continuity, momentum, magnetic induction, microrotation and energy equations governing the above stated problem under the usual boundary layer approximations are as follows.

Continuity Equations:

$$\frac{\partial u}{\partial x} + \frac{\partial v}{\partial y} = 0, \tag{4.22}$$

$$\frac{\partial H_1}{\partial x} + \frac{\partial H_2}{\partial y} = 0, \tag{4.23}$$

Momentum Equation:

$$u\frac{\partial u}{\partial x}+v\frac{\partial u}{\partial y}=\left(\frac{\mu+\zeta_1}{\rho}\right)\frac{\partial^2 u}{\partial y^2}-\frac{\sigma}{\rho}\mu_0 H_2^2 u+\frac{2\zeta_1}{\rho}\frac{\partial N}{\partial y} + \frac{1}{\rho}\frac{M_0}{\bar{H}}(H_1+\tau N H_2)\frac{\partial H_1}{\partial x}+(H_2-\tau N H_1)\frac{\partial H_2}{\partial x}. \tag{4.24}$$

Magnetic Induction Equation:

$$u\frac{\partial H_1}{\partial x}+v\frac{\partial H_1}{\partial y}=H_1\frac{\partial u}{\partial x}+H_2\frac{\partial u}{\partial y}+\nu_0\frac{\partial^2 H_1}{\partial y^2}. \tag{4.25}$$

Microroatation Equation:

$$u\frac{\partial N}{\partial x}+v\frac{\partial N}{\partial y}=\frac{\gamma*}{\rho j}\frac{\partial^2 N}{\partial y^2}-\frac{2\zeta_1}{\rho j}\left(2N+\frac{\partial u}{\partial y}\right)+M_0\tau\bar{H}N. \tag{4.26}$$

Energy Equation:

$$u\frac{\partial T}{\partial x}+v\frac{\partial T}{\partial y}=k_\alpha\frac{\partial^2 T}{\partial y^2}+\frac{\sigma}{\rho c_p}H_2^2u^2. \tag{4.27}$$

Boundary Conditions:

The boundary conditions corresponding to the magneto micropolar fluid are as follows.

$$\left.\begin{aligned} &u=cx,\quad v=0,\quad \frac{\partial H_1}{\partial y}=H_2=0,\quad N=-N_0\frac{\partial u}{\partial y}\quad T=T_w\quad at\quad y=0,\\ &u=ax,\quad H_1=H_e(x)=H_0x,\quad N\longrightarrow 0,\ T\to T_\infty\quad as\quad y\longrightarrow\infty. \end{aligned}\right\} \tag{4.28}$$

4.4 Non-dimensionalization

In this section, we present the process of non-dimensionalization of the mathematical model governing the behavior of the proposed micropolar boundary layer flow. The procedure requires introducing the dimensionless variables and parameters to transform the original equations into a simpler form. By using the dimensionless quantities, we gain a deeper insight into the physical phenomena and make the analysis more tractable. The mathematical model will be transformed into a system of ordinary differential equations (ODEs) using the following similarity transformation [30]

$$\left.\begin{aligned} &u=cxf'(\zeta),\ v=\sqrt{\nu}cf(\zeta),\quad \zeta=\sqrt{\frac{c}{\nu}}y\quad \theta(\zeta)=\frac{T-T_\infty}{T_w-T_\infty},\\ &N=cx\sqrt{\frac{c}{\nu}}g(\zeta),\quad H_1=H_0xh'(\zeta),\quad H_2=-H_0\sqrt{\frac{\nu}{c}}h(\zeta). \end{aligned}\right\} \tag{4.29}$$

The symbol ζ represents the similarity variable. The velocity components in the x and y directions are denoted by u and v, respectively, while W is the microrotation vector and H_1 and H_2 are external magnetic fields.
The identical satisfaction of (4.22) and (4.23) has already been discussed in chapter 3.

4.4.1 Non-Dimensionalization of Momentum Equation

For the momentum equation (4.24), the following derivatives are needed:

$$\begin{aligned}\frac{\partial H1}{\partial x} &= \frac{\partial}{\partial x}(H_0 x h'(\zeta)) \\ &= H_0 h'(\zeta)\frac{\partial}{\partial x}(x) \\ &= H_0 h'(\zeta). \end{aligned} \tag{4.30}$$

$$\begin{aligned}\frac{\partial H2}{\partial x} &= \frac{\partial}{\partial x}\left(- H_0\sqrt{\frac{\nu}{c}}h(\zeta)\right) \\ &= -H_0\sqrt{\frac{\nu}{c}}h'(\zeta)\frac{\partial}{\partial x}(\zeta) \\ &= 0. \end{aligned} \tag{4.31}$$

In this subsection, we transform the governing momentum equation (4.24) into a non-dimensional form. For this purpose, we substitute all the partial derivatives (3.41) -(3.44), (4.30) and (4.31) and the velocity components from expression (4.29) into the equation (4.24) to get the following:

$$\begin{aligned}&(cxf'(\zeta)(cf'(\zeta)) + (-\sqrt{\nu c}f(\zeta)\left(cxf''(\zeta)\sqrt{\frac{c}{\nu}}\right) \\ &= \left(\frac{\mu+\zeta_1}{\rho}\right)c^2 x f'''(\zeta).\frac{1}{\nu} - \frac{\sigma}{\rho}\mu_0\left(H_0^2\left(\sqrt{\frac{\nu}{c}}\right)^2 h^2(\zeta)\right)(cxf'(\zeta)) \\ &\quad + \frac{2\zeta_1}{\rho}c^2 x g'(\zeta).\frac{1}{\nu} + \frac{1}{\rho}\frac{M_0}{\bar{H}}(H_0 x h'(\zeta) \\ &\quad + \tau\left(cx\sqrt{\frac{c}{\nu}}g(\zeta)\right)\left(-H_0\sqrt{\frac{\nu}{c}}\right)h(\zeta))H_0 h'(\zeta) \\ &\quad + (-H_0\left(\sqrt{\frac{\nu}{c}}\right)h(\zeta) - \tau cx\left(\sqrt{\frac{c}{\nu}}\right)g(\zeta)H_0 x h'(\zeta))0.\end{aligned}$$

$$\Rightarrow \quad c^2x(f'(\zeta))^2 - c^2xf(\zeta)f''(\zeta))$$
$$= \left(\frac{\mu}{\rho} + \frac{\zeta_1}{\rho}\right)c^2xf'''(\zeta).\frac{\rho}{\mu} - \frac{\sigma}{\rho}\mu_0\left(H_0^2.\frac{\nu}{c}h^2(\zeta)\right)cxf'(\zeta) + \frac{2\zeta_1}{\rho}c^2xg'(\eta).\frac{\rho}{\mu}$$
$$+ \frac{1}{\rho}\frac{M_0}{\bar{H}}(H_0xh'(\zeta) + \tau cxg(\zeta)(-H_0h(\zeta)))H_0h'(\zeta).$$

$$\Rightarrow \quad c^2x(f'(\zeta)^2 - f(\zeta)f''(\zeta)) = \frac{\mu}{\rho}f'''(\zeta).\frac{\rho}{\mu} + \frac{\zeta_1}{\rho}f'''(\zeta).\frac{\rho}{\mu}c^2x$$
$$- \frac{\sigma}{\rho}\mu_0\left(H_0^2.\frac{\nu}{c}h^2(\zeta)\right)cxf'(\zeta) + \frac{2\zeta_1}{\rho}c^2xg'(\zeta).\frac{\rho}{\mu}$$
$$+ \frac{1}{\rho}\frac{M_0}{\bar{H}}(H_0xh'(\zeta) + \tau cxg(\zeta)(-H_0h(\zeta)))H_0h'(\zeta).$$

$$\Rightarrow \quad \left(f'(\zeta)\right)^2 - f(\zeta)f''(\zeta) = f'''(\zeta) + \frac{\zeta_1}{\mu}f'''(\zeta) - \left(\frac{\sigma\mu_0H_0^2\nu}{\rho c^2}\right)h^2f'(\zeta)$$
$$+ \frac{2\zeta_1}{\mu}g'(\zeta) + \frac{1}{\rho}\frac{M_0}{\bar{H}c}(H_0h'(\zeta) - \tau g(\zeta)H_0h(\zeta))H_0h'(\zeta).$$

$$\Rightarrow \quad \left(f'(\zeta)\right)^2 - f(\zeta)f''(\zeta) = \left(1 + \frac{\zeta_1}{\mu}\right)f'''(\zeta) - \left(\frac{\sigma\mu_0H_0^2\nu}{\rho c^2}\right)h^2f'(\zeta)$$
$$+ 2Kg'(\zeta) + \frac{1}{\rho}\frac{M_0}{\bar{H}c}(H_0^2h'^2(\zeta) - H_0^2\tau g(\zeta)h(\zeta)h'(\zeta)).$$

$$\Rightarrow \quad \left(f'(\zeta)\right)^2 - f(\zeta)f''(\zeta) = (1+K)f'''(\zeta) - \frac{R_m}{R_e}h^2f'(\zeta) + 2Kg'(\zeta)$$
$$+ \frac{M_0}{\rho\bar{H}c}H_0^2(h'^2(\zeta) - \tau g(\zeta)h(\zeta)h'(\zeta)).$$

$$\Rightarrow \quad \left(f'(\zeta)\right)^2 - f(\zeta)f''(\zeta) = (1+K)f'''(\zeta) - \frac{R_m}{R_e}h^2f'(\zeta) + 2Kg'(\zeta)$$
$$+ \frac{H_0^2M_0}{\rho\bar{H}c}h'^2(\zeta) - \frac{M_0H_0^2\tau}{\rho\bar{H}c}g(\zeta)h(\zeta)h'(\zeta).$$

$$\Rightarrow \quad \left(f'(\zeta)\right)2 - f(\zeta)f''(\zeta) = (1+K)f'''(\zeta) - \frac{R_m}{R_e}h^2f'(\zeta) + 2Kg'(\zeta)$$
$$+ \frac{H_0^2}{\rho(\bar{H})^2}h'^2(\zeta) - \beta g(\zeta)h(\zeta)h'(\zeta).$$

$$\Rightarrow \quad \left(f'(\zeta)\right)2 - f(\zeta)f''(\zeta) = (1+K)f'''(\zeta) - \frac{R_m}{R_e}h^2f'(\zeta) + 2Kg'(\zeta)$$
$$+ \alpha h'^2(\zeta) - \beta g(\zeta)h(\zeta)h'(\zeta).$$

$$\Rightarrow \quad (1+K)\,f''' - \left(\frac{R_m}{R_e}\right)h^2f' + 2Kg' + \alpha h'^2 - \beta ghh' - f'^2 + ff'' = 0. \tag{4.32}$$

4.4.2 Non-Dimensionalization of the Magnetic Induction Equation

The complete procedure for the conversion of (4.25) discussed in chapter 3.

$$\lambda h''' - f''h + fh'' = 0. \tag{4.33}$$

4.4.3 Non-Dimensionalization of Microrotation Equation

In this sub-section, we transform the governing microrotation equation (4.26) into the non-dimensional form. For this purpose, we substitute all the partial derivatives (3.50)-(3.52) and (4.15) into the equation (4.26) to get the following:

$$\begin{aligned}
&(cxf'(\zeta))\left(c\sqrt{\frac{c}{\nu}}g(\zeta)\right) + (-\sqrt{\nu c}f(\zeta)\left(cx\left(\sqrt{\frac{c}{\nu}}\right)g'(\zeta)\sqrt{\frac{c}{\nu}}\right)\\
&= \frac{\gamma*}{\rho j}\left(c^2xg''(\zeta)\sqrt{\frac{c}{\nu}}\right).\frac{1}{\nu} - \frac{2\zeta_1}{\rho j}\left(2cx\sqrt{\frac{c}{\nu}}g(\zeta) + cxf''(\zeta)\sqrt{\frac{c}{\nu}}\right) + M_0\tau\bar{H}N.
\end{aligned}$$

$$\begin{aligned}
\Rightarrow\quad &\left(c^2xf'(\zeta)\left(\sqrt{\frac{c}{\nu}}\right)g(\zeta)\right) - \left(c^2xf(\zeta)\sqrt{\frac{c}{\nu}}g'(\zeta)\right) = \frac{(\mu+\frac{\zeta_1}{2}).j}{\rho j}c^2xg''(\zeta)\sqrt{\frac{c}{\nu}}.\frac{1}{\nu}\\
&- \frac{2\zeta_1}{\rho j}\left(2cx\sqrt{\frac{c}{\nu}}g(\zeta) + cxf''(\zeta)\sqrt{\frac{c}{\nu}}\right) + M_0\tau\bar{H}\left(cx\sqrt{\frac{c}{\nu}}g(\zeta)\right).
\end{aligned}$$

$$\begin{aligned}
\Rightarrow\quad &c^2x\sqrt{\frac{c}{\nu}}\left(f'(\zeta)g(\zeta) - f(\zeta)g'(\zeta)\right) = \frac{(\mu+\frac{\zeta_1}{2})}{\rho}c^2xg''(\zeta)\left(\sqrt{\frac{c}{\nu}}\right).\frac{1}{\nu}\\
&- \frac{2\zeta_1}{\rho j}cx\sqrt{\frac{c}{\nu}}\left(2g(\zeta) + f''(\zeta)\right) + M_0\tau\bar{H}.cx\sqrt{\frac{c}{\nu}}g(\zeta).
\end{aligned}$$

$$\Rightarrow\quad f'(\zeta)g(\zeta) - fg'(\zeta) = \frac{\mu(1+\frac{\zeta_1}{2\mu})}{\rho}g''(\zeta).\frac{1}{\nu} - \frac{2\zeta_1}{\rho jc}(2g(\zeta) + f''(\zeta)) + \frac{M_0\tau\bar{H}}{c}g(\zeta).$$

$$\Rightarrow\quad f'(\zeta)g(\zeta) - fg'(\zeta) = \frac{\mu(1+\frac{\zeta_1}{2\mu})}{\rho}g''(\zeta).\frac{\rho}{\mu} - \frac{2\zeta_1}{\rho jc}(2g(\zeta) + f''(\zeta)) + \frac{M_0\tau\bar{H}}{c}g(\zeta).$$

$$\Rightarrow\quad f'(\zeta)g(\zeta) - fg'(\zeta) = \left(1+\frac{K}{2}\right)g''(\zeta).\frac{\rho}{\mu} - \beta^*(2g(\zeta) + f''(\zeta)) + \frac{\beta}{\alpha}g(\zeta).$$

$$\Rightarrow\quad \left(1+\frac{K}{2}\right)g''(\zeta) - \beta^*(2g(\zeta) + f''(\zeta)) + \frac{\beta}{\alpha}g(\zeta) - f'(\zeta)g(\zeta) + fg'(\zeta) = 0.$$

$$\Rightarrow\quad \left(1+\frac{K}{2}\right)g'' - \beta^*(2g + f'') + \frac{\beta}{\alpha}g - f'g + fg' = 0. \tag{4.34}$$

4.4.4 Non-Dimensionalization of Energy Equation

In this sub-section, we discuss the non-dimensionalization process of the energy equation (4.27) for our micropolar boundary layer flow.

$$\theta(\zeta) = \frac{T - T_\infty}{T_w - T_\infty}$$

$$T = T_\infty + (T_w - T_\infty)\theta(\zeta). \tag{4.35}$$

$$\Rightarrow \quad \frac{\partial T}{\partial x} = 0. \tag{4.36}$$

Now, differentiating equation (4.35) w.r.t y, we obtain

$$\frac{\partial T}{\partial y} = (T_w - T_\infty)\theta'(\zeta).\frac{\partial \zeta}{\partial y}$$

$$\frac{\partial T}{\partial y} = (T_w - T_\infty)\theta'(\zeta).\sqrt{\frac{c}{\nu}}. \tag{4.37}$$

$$\Rightarrow \quad \frac{\partial^2 T}{\partial y^2} = \frac{c}{\nu}(T_w - T_\infty)\theta''(\zeta). \tag{4.38}$$

Now, we substitute the partial derivatives (4.36)-(4.38) and velocity components u and v from (4.29) into equation (4.27) to get the following:

$$cxf'(\zeta)(0) - \sqrt{\nu c}f(\zeta)(T_w - T_\infty)\theta'(\zeta).\left(\sqrt{\frac{c}{\nu}}\right)$$
$$= k_\alpha c(T_w - T_\infty)\theta''(\zeta).\frac{1}{\nu} + \frac{\sigma}{\rho c_p}\left(H_0^2.\frac{\nu}{c}h^2(\zeta)\right)c^2x^2f'^2(\zeta).$$

$$\Rightarrow \quad -c(T_w - T_\infty)f(\zeta)\theta'(\zeta) = k_\alpha c(T_w - T_\infty)\theta''(\zeta).\frac{1}{\nu} + \frac{\sigma}{\rho c_p}H_0^2.\frac{\nu}{c}h^2(\zeta)c^2x^2f'^2(\zeta).$$

$$\Rightarrow \quad -c(T_w - T_\infty)f(\zeta)\theta'(\zeta) = c(T_w - T_\infty)k_\alpha\theta''(\zeta).\frac{1}{\nu} + \frac{\sigma}{\rho c_p}H_0^2.\frac{\nu}{c}h^2(\zeta)cx^2f'^2(\zeta).$$

$$\Rightarrow \quad -f(\zeta)\theta'(\zeta) = k_\alpha\theta''(\zeta).\frac{1}{\nu} + \frac{\sigma H_0^2\nu}{\rho c^2}h^2(\zeta).\frac{cx^2}{c_p(T_w - T_\infty)}f'^2(\zeta).$$

$$\Rightarrow \quad -f(\zeta)\theta'(\zeta) = \frac{k_\alpha}{\nu}\theta''(\zeta) + \frac{Rm}{Re}h^2(\zeta).Ecf'^2(\zeta).$$

$$\Rightarrow \quad -f(\zeta)\theta'(\zeta) = K^*\theta''(\zeta) + \frac{Rm}{Re}h^2(\zeta).Ecf'^2(\zeta).$$

$$\Rightarrow \quad K^*\theta''(\zeta) + \frac{Rm}{Re}h^2(\zeta).Ecf'^2(\zeta) + f(\zeta)\theta'(\zeta) = 0. \tag{4.39}$$

4.4.5 Non-Dimensionalization of Boundary Conditions

The boundary conditions for equations (4.24)-(4.26) have already been non-dimensionalized in Chapter 3. Here, we will non-dimensionalize the corresponding boundary condition for equation (4.27) using equation (4.29) as follows:

$$\bullet \quad T = Tw, \qquad at \quad y = 0.$$

$$\Rightarrow \quad (T_w - T_\infty)\theta(\zeta) + T_\infty = Tw, \qquad at \quad \zeta = 0.$$

$$\Rightarrow \quad (T_w - T_\infty)\theta(\zeta) = Tw - T_\infty, \qquad at \quad \zeta = 0.$$

$$\Rightarrow \quad \theta(\zeta) = 1, \qquad at \quad \zeta = 0.$$

$$\bullet \quad T \longrightarrow T\infty, \qquad as \quad y \longrightarrow \infty.$$

$$\Rightarrow \quad (T_w - T_\infty)\theta(\zeta) + T_\infty \longrightarrow T\infty, \qquad as \quad \zeta \longrightarrow \infty.$$

$$\Rightarrow \quad \theta(\zeta) \longrightarrow 0, \qquad as \quad \zeta \longrightarrow \infty.$$

4.4.6 Non-dimensionalization of the Skin-friction and Nusselt Number

The skin friction have already been discussed in chapter 3.

Nusselt number

$$\begin{aligned} Nu &= \frac{xk(Tw - T_\infty)\theta'(\zeta)\sqrt{\frac{c}{\nu}}}{k(Tw - T_\infty)} \\ &= x\sqrt{\frac{c}{\nu}}\theta'(\zeta) \\ &= \sqrt{\frac{cx^2}{\nu}}\theta'(\zeta) \\ &= \sqrt{\frac{(cx)x}{\nu}}\theta'(\zeta) \\ &= \sqrt{\frac{u_w x}{\nu}}\theta'(\zeta) \end{aligned}$$

$$= \sqrt{Re_x}\theta'(\zeta)$$
$$\Rightarrow Re_x^{-1/2} Nu = \theta'(\zeta). \tag{4.40}$$

4.5 Solution Framework

In order to solve the ODEs (4.32), (4.33) and (4.34) by the shooting method:

$$f(\zeta) = T_1,\ f'(\zeta) = T_1' = T_2,\ f''(\zeta) = T_2' = T_3,\ h(\zeta) = T_4,$$
$$h'(\zeta) = T_4' = T_5,\ h''(\zeta) = T_5' = T_6,\ g(\zeta) = T_7,\ g'(\zeta) = T_7' = T_8.$$

The system of equations (4.32), (4.33) and (4.34) can be represented in the form of the following first-order coupled ODEs:

$$\begin{aligned}
&T_1{}' = T_2, && T_1(0) = 0,\\
&T_2' = T_3, && T_2(0) = 1,\\
&T_3' = \frac{1}{1+K}\left(\frac{Rm}{Re}(T_4)^2 T_2 - 2KT_8 - \alpha T_5^2 + \beta T_7 T_4 T_5 + T_2^2 - T_1 T_3\right), && T_3(0) = p,\\
&T_4' = T_5, && T_4(0) = 0,\\
&T_5' = T_6, && T_5(0) = q,\\
&T_6' = \lambda(T_4 T_3 - T_6 T_1), && T_6(0) = 0,\\
&T_7' = T_8, && T_7(0) = -N_0(t),\\
&T_8' = \frac{2}{K+2}\left(\beta^*(2T_7 + T_3) + \frac{\beta}{\alpha}T_7 + T_2 T_7 - T_1 T_8\right), && T_8(0) = w,
\end{aligned}$$

where p, q and w are the missing initial conditions. Now, the Runge-Kutta method of order four will be used to solve the above mentioned first order initial value problem. It is necessary to choose the missing conditions, such that:

$$\left.\begin{aligned}
T_2(p,q,w) - A^* &= 0,\\
T_5(p,q,w) - 1 &= 0,\\
T_7(p,q,w) &= 0,
\end{aligned}\right\} \tag{4.41}$$

Newton's method has been used to solve the algebraic equation (4.41) numerically. This formula has the following itreative form:

$$\begin{bmatrix} p \\ q \\ w \end{bmatrix}_{(n+1)} = \begin{bmatrix} p \\ q \\ w \end{bmatrix}_{(n)} \begin{bmatrix} \frac{\partial T_2}{\partial p} & \frac{\partial T_2}{\partial q} & \frac{\partial T_2}{\partial w} \\ \frac{\partial T_5}{\partial p} & \frac{\partial T_5}{\partial q} & \frac{\partial T_5}{\partial w} \\ \frac{\partial T_7}{\partial p} & \frac{\partial T_7}{\partial q} & \frac{\partial T_7}{\partial w} \end{bmatrix}_{(n)} \begin{bmatrix} T_2 - A^* \\ T_5 - 1 \\ T_7 \end{bmatrix}_{(n)}$$

To successfully iterate the above formula, we need the following new notations:

$$\frac{\partial T_1}{\partial p} = T_9, \quad \frac{\partial T_2}{\partial p} = T_{10}, \quad \frac{\partial T_3}{\partial p} = T_{11}, \quad \frac{\partial T_4}{\partial p} = T_{12}, \frac{\partial T_5}{\partial p} = T_{13}, \quad \frac{\partial T_6}{\partial p} = T_{14},$$

$$\frac{\partial T_7}{\partial p} = T_{15}, \quad \frac{\partial T_8}{\partial p} = T_{16}, \quad \frac{\partial T_1}{\partial q} = T_{17}, \quad \frac{\partial T_2}{\partial q} = T_{18}, \quad \frac{\partial T_3}{\partial q} = T_{19}, \frac{\partial T_4}{\partial q} = T_{20},$$

$$\frac{\partial T_5}{\partial q} = T_{21}, \quad \frac{\partial T_6}{\partial q} = T_{22}, \quad \frac{\partial T_7}{\partial q} = T_{23}, \quad \frac{\partial T_8}{\partial q} = T_{24}, \quad \frac{\partial T_1}{\partial w} = T_{25}, \frac{\partial T_2}{\partial w} = T_{26},$$

$$\frac{\partial T_3}{\partial w} = T_{27}, \quad \frac{\partial T_4}{\partial w} = T_{28}, \quad \frac{\partial y_5}{\partial w} = T_{29}, \quad \frac{\partial T_6}{\partial w} = T_{30}, \quad \frac{\partial T_7}{\partial w} = T_{31}, \quad \frac{\partial T_8}{\partial w} = T_{32},$$

The Netwon's iterative technique takes on the following form, as a result of the above notations:

$$\begin{bmatrix} p \\ q \\ w \end{bmatrix}_{(n+1)} = \begin{bmatrix} p \\ q \\ w \end{bmatrix}_{(n)} \begin{bmatrix} T_9 & T_{17} & T_{25} \\ T_{12} & T_{20} & T_{28} \\ T_{15} & T_{23} & T_{31} \end{bmatrix}_{(n)} \begin{bmatrix} T_2 - A^* \\ T_5 - 1 \\ T_7 \end{bmatrix}_{(n)}.$$

To find the missing derivatives present in the Newton formula, the following initial value problem, will have to be tackled.

$$T_9' = T_{10}, \qquad T_9(0) = 0,$$

$$T_{10}' = T_{11}, \qquad T_{10}(0) = 0,$$

$$T_{11}' = \frac{1}{1+K}\left(\frac{Rm}{Re}T_4^2 T_{10} + T_2 2T_4 T_{12} - 2KT_{16} - 2\alpha T_5 T_{13} + \beta(T_7 T_4 T_{13} + T_7 T_{12} T_5 + T_{15} T_4 T_5) + 2T_2 T_{10} - T_1 T_{11} + T_3 T_9\right), \qquad T_{11}(0) = 1.$$

$$T_{12}' = T_{13}, \qquad T_{12}(0) = 0,$$

$$T_{13}' = T_{14}, \qquad T_{13}(0) = 0,$$

$$T'_{14} = \lambda(T_4T_{11} + T_3T_{12} - T_6T_9 - T_1T_{14}), \qquad T_{14}(0) = 0.$$

$$T'_{15} = T_{16}, \qquad T_{15}(0) = -N_0,$$

$$T'_{16} = \frac{2}{K+2}\Bigg(\beta^*(2T_{15}+T_{11})+\frac{\beta}{\alpha}T_{15} \quad +T_2T_{15}+T_7T_{10}-T_1T_{16}-T_8T_9\Bigg), \qquad T_{16}(0) = 0.$$

$$T'_{17} = T_{18}, \qquad T_{17}(0) = 0,$$

$$T'_{18} = T_{19}, \qquad T_{18}(0) = 0,$$

$$T'_{19} = \frac{1}{1+K}\Bigg(\frac{Rm}{Re}T_4^2T_{18} + T_2 2T_4T_{20} - 2KT_{24} - 2\alpha T_5T_{21}$$
$$+ \beta(T_7y_4T_{21} + T_7T_{20}T_5 + T_{23}T_4T_5) + 2T_2T_{18} - T_1T_{19} + T_3T_{17}\Bigg), \qquad T_{19}(0) = 0.$$

$$T'_{20} = T_{21}, \qquad T_{20}(0) = 0,$$

$$T'_{21} = T_{22}, \qquad T_{21}(0) = 1,$$

$$T'_{22} = \lambda(T_4T_{19} + T_3T_{20} - T_6T_{17} - T_1T_{22}), \qquad T_{22}(0) = 0.$$

$$T'_{23} = T_{24}, \qquad T_{23}(0) = 0,$$

$$T'_{24} = \frac{2}{K+2}\Bigg(\beta^*(2T_{23} + T_{19}) + \frac{\beta}{\alpha}T_{23}$$
$$+ T_2T_{23} + T_7T_{18} - T_1T_{24} - T_8T_{17}\Bigg), \qquad T_{24}(0) = 0.$$

$$T'_{25} = T_{26}, \qquad T_{25}(0) = 0,$$

$$T'_{26} = T_{27}, \qquad T_{26}(0) = 0,$$

$$T'_{27} = \frac{1}{1+K}\Bigg(\frac{Rm}{Re}T_4^2T_{26} + T_2 2T_4T_{28} - 2KT_{32} - 2\alpha T_5T_{29}$$
$$+ \beta(T_7T_4T_{29} + T_7T_{28}T_5 + T_{31}T4T_5) + 2T_2T_{26} - T_1T_{27} + T_3T_{25}\Bigg) \qquad T_{27}(0) = 0.$$

$$T'_{28} = T_{29}, \qquad T_{28}(0) = 0,$$

$$T'_{29} = T_{30}, \qquad T_{29}(0) = 0,$$

$$T'_{30} = \lambda(T_4T_{27} + T_3T_{28} - T_6T_{25} - T_1T_{30}), \qquad T_{30}(0) = 0.$$

$$T'_{31} = T_{32}, \qquad T_{31}(0) = 0,$$

$$T'_{32} = \frac{2}{K+2}\Bigg(\beta^*(2T_{31} + T_{27}) + \frac{\beta}{\alpha}T_{31} \qquad T_{32}(0) = 1.$$
$$+ y_2T_{31} + y_7T_{26} - T_1T_{32} - T_8T_{25}\Bigg),$$

Following stopping criteria is used for Newtons's method:

$$\max\left\{\left|T_2\left(\zeta_\infty,p,q,w\right)-A^*\right|,\left|T_5\left(\zeta_\infty,p,q,w\right)-1\right|,\left|T_7\left(\zeta_\infty,p,q,w\right)\right|\right\}<\epsilon,$$

Now, to solve the energy equation numerically by using shooting method, f and f' and h will be taken as a known functions. The notations below are used for the implementation of the shooting method.

$$\theta(\zeta)=Z_1,\qquad \theta'(\zeta)=Z_1'=Z_2,\qquad \theta''(\zeta)=Z_2'$$

The following system of first-order ODEs is created for the energy equation.

$$\begin{aligned} Z_1' &= Z_2, & Z_1(0)&=1,\\ Z_2' &= \left(\frac{1}{K^*}\right)\left[-\frac{Rm}{Re}Ech^2f'^2-fZ_2\right] & Z_2(0)&=s. \end{aligned}$$

To utilize the Runge-Kutta 4th order (RK4) method for numerical solution of the above mentioned initial value problem, the condition s within the system of equations needs to be carefully chosen. The missing condition s is to be chosen such that.

$$Z_1(\zeta_\infty,s)=0.$$

Newton's method will be used to find s with the following iterative scheme:

$$s^{(n+1)}=s^n-\frac{Z_1\left(\zeta_\infty,s^{(n)}\right)}{\left(\frac{\partial}{\partial s}Z_1\left(\zeta_\infty,s\right)\right)^{(n)}}.$$

We further introduce the following notations:

$$\frac{\partial z_1}{\partial s}=Z_3,\qquad \frac{\partial z_2}{\partial s}=Z_4,$$

As a result these new notations, the Newton's iterative scheme gets the form:

$$s^{(n+1)}=s^n-\frac{Z_1(\zeta_\infty,s^{(n)})}{Z_3(\zeta_\infty,s^{(n)})}.$$

Now differentiating the most recently presented system of two first order ODEs with respect to s, we get another system of ODEs, as follows:

$$Z_3' = Z_4, \qquad Z_3(0) = 0,$$

$$Z_4' = \left(\frac{1}{K^*}\right)\Big[- fZ_4\Big] \qquad Z_4(0) = 1.$$

The stopping criteria for the Newton's techniques is set as.

$$|Z_1(\zeta_\infty, s)| < \epsilon.$$

4.6 Results Interpretation

While transforming the governing PDEs describing the fluid flow into a system of ODEs, several crucial parameters emerge. The impact of these physical parameters on the hydrodynamic velocity $f'(\eta)$, macrorotational velocity $g(\eta)$, and magnetic induction $h'(\eta)$ distributions is thoroughly investigated through the use of graphical representations. The significance and interpretations of the impact of each parameter in this study are discussed in detail, and the study's results are comprehensively presented.

4.6.1 Analysis of Computational Result

This section is devoted to an investigation of the influence of various physical parameters on the coefficient of skin friction $Re^{\frac{1}{2}}Cf_x$. An increase in the micropolar constant, denoted as K, as well as in magnetization, represented by β, and the magnetic Reynolds number, denoted as Rm, leads to a reduction in the coefficient of skin friction. Conversely, for higher values of the micro inertial coupling parameter, denoted as β^*, and the Reynolds number, denoted as Re, the skin friction coefficient also exhibits an increase, as summarized in Table 4.1. Furthermore, Table 4.2 provides an overview of the conditions corresponding to the missing initial value problem (IVP) for the parameter values presented in Table 1.

TABLE 4.1: The numerical results of $(Re_x)^{1/2}Cf_x$ and $(Re_x)^{-1/2}Nu_x$.

α	K	λ	β	β^*	Re	Rm	N_0	A^*	Ec	K^*	$Re^{1/2}Cf_x$	$Re^{-1/2}Nu_x$
1.0	0.2	0.5	0.3	0.1	10	0.1	2.0	1.0	0.2	0.2	-0.367205	-3.984554
0.6											-0.840236	-3.316414
0.7											-0.770976	-3.466088
0.8											-0.674206	-3.623007
	0.05										-0.283715	-4.078440
	0.1										-0.305559	-4.056018
	0.15										-0.332594	-4.026027
		0.1									-0.365789	-3.965751
		0.2									-0.368664	-3.970817
		0.3									-0.369232	-3.975571
			0.2								-0.347773	-4.004196
			0.4								-0.390230	-3.960581
			0.5								-0.417955	-3.930664
				0.0							-0.369465	-3.997120
				0.15							-0.362630	-3.987696
				0.2							-0.365566	-3.990536
					6						-0.482897	-3.831159
					12						-0.328315	-4.032636
					18						-0.249571	-4.125680
						0.2					-0.524927	-3.770707
						0.3					-0.615757	-3.628363
						0.4					-0.675648	-3.522731
							2.1				-0.379156	-3.967343
							2.12				-0.381708	-3.963630
							2.13				-0.383005	-3.961738
								1.1			-0.570630	-3.775438
								1.2			-0.681542	-3.641917
								1.3			-0.749284	-3.551162
									0.1		-0.367205	-4.001512
									0.3		-0.367205	-3.967595
									0.4		-0.367205	-3.950637
										0.1	-0.367205	-5.740823
										0.3	-0.367205	-3.220232
										0.4	-0.367205	-2.770200

TABLE 4.2: Numerical Results for the Missing Initial Value Problem (IVP).

α	K	λ	β	β^*	Re	Rm	N_0	A^*	Ec	K^*	$f''(0)$	$h'(0)$	$g'(0)$	$\theta'(0)$
1.0	0.2	0.5	0.3	0.1	10	0.1	2.0	1.0	0.2	0.2	-0.459006	0.846533	-0.969997	-3.984554
0.6											-1.050295	0.619311	-1.630550	-3.316414
0.7											-0.963720	0.664191	-1.664933	-3.466088
0.8											-0.842758	0.715439	-1.574037	-3.623007
	0.05										-0.298647	0.880815	-0.663494	-4.078440
	0.1										-0.339510	0.872562	-0.745405	-4.056018
	0.15										-0.391287	0.861584	-0.843947	-4.026027
		0.1									-0.457236	0.892257	-0.961892	-3.965751
		0.2									-0.460830	0.870277	-0.970731	-3.975571
		0.3									-0.461540	0.858510	-0.973342	-3.975571
			0.2								-0.434716	0.853555	-0.958650	-4.004196
			0.4								-0.4877886	0.838010	-0.982817	3.960581
			0.5								-0.522444	0.827451	-0.996837	-3.930664
				0.0							-0.461831	0.843680	-0.909359	-3.977120
				0.15							-0.457900	0.847740	-0.998423	-3.987696
				0.2							0.456957	0.848831	-1.025834	-3.990536
					6						-0.603621	0.791776	-1.235927	-3.831159
					12						-0.410394	0.864120	-0.875643	-4.032636
					18						-0.311964	0.898634	-0.677864	-4.125680
						0.2					-0.656158	0.770857	-1.326334	-3.770707
						0.3					-0.769697	-0.723432	-1.508009	-3.628363
						0.4					-0.844560	0.690250	-1.615322	-3.522731
							2.1				-0.486098	0.840329	-1.075478	-3.967343
							2.12				-0.491892	0.838996	-1.097934	-3.963630
							2.13				-0.494839	0.838316	-1.109343	-3.961738
								1.1			-0.713288	0.702176	-1.437419	-0.570630
								1.2			-0.851928	0.606889	-1.662355	-3.641917
								1.3			-0.936605	0.538530	-1.786689	-3.551162
									0.1		-0.459006	0.846533	-0.969997	-4.001512
									0.3		-0.459006	0.846533	-0.969997	-3.967595
									0.4		-0.459006	0.846533	-0.969997	-3.950637
										0.1	-0.459006	0.846533	-0.969997	-5.740823
										0.3	-0.459006	0.846533	-0.969997	-3.220232
										0.4	-0.459006	0.846533	-0.969997	-2.770200

4.6.2 Hydrodynamic Velocity Profile

In Figure 4.1, the increasing hydrodynamics velocity profile for different values of Reynolds number (Re) are shown with the varying values of magnetization parameter. As Re increases, the ratio of inertial forces to viscous forces in the fluid flow becomes greater. This amplification in inertia causes fluid particles near the boundary to accelerate more rapidly, resulting in a steeper velocity gradient and a more pronounced velocity profile. Essentially, higher Reynolds numbers signify that the fluid is less influenced by viscosity and more by inertia, leading to a more dynamic flow with a sharper velocity change near the boundary.

Figure 4.2 exhibits the diminishing hydrodynamics velocity profile as magnetic Reynolds number (Rm) increases. This trend is a consequence of the intricate interaction between the magnetic field and the fluid flow. With the escalation of Rm, magnetic effects become increasingly dominant, culminating in the generation of substantial Lorentz forces that act to suppress the velocity gradient. These Lorentz forces counteract the fluid's motion, effectively damping the hydrodynamics and resulting in a flatter velocity profile. This behavior is typical in magnetohydrodynamic (MHD) flows, where magnetic forces significantly modify fluid dynamics.

Turning to Figure 4.3, an augmentation in the hydrodynamics velocity profile with an increasing micropolar constant (K) can be elucidated by considering the characteristics of micropolar fluids. A higher value of K signifies a greater contribution of microrotation to the flow. Microrotation introduces additional rotational effects within the fluid, leading to an increased angular velocity and, consequently, a more pronounced velocity profile. In essence, higher values of K enhance the rotational aspects of the flow, causing the velocity to change more dramatically near the boundary.

Figure 4.4 portrays the decreasing behavior of the hydrodynamics velocity profile near the sheet as the magnetization parameter (β) increases. This phenomenon arises from the magnetic effects on fluid flow. As β increases, the magnetic field exerts a more potent influence on the fluid, causing fluid particles to align more with the field's direction. This

alignment suppresses the fluid's intrinsic rotational motion and dampens the velocity gradient, resulting in a flatter velocity profile. Essentially, higher values of β correspond to stronger magnetization, which significantly alters the flow dynamics and reduces the hydrodynamic velocity gradient.

4.6.3 Macrorotational Velocity Profile

In the study of magneto-micropolar boundary layer models, the macrorotational velocity profile $g(\zeta)$ takes centeral stage due to its crucial role in understanding the fluid's overall rotational behavior, especially in the presence of Micromagnetorotation (MMR) effects. Figures 4.5 to 4.8 investigate how various parameters influence this profile.

Figure 4.5 reveals an unexpected behavior; as the Re increases, initially the macrorotational velocity profile decreases near the stretching plate. This decline stems from the dominance of fluid inertia at higher Re. However, as we move away from the plate, the boundary layer characteristics evolve, and rotational effects start to prevail, leading to a reversal in the profile's behavior. This intriguing reversal signifies the transition from an inertia-dominated region close to the plate to a rotationally influenced area further away.

Figure 4.6 sheds light on the influence of the Rm on the macrorotational velocity profile. As Rm rises, magnetic effects intensify, promoting fluid rotation and elevating the macrorotational profile. Nevertheless, near the stretching plate, this trend reverses due to the intricate interaction between magnetic forces, resulting in a complex behavior with a reversal close to the plate.
Moving to Figure 4.7, the impact of the micropolar constant (K) becomes evident as the macrorotational velocity profile increases with higher K. This enhancement is attributed to the heightened contribution of microrotation, intensifying fluid rotation and overall increasing the macrorotational velocity profile.

Lastly, Figure 4.8 explores the effect of the magnetization parameter (β) on the macrorotational velocity profile. An initial increase is observed as β rises, primarily due to

enhanced fluid alignment with the magnetic field, which intensifies fluid rotation. However, away from the stretching surface, the fluid's response to magnetic effects becomes more intricate, resulting in a reverse behavior.

4.6.4 Magnetic Induction Profile

Figure 4.9 delves into the effect of Reynolds number (Re) on the magnetic induction profile. Notably, as Re escalates, a discernible increase in the magnetic induction profile is observed. This phenomenon stems from heightened fluid dynamics driven by increased inertia. With rising Reynolds numbers, the fluid's momentum becomes more pronounced, enabling it to more effectively transmit magnetic effects throughout the boundary layer.

Figure 4.10 shifts the focus to the micro-inertial coupling parameter (β^*) and its influence on the magnetic induction profile. Here, an intriguing trend emerges: an ascent in the magnetic induction profile with increasing values of β^*. This trend signifies the heightened interplay between micro-inertial effects and magnetization. Greater β^* values denote a more substantial contribution of micropolar fluid characteristics to the fluid's magnetic field response, amplifying the magnetic induction profile.

Figure 4.11 investigates the role of the micropolar constant (K) in shaping the magnetic induction profile. As K assumes higher values, a notable elevation in the magnetic induction profile becomes evident. This enhancement is attributed to the augmented influence of micropolar characteristics on the fluid's response to the magnetic field, resulting in an intensified magnetic induction profile.

Figure 4.12 turns attention to the magnetization parameter (β) and its impact on the magnetic induction profile. Initially, as β increases, a decrease in the profile is observed, attributable to the strengthening influence of the magnetic field, aligning fluid particles more closely with the field's direction. Intriguingly, this behavior undergoes a reversal after a specific distance from the sheet.

4.6.5 Temperature Profile

Here we examine the influence of several physical parameters on the temperature distribution, denoted as $\theta(\zeta)$. In Figure 4.13, we observe that increasing the Eckert number Ec leads to higher fluid temperatures. Physically, the effect of the Eckert number on the temperature distribution can be understood through the fluid's energy conversion. With higher Ec values, the fluid's kinetic energy dominates, and the excessive kinetic energy is converted into thermal energy. This process leads to increase the heat generation within the fluid, subsequently raising the fluid temperature.
Figure 4.14 elucidates the influence of the Magnetic Reynolds number Rm on the temperature distribution $\theta(\zeta)$. Notably, it is observed that higher values of the magnetic Reynolds parameter contribute to a discernible augmentation in fluid temperature.

4.6.6 Graphically Behavior of Physical Quantities

In Figure 4.15, the variation in the coefficient of skin friction is depicted concerning the magnetic Reynolds number (Rm) and the micro-inertial coupling parameter (β^*). Clearly, the coefficient of skin friction experiences a decrease with higher values of β^*. Figure 4.16 delves into the analysis of $Re_x^{1/2}Cf_x$ for different values of the micropolar constant (K) and the magnetization parameter (β) for a micropolar fluid.

It is evident that the coefficient of skin friction undergoes a decrease with increasing values of these parameters, indicating that elevated K and β lead to a more rapid fluid velocity gradient. In Figure 4.17, the impact of the micropolar constant (K) and the micro-inertial coupling parameter (β^*) on the local Nusselt number ($Re_x^{-1/2}Nu_x$) is explored, taking into account the MMR effect. Higher values of K and β^* correlate with an increased local Nusselt number, signifying enhanced heat transfer characteristics.
Figure 4.18 depicts the fluctuation in $Re_x^{-1/2}Nu_x$ due to changes in Eckert (Ec) and the magnetization parameter (β) under the influence of the MMR effect. Elevated values of Ec and β enhance $Re_x^{-1/2}Nu_x$, showcasing improved heat transfer performance. Conversely, lower values of Ec and β may reduce $Re_x^{-1/2}Nu_x$, indicating a potential decrease in heat transfer efficiency.

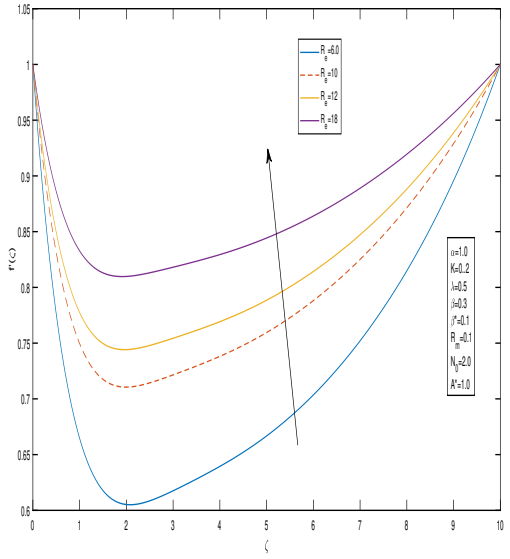

FIGURE 4.1: Effect of Re on $f'(\zeta)$

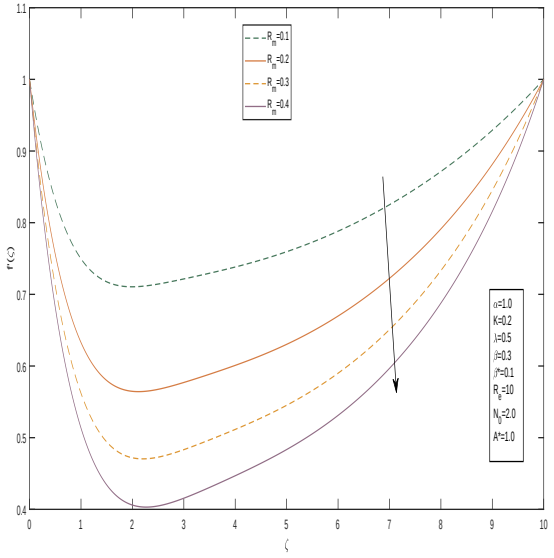

FIGURE 4.2: Effect of Rm on $f'(\zeta)$

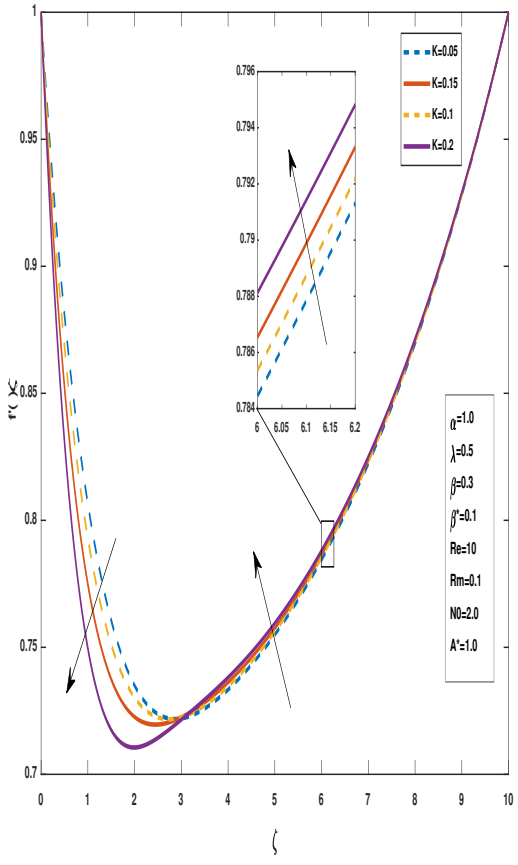

FIGURE 4.3: Effect of K on $f'(\zeta)$

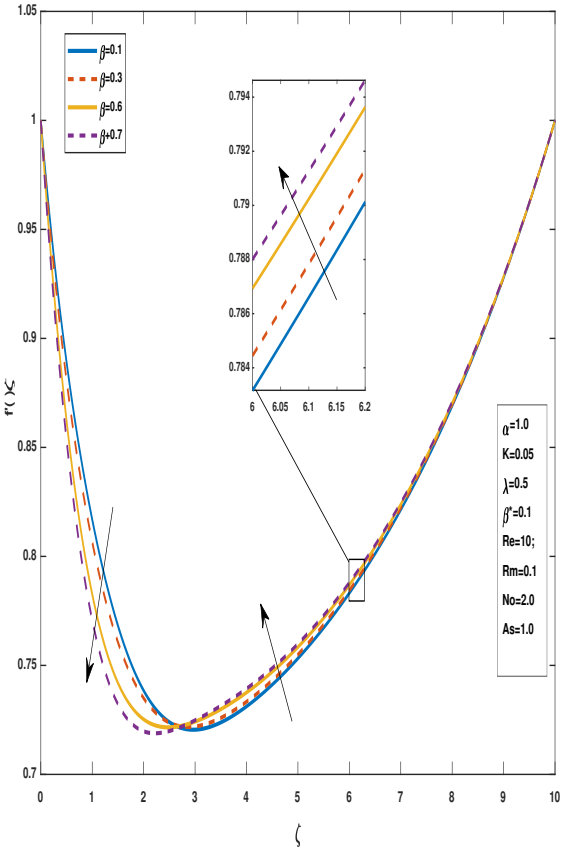

FIGURE 4.4: Effect of β on $f'(\zeta)$

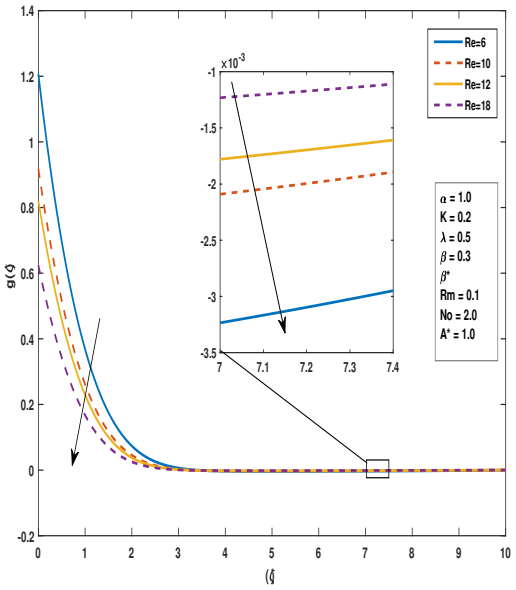

FIGURE 4.5: Effect of Re on $g(\zeta)$

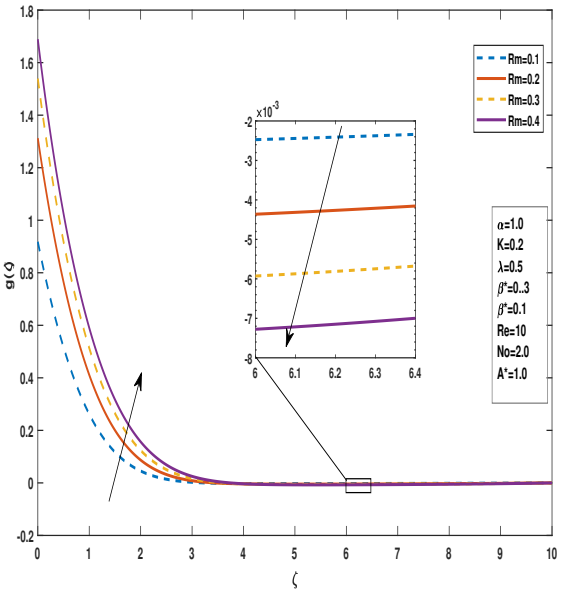

FIGURE 4.6: Effect of Rm on $g(\zeta)$

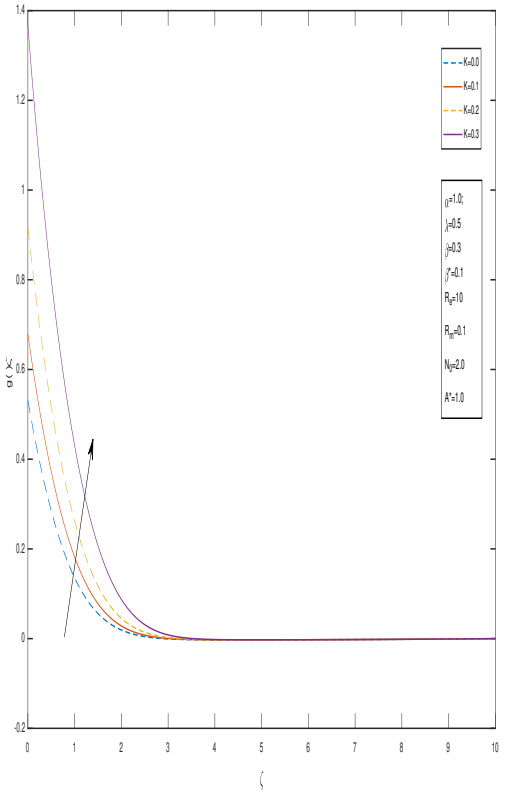

FIGURE 4.7: Effect of K on $g(\zeta)$

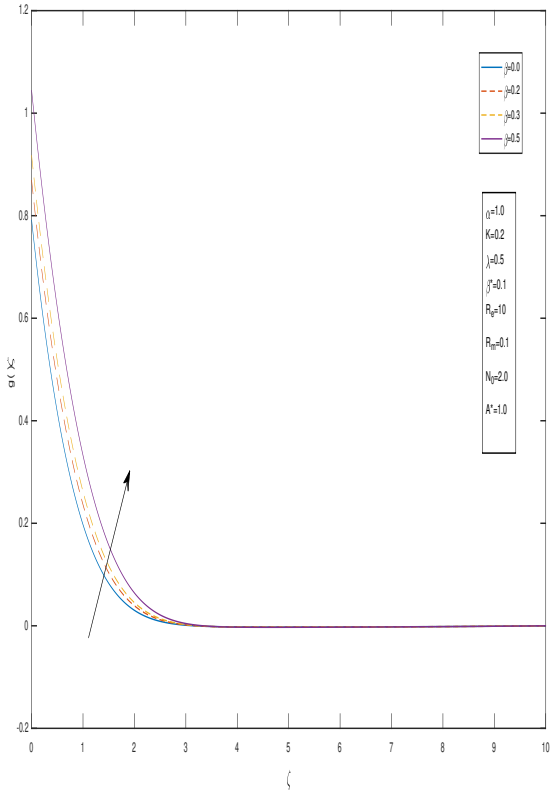

FIGURE 4.8: Effect of β on $g(\zeta)$

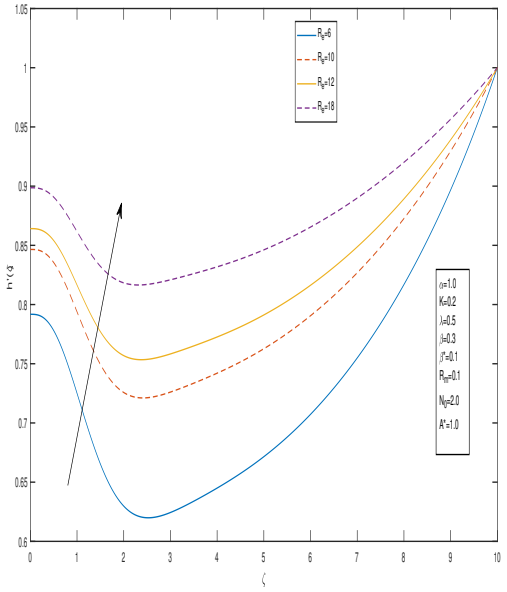

FIGURE 4.9: Effect of Re on $h'(\zeta)$

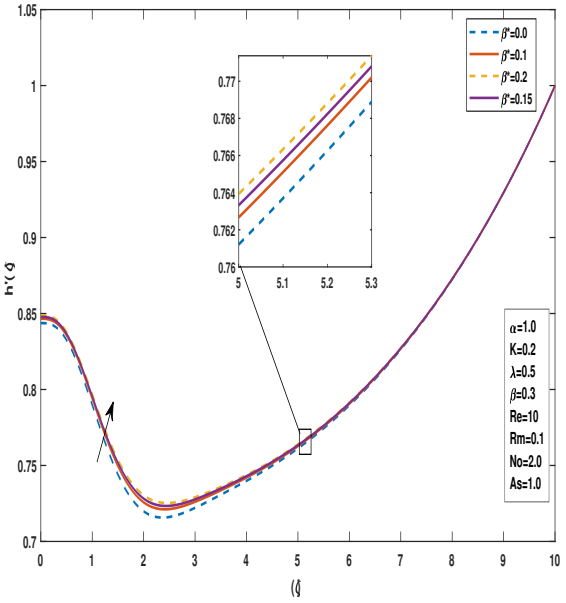

FIGURE 4.10: Effect of β^* on $h'(\zeta)$

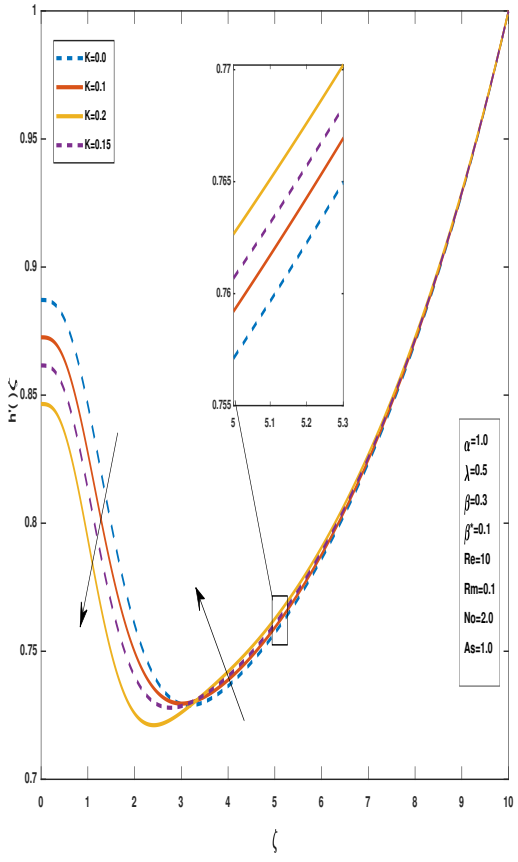

FIGURE 4.11: Effect of K on $h'(\zeta)$

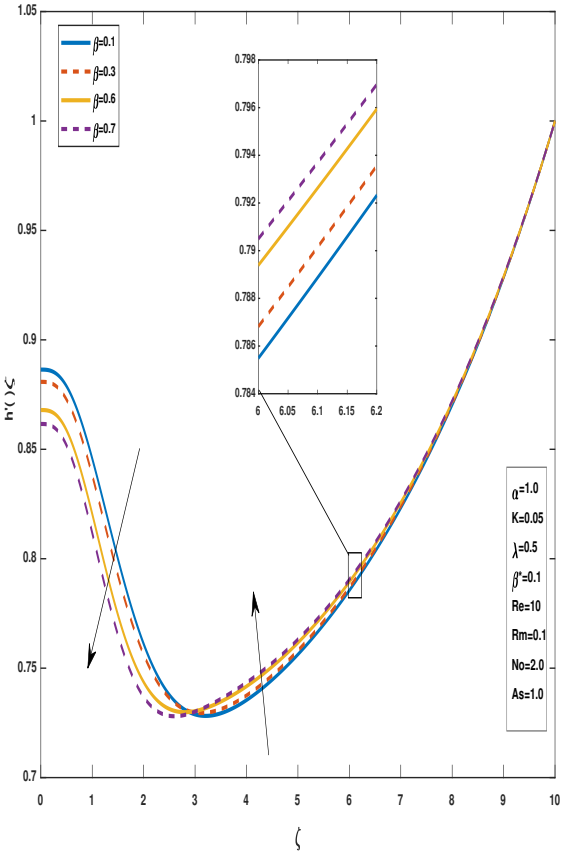

FIGURE 4.12: Effect of β on $h'(\zeta)$

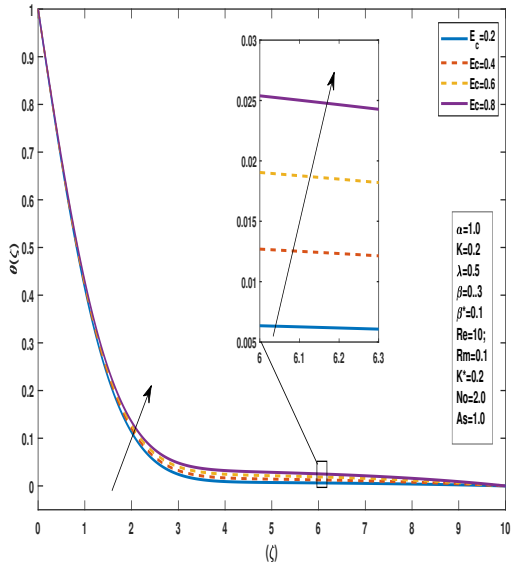

FIGURE 4.13: Effect of Ec on $\theta(\zeta)$

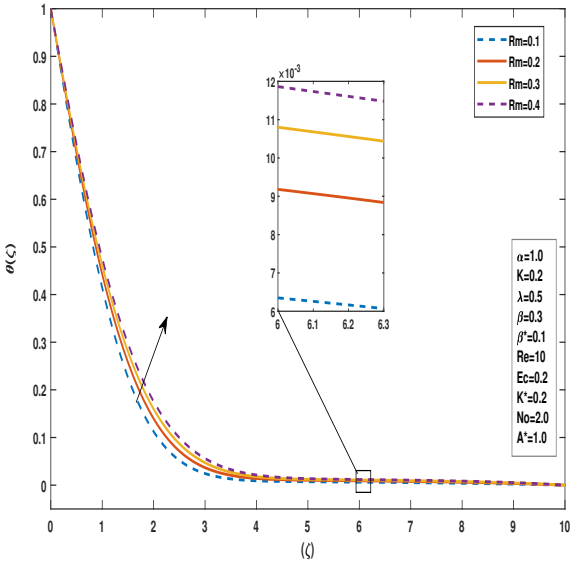

FIGURE 4.14: Effect of Rm on $\theta(\zeta)$

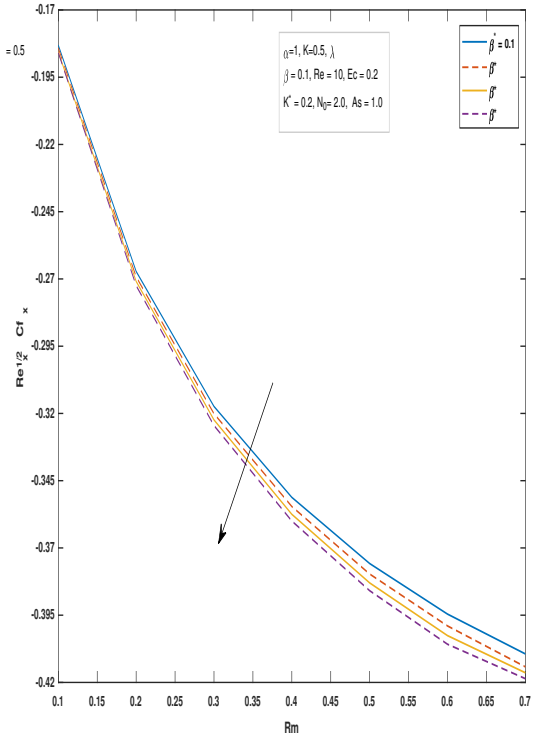

FIGURE 4.15: Skin friction coefficients $Re_x^{1/2}Cf_x$ vs Rm for various values of β^*

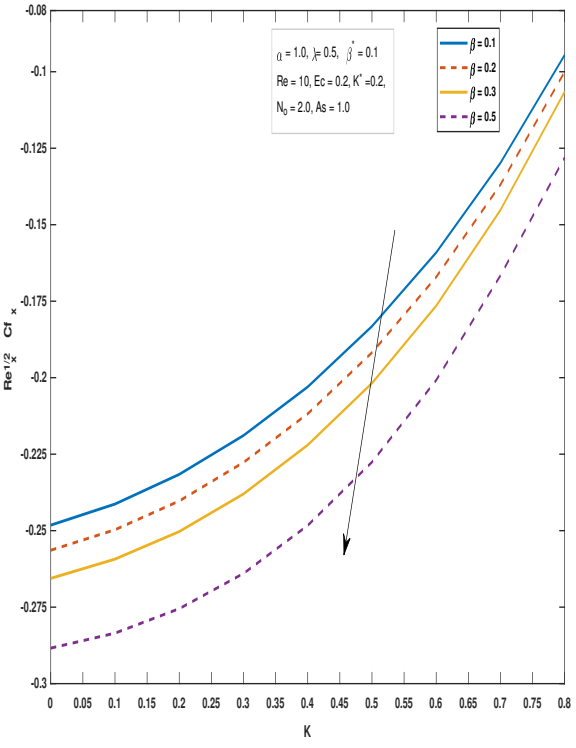

FIGURE 4.16: Skin friction coefficients $Re_x^{1/2}Cf_x$ vs K for various values of β

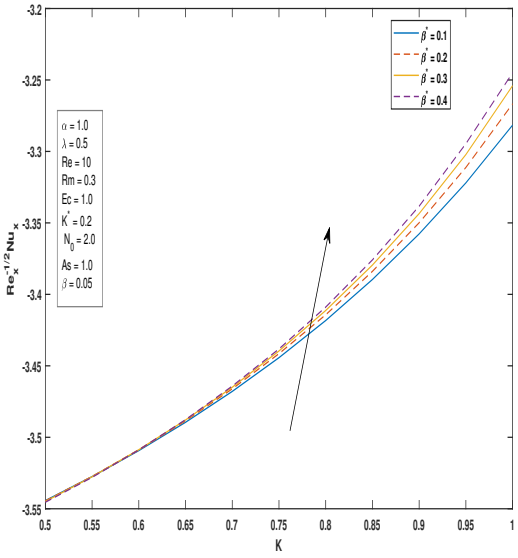

FIGURE 4.17: Local Nusselt number $Re_x^{-1/2}Nu_x$ vs K for various values of β^*

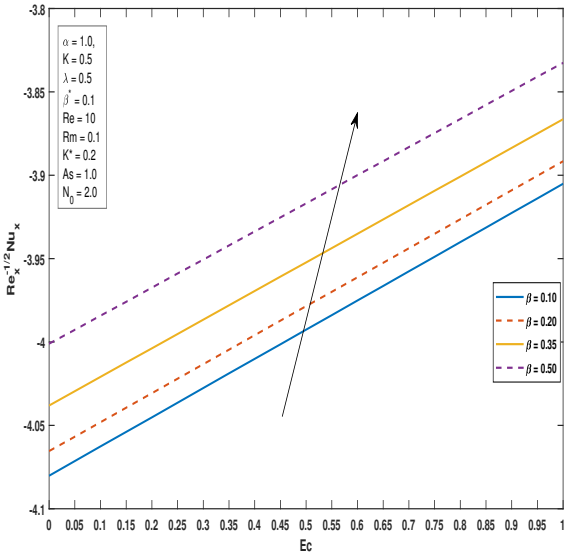

FIGURE 4.18: Local Nusselt number $Re_x^{-1/2}Nu_x$ vs Ec for various values of β

Chapter 5

Conclusions

The key findings of this investigation are as follows:

- The velocity boundary layer thickness is reduced by increasing the value of MMR.
- In the presence of MMR, the microrotation boundary layer thickness is lower than that in the absence of MMR near the stretching plate.
- The magnetic induction profile increases by increasing the values of MMR.
- The skin friction coefficient decreases by increasing the MMR parameter.
- Higher Eckert numbers result in elevated fluid temperatures due to an increased conversion of kinetic energy into thermal energy.
- Higher micropolar constant and micro-inertial coupling parameter lead to increase the heat transfer rate.
- Elevated micropolar constant leads to strengthen the magnetic induction profiles.
- The flow and thermal properties of micropolar fluids are further altered by the presence of a magnetic field.
- Results indicate that micromagnetorotation significantly alters the boundary layer thickness and velocity profiles.

- Essentially, higher Reynolds numbers signify that the fluid is less influenced by viscosity and more by inertia, leading to a more dynamic flow with a sharper velocity change near the boundary.
- The inclusion of micropolar effects, specifically micromagnetorotation, enhances heat transfer rates.
- The impact of viscous dissipation on the flow is measured by the Eckert number (Ec). Higher viscous dissipation effects are indicated by an increasing Eckert number.
- Through the Lorentz force, the magnetic field creates extra drag, which raises the skin friction coefficient by increasing the barrier to fluid flow.

Bibliography

[1] A Cemal Eringen. Simple microfluids. *International Journal of Engineering Science*, 2(2):205–217, 1964.

[2] Roslinda Nazar, Norsarahaida Amin, Diana Filip, and Ioan Pop. Stagnation point flow of a micropolar fluid towards a stretching sheet. *International Journal of Non-Linear Mechanics*, 39(7):1227–1235, 2004.

[3] Krishnendu Bhattacharyya, Swati Mukhopadhyay, GC Layek, and Ioan Pop. Effects of thermal radiation on micropolar fluid flow and heat transfer over a porous shrinking sheet. *International Journal of Heat and Mass Transfer*, 55(11-12):2945–2952, 2012.

[4] S Nadeem, MN Khan, and Nadeem Abbas. Transportation of slip effects on nanomaterial micropolar fluid flow over exponentially stretching. *Alexandria Engineering Journal*, 59(5):3443–3450, 2020.

[5] SE Ghasemi and Sina Gouran. Mathematical simulation of laminar micropolar fluid flow between two disks for two different geometries. *Waves in Random and Complex Media*, pages 1–22, 2023.

[6] AC Eringen. Micromorhic field theories i: Foundations and solids, 1999.

[7] A Cemal Eringen. *Microcontinuum field theories: II. Fluent media*, volume 2. Springer Science & Business Media, 2001.

[8] RC Chaudhary and Abhay Kumar Jha. Effects of chemical reactions on mhd micropolar fluid flow past a vertical plate in slip-flow regime. *Applied mathematics and Mechanics*, 29:1179–1194, 2008.

[9] Surbhi Sharma, Amit Dadheech, Amit Parmar, Jyoti Arora, Qasem Al-Mdallal, and S Saranya. Mhd micro polar fluid flow over a stretching surface with melting and slip effect. *Scientific reports*, 13(1):10715, 2023.

[10] Lakshmi Appidi, P Pramod Kumar, Sweta Matta, and Bala Siddulu Malga. Effects of chemical reaction and thermal radiation on mhd free convective flow of micro polar fluid past an infinite moving vertical porous plate with viscous dissipation. *Heat Transfer*, 52(3):2922–2939, 2023.

[11] M Turkyilmazoglu. Flow of a micropolar fluid due to a porous stretching sheet and heat transfer. *International Journal of Non-Linear Mechanics*, 83:59–64, 2016.

[12] Iswar Chandra Mandal, Swati Mukhopadhyay, and Kuppalapalle Vajravelu. Melting heat transfer of mhd micropolar fluid flow past an exponentially stretching sheet with slip and thermal radiation. *International Journal of Applied and Computational Mathematics*, 7:1–18, 2021.

[13] Fairul Naim Abu Bakar and Siti Khuzaimah Soid. Mhd stagnation-point flow and heat transfer over an exponentially stretching/shrinking vertical sheet in a micropolar fluid with a buoyancy effect. *Journal of Advanced Research in Numerical Heat Transfer*, 8(1):50–55, 2022.

[14] Waqar Khan Usafzai and Emad H Aly. Hiemenz flow with heat transfer in a slip condition micropolar fluid model: Exact solutions. *International Communications in Heat and Mass Transfer*, 144:106775, 2023.

[15] Rashmi Agrawal, Sonu Kumar Saini, and Pradeep Kaswan. Numerical modeling of mhd micropolar fluid flow and melting heat transfer under thermal radiation and joule heating. *International Journal for Computational Methods in Engineering Science and Mechanics*, 24(2):143–154, 2023.

[16] Kyriaki-Evangelia Aslani and Ioannis E Sarris. Effect of micromagnetorotation on magnetohydrodynamic poiseuille micropolar flow: Analytical solutions and stability analysis. *Journal of Fluid Mechanics*, 920:A25, 2021.

[17] Edward J Shaughnessy, Ira M Katz, and James P Schaffer. *Introduction to fluid mechanics*, volume 8. Oxford University Press New York, 2005.

[18] Donald F Young, TH (Theodore Hisao) Okiishi, and Wade Huebsch. *Fundamentals of fluid mechanics*. Wiley, 2006.

[19] RK Bansal. *A textbook of fluid mechanics*. Firewall Media, 2005.

[20] Peter A Davidson and Andre Thess. *Magnetohydrodynamics*, volume 418. Springer Science & Business Media, 2002.

[21] Yunus A Cengel and John M Cimbala. Fluid kinematics. *Fluid Mechanics Fundamentals and Applications, Mc Graw Hill Higher Education*, pages 121–170, 2006.

[22] Roland W Lewis, Perumal Nithiarasu, and Kankanhalli N Seetharamu. *Fundamentals of the finite element method for heat and fluid flow*. John Wiley & Sons, 2004.

[23] Robert W Fox, AT McDonald, and PJ Pitchard. Introduction to fluid mechanics, 2004, 2006.

[24] Alexander J Smits. A physical introduction to fluid mechanics. *(No Title)*, 2000.

[25] RK Rajput. *A textbook of fluid mechanics*. S. Chand, 2008.

[26] Royal Eugene Collins. Flow of fluids through porous materials. 1976.

[27] Junuthula Narasimha Reddy and David K Gartling. *The finite element method in heat transfer and fluid dynamics*. CRC press, 2010.

[28] J Kuneš. Thermomechanics. *Dimensionless Physical Quantities in Science and Engineering. Elsevier, Oxford*, pages 173–283, 2012.

[29] D Nikodijevic, D Milenkovic, and Z Stamenkovic. Mhd couette two-fluid flow and heat transfer in presence of uniform inclined magnetic field. *Heat and Mass Transfer*, 47(12):1525–1535, 2011.

[30] Muhammad Sabeel Khan and Isma Hameed. A new magneto-micropolar boundary layer model for liquid flows–effect of micromagnetorotation (mmr). *arXiv preprint arXiv:2308.08457*, 2023.